

**APPLICATION OF A HYDROCHEMICAL MODEL AND A
MULTIVARIATE SOIL-SOLUTION MIXING MODEL TO ALPINE
WATERSHEDS IN THE SIERRA NEVADA, CALIFORNIA**

By Richard P. Hooper and Norman E. Peters

U.S. GEOLOGICAL SURVEY

Water-Resources Investigations Report 93-4030

Prepared in cooperation with the

CALIFORNIA AIR RESOURCES BOARD



Atlanta, Georgia

1993

U.S. DEPARTMENT OF THE INTERIOR

BRUCE BABBITT, Secretary

U.S. GEOLOGICAL SURVEY

Dallas L. Peck, Director

For additional information write to:

District Chief, WRD
U.S. Geological Survey
3039 Amwiler Rd., Suite 130
Atlanta, GA 30360-2428

Copies of this report can be purchased from:

U.S. Geological Survey
Books and Open-File Reports Section
Box 25425, Federal Center
Denver, CO 80225

CONTENTS

Page

| | |
|---|----|
| Abstract | 1 |
| Introduction | 2 |
| Purpose and scope | 2 |
| Site description | 2 |
| Background | 6 |
| Alpine Lake Forecaster | 6 |
| Multivariate soil-solution mixing model | 11 |
| Application of the Alpine Lake Forecaster to four Alpine Watersheds | 13 |
| Approach | 13 |
| Geochemical results | 13 |
| Evaluation of residence-time formulation | 19 |
| Discussion | 19 |
| Sensitivity analysis of the Alpine Lake Forecaster | 24 |
| Analysis of stream transect data | 27 |
| Multivariate soil-solution mixing model | 31 |
| Summary | 37 |
| References cited | 38 |
| Appendix—Mixing diagrams | 40 |

ILLUSTRATIONS

Page

| | |
|---|----|
| Figure 1.—Location of Emerald, Topaz, and Pear Lakes | 3 |
| Figure 2.—Location of Crystal Lake | 4 |
| Figure 3.—Location of Ruby Lake | 5 |
| Figure 4.—Relation between sum-of-base-cations and silica concentration in streamwater samples collected from inlets to Emerald Lake, 1986 | 7 |
| Figure 5.—Relation between weathering ratio (K) and 10-day average discharge | 9 |
| Figure 6.—Relation between sum-of-base-cations concentration and both acid neutralizing capacity and silica concentration for inlet and lake samples at Crystal Lake | 14 |
| Figure 7.—Relation between sum-of-base-cations concentration and both acid neutralizing capacity and silica concentration for the combined inlets at Crystal Lake | 15 |
| Figure 8.—Relation between silica and sum-of-base-cations concentrations in inflow and outflow samples at Crystal Lake on various sampling dates | 16 |
| Figure 9.—Relation between sum-of-base-cations concentration and both acid neutralizing capacity and silica concentration for Ruby Lake | 17 |
| Figure 10.—Relation between sum-of-base-cations concentration and both acid neutralizing capacity and silica concentration for the 1-meter sampling site in the lake, the outflow, and combined inlets, Ruby Lake | 18 |
| Figure 11.—Relation between sum-of-base-cations concentration and both acid neutralizing capacity and silica concentration for all data at Topaz Lake | 20 |
| Figure 12.—Relation between sum-of-base-cations concentration and acid neutralizing capacity at Pear Lake .. | 21 |
| Figure 13.—Relation between sum-of-base-cations concentration and acid neutralizing capacity at Pear Lake, excluding two samples with high acid neutralizing capacity | 21 |
| Figure 14.—Relation between the weathering ratio (K) and daily mean discharge for Crystal Lake | 22 |

ILLUSTRATIONS--Continued

| | Page |
|---|------|
| Figure 15.—Relation between the weathering ratio (K) and daily mean discharge for Ruby Lake..... | 22 |
| Figure 16.—Relation between the weathering ratio (K) and daily mean discharge for Topaz Lake. | 23 |
| Figure 17.—Relation between weathering ratio and 10-day average discharge for a range of stoichiometric coefficients..... | 25 |
| Figure 18.—Calculated alkalinity for an inlet to Emerald Lake during 1986 for a range of stoichiometric coefficients (c)..... | 26 |
| Figure 19.—Location of stream and lysimeter sites sampled along a major inlet to Emerald Lake. | 28 |
| Figure 20.—Silica concentration along the major inflow to Emerald Lake on various sampling dates..... | 29 |
| Figure 21.—Sum of base cations concentration along the major inflow to Emerald Lake on various sampling dates..... | 30 |
| Figure 22.— Mixing diagram relating calcium and alkalinity..... | 41 |
| Figure 23.— Mixing diagram relating chloride and alkalinity. | 41 |
| Figure 24.— Mixing diagram relating nitrate and alkalinity. | 42 |
| Figure 25.— Mixing diagram relating sulfate and alkalinity..... | 42 |
| Figure 26.—Mixing diagram relating magnesium and alkalinity..... | 43 |
| Figure 27.—Mixing diagram relating sodium and alkalinity. | 43 |
| Figure 28.—Mixing diagram relating potassium and alkalinity. | 44 |
| Figure 29.—Mixing diagram relating silica and alkalinity..... | 44 |
| Figure 30.—Mixing diagram relating nitrate and chloride. | 45 |
| Figure 31.—Mixing diagram relating sulfate and chloride..... | 45 |
| Figure 32.—Mixing diagram relating calcium and chloride..... | 46 |
| Figure 33.—Mixing diagram relating magnesium and chloride..... | 46 |
| Figure 34.—Mixing diagram relating sodium and chloride..... | 47 |
| Figure 35.—Mixing diagram relating potassium and chloride. | 47 |
| Figure 36.—Mixing diagram relating silica and chloride..... | 48 |
| Figure 37.—Mixing diagram relating sulfate and nitrate..... | 48 |
| Figure 38.—Mixing diagram relating calcium and nitrate..... | 49 |
| Figure 39.—Mixing diagram relating magnesium and nitrate..... | 49 |
| Figure 40.—Mixing diagram relating sodium and nitrate. | 50 |
| Figure 41.—Mixing diagram relating potassium and nitrate..... | 50 |
| Figure 42.—Mixing diagram relating silica and nitrate. | 51 |
| Figure 43.—Mixing diagram relating calcium and sulfate. | 51 |
| Figure 44.—Mixing diagram relating magnesium and sulfate. | 52 |
| Figure 45.—Mixing diagram relating sodium and sulfate. | 52 |
| Figure 46.—Mixing diagram relating potassium and sulfate..... | 53 |
| Figure 47.—Mixing diagram relating silica and sulfate. | 53 |
| Figure 48.—Mixing diagram relating magnesium and calcium. | 54 |
| Figure 49.—Mixing diagram relating sodium and calcium..... | 54 |
| Figure 50.—Mixing diagram relating potassium and calcium..... | 55 |
| Figure 51.—Mixing diagram relating silica and calcium. | 55 |
| Figure 52.—Mixing diagram relating sodium and magnesium. | 56 |
| Figure 53.—Mixing diagram relating potassium and magnesium..... | 56 |
| Figure 54.—Mixing diagram relating silica and magnesium..... | 57 |
| Figure 55.—Mixing diagram relating potassium and sodium. | 57 |
| Figure 56.—Mixing diagram relating silica and sodium. | 58 |
| Figure 57.—Mixing diagram relating silica and potassium..... | 58 |
| Figure 58.—Relation between first and second principal components for streamwater and soil solutions | 33 |

TABLES

| | <u>Page</u> |
|--|-------------|
| Table 1.—Characteristics of selected watersheds in the study area..... | 8 |
| Table 2.—Hydrologic and chemical inputs to the Alpine Lake Forecaster..... | 10 |
| Table 3.—Statistics of regression models relating weathering ratio and 10-day average discharge..... | 24 |
| Table 4.—Variance explained by principal component..... | 32 |
| Table 5.—Soil-solution statistics for shallow lysimeter at bench meadow site..... | 34 |
| Table 6.—Soil-solution statistics for deep lysimeter at bench meadow site..... | 34 |
| Table 7.—Soil-solution statistics for shallow lysimeter at ridge site..... | 35 |
| Table 8.—Soil-solution statistics for deep lysimeter at ridge site | 35 |
| Table 9.—Soil-solution statistics for shallow lysimeter at inlet meadow site | 36 |
| Table 10.—Soil-solution statistics for deep lysimeter at inlet meadow site | 36 |

CONVERSION FACTORS, VERTICAL DATUM AND ACRONYMS AND ABBREVIATIONS

| Multiply | by | To obtain |
|---|---------|-----------------------|
| <i>Length</i> | | |
| millimeter (mm) | 0.03937 | inch |
| meter (m) | 3.281 | foot |
| kilometer (km) | 0.6214 | mile |
| <i>Area</i> | | |
| hectare (ha) | 2.471 | acre |
| square meter (m ²) | 10.76 | square foot |
| <i>Volume</i> | | |
| liter (L) | 0.2642 | gallon |
| cubic meter (m ³) | 35.31 | cubic foot |
| <i>Flow</i> | | |
| cubic meter per day (m ³ /d) | 264.2 | gallon per day |
| liters per second (L/s) | 0.0353 | cubic feet per second |

VERTICAL DATUM

In this report, “sea level” refers to the National Geodetic Vertical Datum of 1929—a geodetic datum derived from a general adjustment of the first-order level nets of the United States and Canada, formerly called Sea Level Datum of 1929.

ACROYNMS AND ABBREVIATIONS

| | |
|--------|---|
| ALF | Alpine Lake Forecaster |
| ANC | Acid Neutralizing Capacity |
| EMMA | End-Member Mixing Analysis |
| ILWAS | Integrated Lake/Watershed Acidification Study |
| IWS | Integrated Watershed Study |
| PCA | Principal Components Analysis |
| PC | Principal Component |
| SBC | Sum of Base Cations |
| µeq/L | microequivalents per liter |
| µmol/L | micromoles per liter |

**APPLICATION OF
A HYDROCHEMICAL MODEL AND
A MULTIVARIATE SOIL-SOLUTION MIXING MODEL
TO ALPINE WATERSHEDS IN THE
SIERRA NEVADA, CALIFORNIA**

By

Richard P. Hooper and Norman E. Peters

ABSTRACT

A computer model that was developed to simulate the hydrology and geochemical reactions at Emerald Lake in California can be applied to three of the four alpine lake watersheds in the Sierra Nevada, California studied in this investigation. The four watersheds were less intensively characterized than the Emerald Lake watershed for which the model, called the Alpine Lake Forecaster (ALF), was originally designed. Reliable parameter estimation for this model requires that samples be collected over the broadest possible range of discharge from the watershed, such as from baseflow to peak snowmelt discharge. A sensitivity analysis of the geochemical formulation of ALF indicates that the streamwater chemical response to acidic snowmelt is highly dependent upon the proportion of more readily weatherable minerals that are contained in the bedrock. The slope of the regression line relating the sum-of-bases concentration to silica concentration may serve to quantify the relative sensitivity of the watershed to acidification. To further elucidate hydrologic flowpaths in alpine basins, a multivariate mixing model was developed that explains variation in streamwater chemistry as mixtures of soil solutions. Because soil-solution data were available only from Emerald Lake, the mixing model was developed for that site. The results indicate that two soil environments—the bench meadow and the inlet meadow or ridge site—may explain most of the observed variation in stream chemistry, and indicate that there is a source of calcium to the surface water that has not been identified.

INTRODUCTION

The Alpine Lake Forecaster (ALF) is a computer simulation model developed to predict the effects of acid deposition on streamwater and lake-water quality in alpine catchments (Hooper, West, and Peters, 1990). ALF consists of a hydrologic model, which is designed for snowmelt periods, coupled with a geochemical model that contains primary mineral weathering reactions and carbonate equilibria. ALF was developed using data from the Emerald Lake watershed in Sequoia National Park, California. This watershed was the subject of an intensive 5-year investigation under the Integrated Watershed Study (IWS) of the California Air Resources Board to understand “the influence of atmospheric inputs on watershed processes, surface-water chemistry, and aquatic biota in an ecosystem representative of alpine watersheds at high elevations in the Sierra Nevada” (Tonnessen, 1991, p. 1537). The investigation included extensive characterization of the watershed, complete with topographic, bathymetric, geologic, soils, and vegetation mapping, and surveys of aquatic biota. During winter months, snow inputs were measured on an event basis, and a snow survey of the entire basin was made at maximum snow accumulation (Dozier and others, 1989). Discharge from the lake was monitored continuously and inlet stages were recorded manually when samples were collected. Streams were sampled routinely on a bi-weekly basis and more intensively during a few summer rainstorms (Melack and others, 1989). Radiation measurements at multiple sites within the basin also were recorded for the development of an energy-based snowmelt model (Marks, 1988; Dozier and others, 1989).

Purpose and Scope

This report presents three distinct model analyses using data from both Emerald Lake and other alpine lakes in the Sierra Nevada. First, ALF was calibrated to four less intensively studied alpine lake watersheds—Pear, Ruby, Topaz, and Crystal Lake. The purpose of this investigation was to assess whether sufficient data were available to calibrate the model, to determine the suitability of the model to these watersheds, and to assess the need for design changes for future field efforts where ALF was to be used. Second, a sensitivity analysis of ALF was performed that required the more complete streamwater chemistry record available at Emerald Lake. Because the hydrologic model in ALF does not contain any calibrated parameters, this analysis focused on the weathering formulation contained within the geochemical model. Finally, a multivariate soil-solution mixing model was developed that attempts to explain variation in streamwater chemistry by varying the proportions of soil solutions that compose the streamwater. This analysis can indicate which areas of the watershed are contributing to streamflow and the hydrologic pathways by which the water flows through the watershed. Because soil solution data are available only from Emerald Lake, that data set is used for this analysis as well.

Site Description

Data analyzed in this report were collected from five alpine watersheds in the Sierra Nevada, Calif. Three of the watersheds, Emerald Lake, Pear Lake, and Topaz Lake (fig. 1), are on the western slope, and the other two, Crystal Lake (fig. 2) and Ruby Lake (fig. 3), are on the eastern slope. Characteristics of the watersheds are summarized in table 1. More extensive descriptions of the watersheds are provided by Melack and others (1989) and Sickman and Melack (1989). In these watersheds, snow predominates over rainfall and snowmelt is the major source of streamflow.

Pear, Ruby, Topaz and Crystal Lake watersheds were studied much less intensively than was the Emerald Lake watershed. Topographic and geologic data were obtained from available maps for these watersheds. Inputs to the watersheds were estimated from snow surveys at maximum accumulation and from rain gages during the non-snow season. The lakes were sampled bi-monthly at four depths, from October 1986 to June 1988, and inlets and lake outlets were sampled contemporaneously when possible. These data were collected to describe seasonal variability of acid neutralizing capacity (ANC) and other solutes within the lakes, to identify seasonal increases and decreases in ANC, and to quantify the acidic deposition to these four watersheds (Sickman and Melack, 1989, p. 1). This investigation will be referred to as the “Four-Lake Study.”

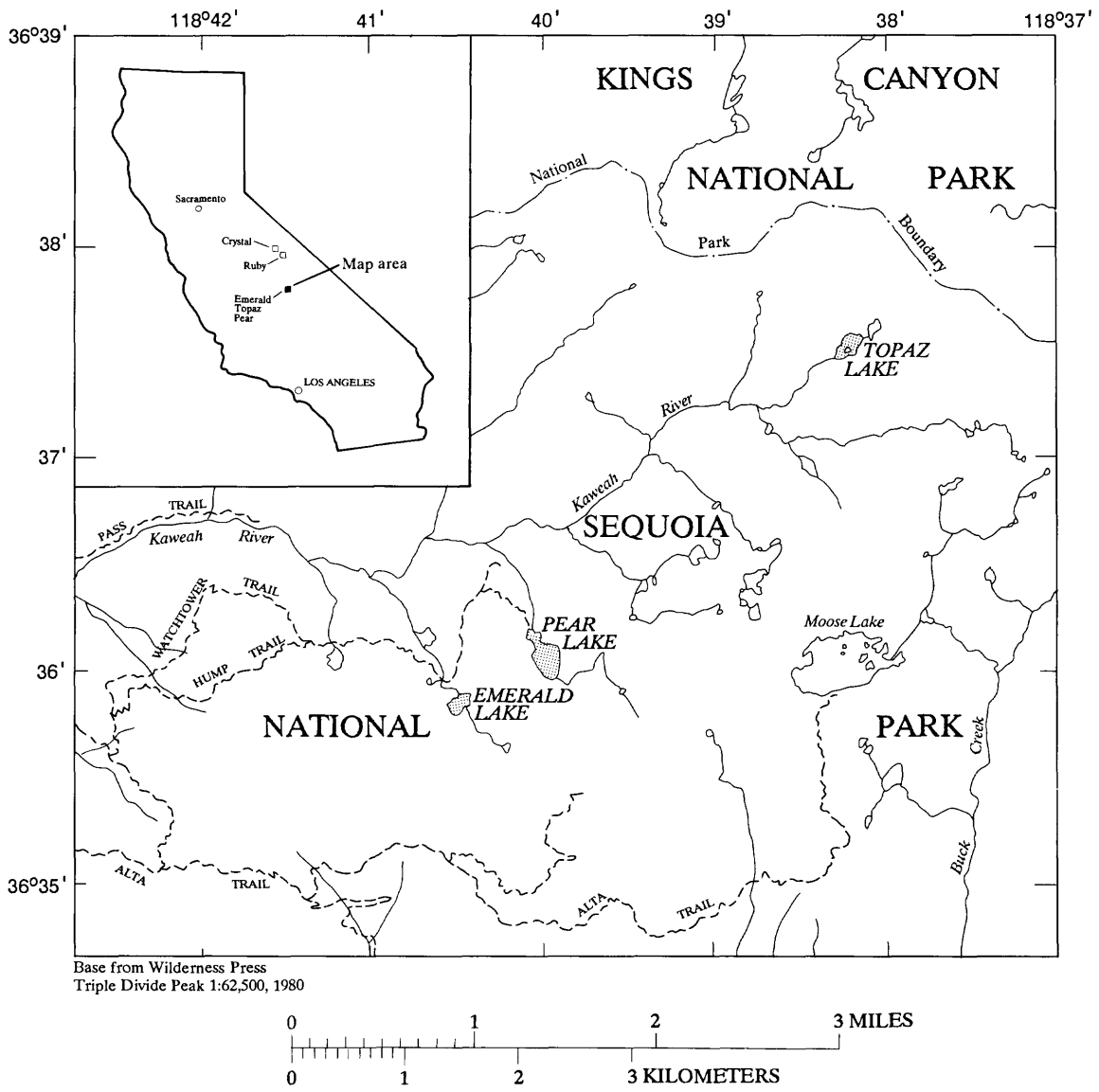


Figure 1.—Location of Emerald, Topaz, and Pear Lakes.

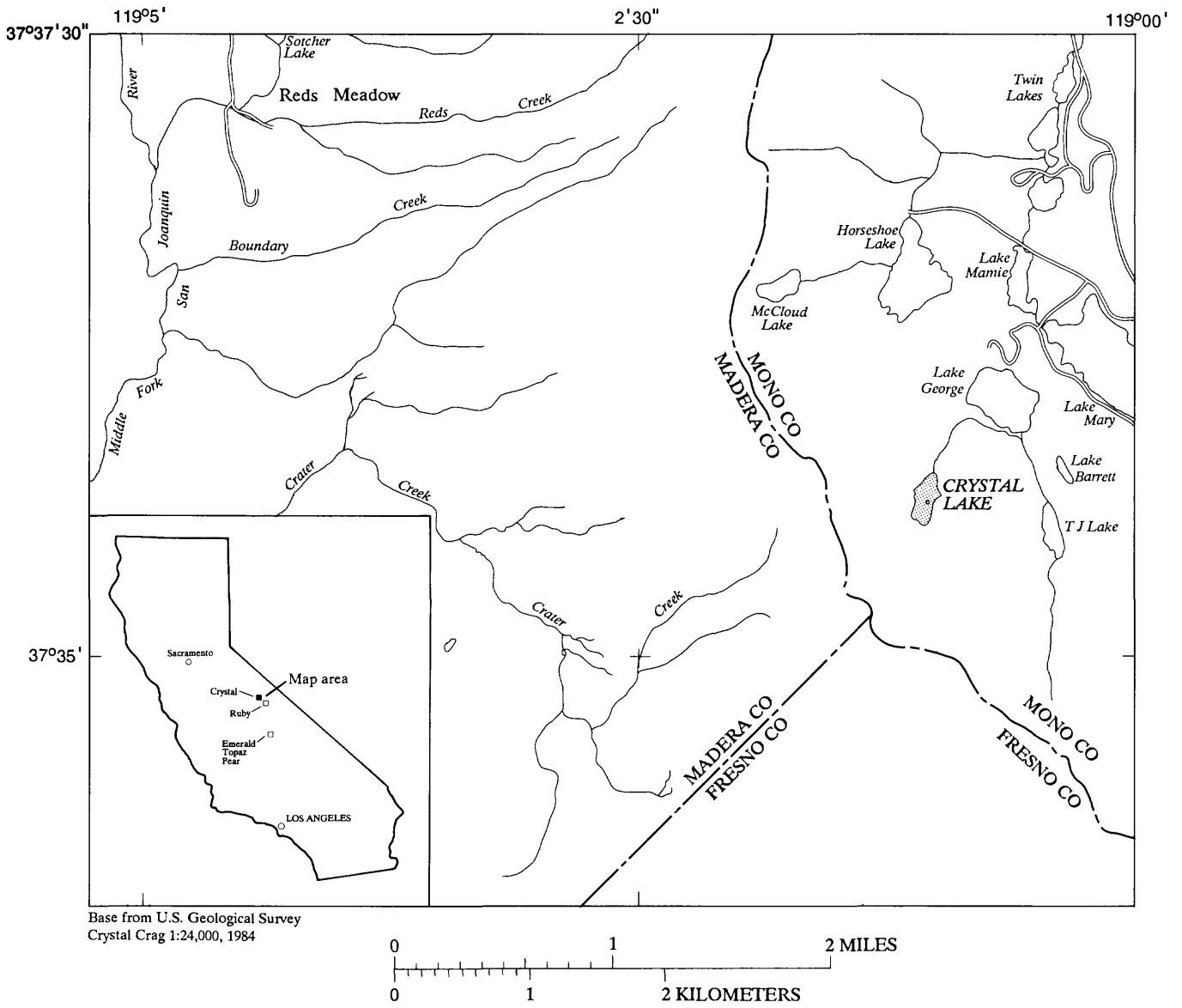


Figure 2.—Location of Crystal Lake.

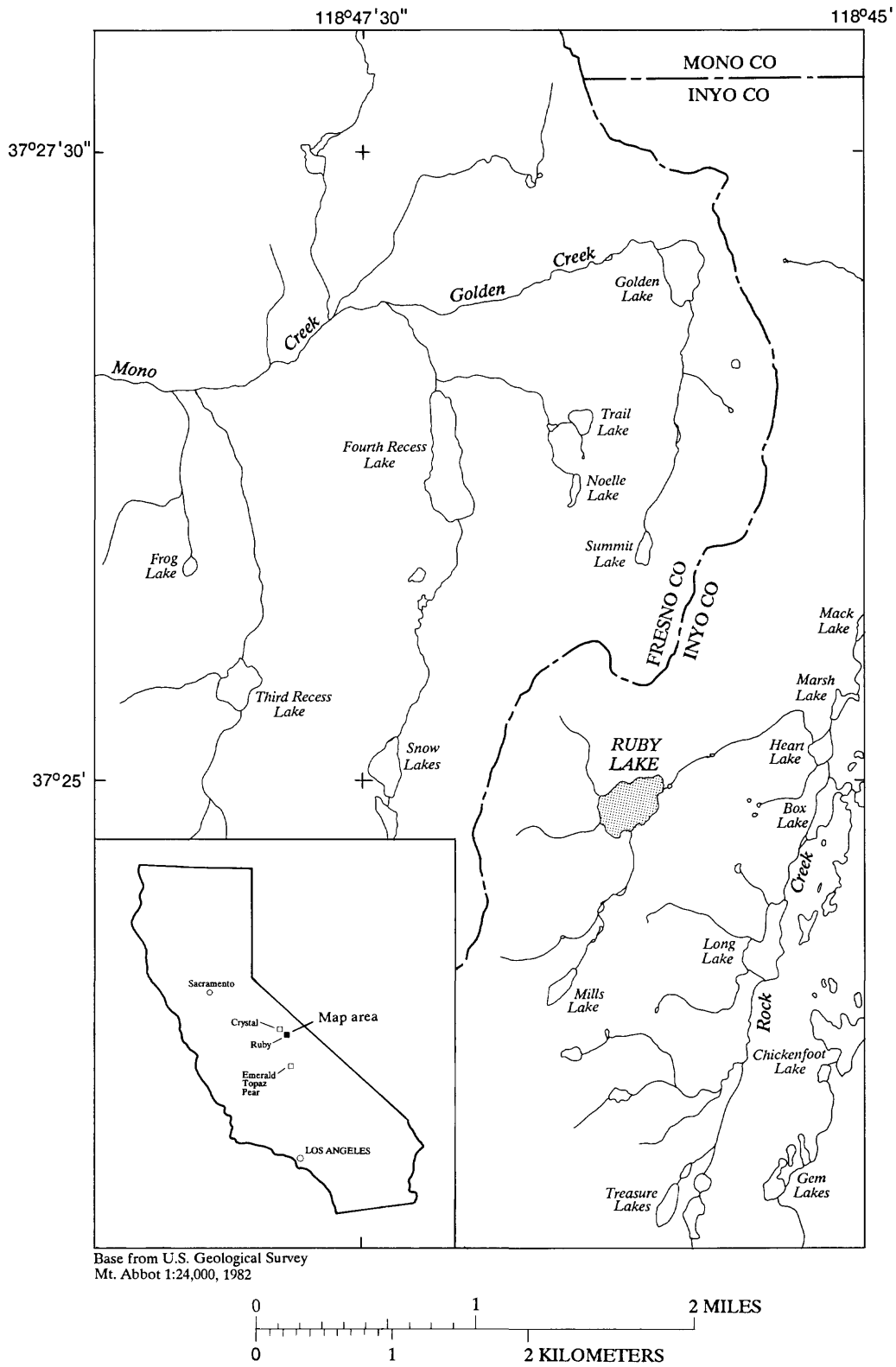


Figure 3.—Location of Ruby Lake.

Background

This section provides information on the structure of ALF and its past application to Emerald Lake, as described by Hooper, West, and Peters (1990), that will be needed for the sensitivity analysis of ALF and for its application to the Four-Lake data set. In addition, the theoretical background for the alternate interpretation of the Emerald Lake data using end-member mixing analysis (EMMA) is presented. This discussion integrates the findings of Christophersen and others (1990), Hooper, Christophersen, and Peters (1990), and Christophersen and Hooper (1992).

Alpine Lake Forecaster

The Alpine Lake Forecaster (ALF) consists of coupled hydrologic and chemical models. The hydrologic model was developed to eliminate the need to adjust or “fit” parameters by assuming that daily discharge from the lake was equal to daily snowmelt. However, this assumption limits the application of ALF to snowmelt periods and to catchments where ground-water and lake storage are constant or vary by small amounts relative to the water flux. Emerald Lake seemed to meet these constraints (Hooper, West, and Peters, 1990, p. 6). The snowpack was assumed to melt in each terrestrial subbasin proportionately to its potential solar insolation; the insolation was calculated as a function of latitude, slope inclination, aspect, and day of year using an algorithm developed by Swift (1976). Based on these characteristics, Emerald Lake watershed was divided into seven subbasins. The epilimnion of the lake received water from the terrestrial subbasins and discharged water to the outflow of the lake. The proportion of the lake volume containing ice, epilimnion, and hypolimnion was determined by combining the lake bathymetry and the temperature profiles that were collected approximately biweekly. These data were linearly interpolated to provide the daily values required by the model.

The hydrologic model is complicated by rainfall that occurs during the snowmelt period. If the discharge increases on a day when rainfall is recorded, all of the increase in discharge is assumed to be from rainfall, if the rainfall volume is sufficient. If not, the discharge volume unaccounted for by the rainfall is presumed to be supplied from the snow pack. If rainfall volume exceeds the increase in discharge (as was usually the case), the “excess” rainfall is areally proportioned (along with the solutes it contains) among the subbasins and is added to the snowpack. At Emerald Lake, rainfall was minor in 1986, but provided more than 10 percent of the precipitation in 1987 (Hooper, West, and Peters, 1990).

The chemical model includes primary mineral weathering, the carbonate buffering system, and a simplified representation of the nitrogen cycle. Sulfate and chloride are treated as conservative constituents in the model. For the carbonate system, the lake is assumed to be closed to the atmosphere when covered by ice and open to the atmosphere at other times. The terrestrial part of the watershed is assumed to be open to the atmosphere at all times. The partial pressure of carbon dioxide, to which water equilibrates in the open system, is a parameter in the model that must be adjusted. For the nitrogen cycle, the year is divided into biotically active and inactive seasons. During the biotically active season, all ammonium is assumed to be taken up by the biota; thus, every mole of ammonium is exchanged for one mole of hydrogen ion. In addition, a portion of the nitrate also is retained, along with an equivalent amount of hydrogen ion. During the biotically inactive season, all of the ammonium is assumed to be oxidized to nitrate and two moles of hydrogen ion; the biota are assumed to retain no nitrate. After biotic uptake, if any, nitrate is treated as a conservative constituent. At Emerald Lake, the entire snowmelt period was assumed to be biotically active, and 10 percent of the nitrate was assumed to be retained by the biota.

Cation exchange was not included as an alkalinity generating mechanism based upon three factors:

- The conclusions of other researchers that weathering was the dominant process at Emerald Lake (Weintraub, 1986; Lund and others, 1987),
- The lack of detailed soil-solution information during the snowmelt period, and
- The observation that dissolved silica, a product of primary weathering, was well correlated with the sum of base cations (SBC) in solution (that is, the sum of sodium, potassium, calcium, and magnesium) as shown in figure 4.

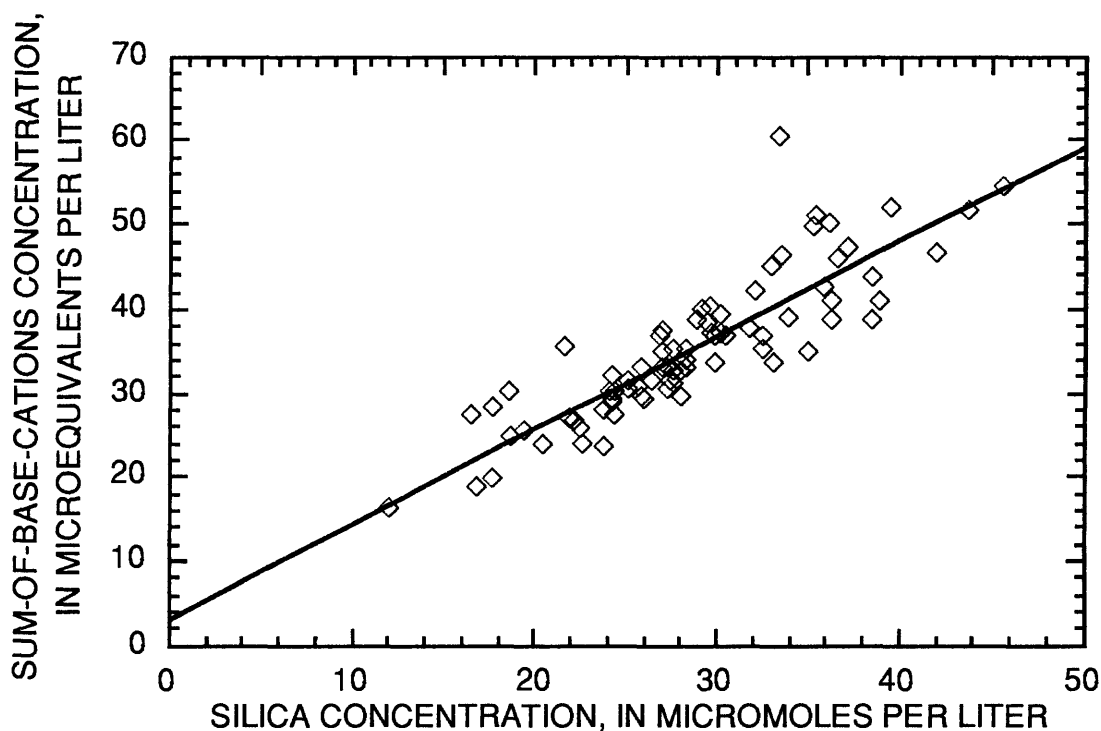


Figure 4.—Relation between sum-of-base-cations and silica concentration in streamwater samples collected from inlets to Emerald Lake, 1986.

The bedrock at Emerald Lake is dominated by quartz and feldspar and contains minor amounts of biotite and hornblende. The existence of secondary minerals in the soils indicates that the weathering reactions are incongruent (Weintraub, 1986); that is, the dissolution reaction involves the formation of a secondary mineral, such as a clay. In the absence of detailed mineral-weathering data, however, the stoichiometries of the weathering reactions were simplified by combining the individual aluminosilicate minerals into one reactant called rock. Because cation exchange reactions were not included, the individual base cations also were not tracked separately, but rather were lumped into one reactant, sum of base cations (SBC). The slope of the least-squares regression of SBC concentration on dissolved silica is 1.2 (fig. 4), and therefore, the following dissolution reaction is consistent with these data

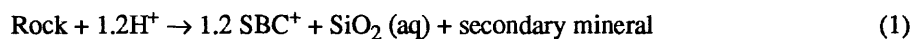


Table 1.—Characteristics of selected watersheds in the study area
[ha, hectare; m, meter]

| Watershed | Latitude | Longitude | Drainage area (ha) | Relief (m) | Lake area (ha) | Lake altitude (m) | Maximum depth (m) | Aspect | Lake volume (m) | Bedrock type |
|-----------|------------|-------------|--------------------|------------|----------------|-------------------|-------------------|-----------|-----------------|---|
| Emerald | 36°35'49"N | 118°40'30"W | 120 | 616 | 0.7 | 2,800 | 10 | northwest | 60,000 | Granite, granodiorite, aplite |
| Topaz | 36°37'30"N | 118°38'11"W | 142 | 244 | 5.2 | 3,219 | 5.0 | north | 74,000 | Granodiorite with abundant mafic inclusions |
| Pear | 36°36'02"N | 118°40'00"W | 136 | 471 | 8.0 | 2,904 | 27 | northwest | 578,000 | Granite with sparse mafic inclusions |
| Crystal | 37°35'36"N | 119°01'05"W | 129 | 293 | 5.0 | 2,951 | 14 | north | 320,000 | Granite in east and south; volcanic elsewhere |
| Ruby | 37°24'50"N | 118°46'15"W | 424 | 754 | 12.6 | 3,426 | 35 | northeast | 2,156,000 | Quartz monzonite |

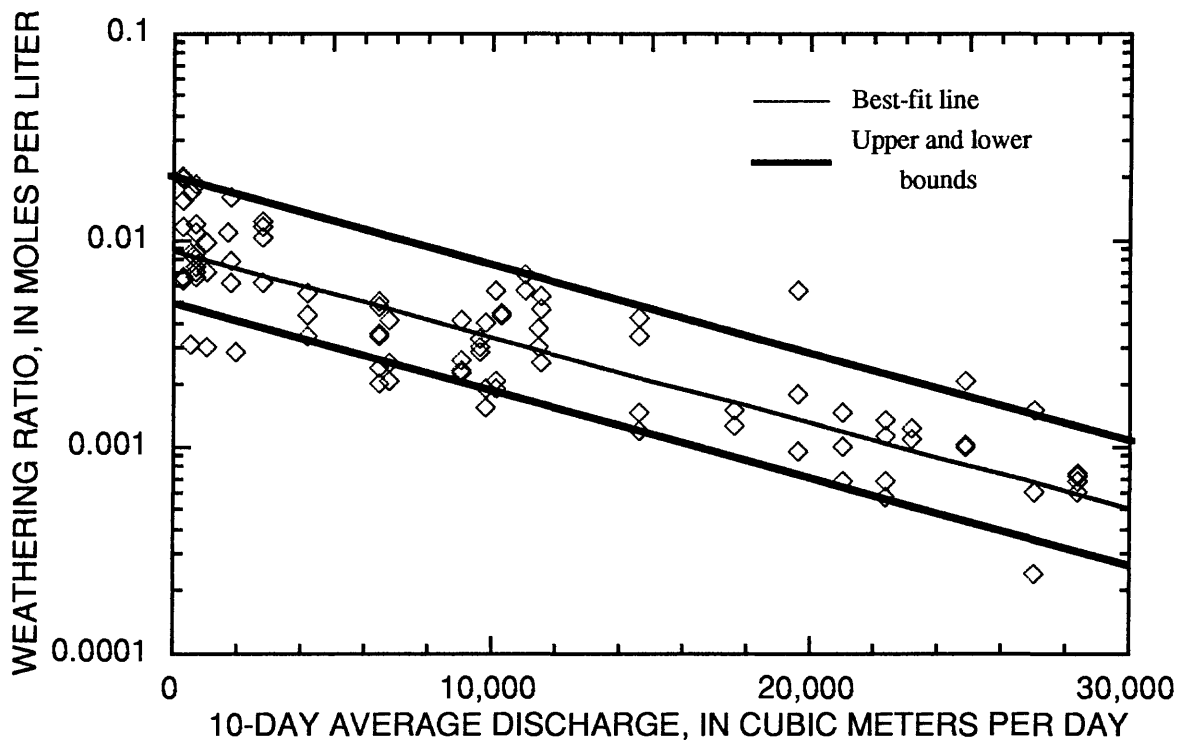


Figure 5.—Relation between weathering ratio (K) and 10-day average discharge.

Reaction 1, however, is subject to kinetic constraints. The hydrologic model does not permit an explicit calculation of the residence time of water within the terrestrial system, so a standard kinetic model cannot be fit to the data. Instead, lake discharge, averaged over the 10 days prior to the sample collection, was used as a surrogate for residence time. At Emerald Lake, a regression of the log of the weathering ratio, K, where

$$K = \frac{[\text{SBC}^+]^{1.2}[\text{SiO}_2]}{[\text{H}^+]^{1.2}} \quad (2)$$

on the average discharge (fig. 5) yields the following equation,

$$K = 0.0082 \cdot 10^{-0.000044Q'} \quad (3)$$

where Q' is the 10-day average discharge. Equation 3 explains 80 percent of the variation in the data. In the original application of ALF to Emerald Lake, two different intercepts—0.005 and 0.02—were used to display the sensitivity of the predictions to uncertainty in this equation. These values were chosen because they enclosed most of the scatter in the data (fig. 5).

A modified Newton's method (Morel and Morgan, 1972) was used to solve the system of non-linear equations that form the chemical model. Temperature corrections were made for the carbonate system and for the hydrolysis of water, but activity corrections were not made because of the low ionic strength of the surface water. The mathematical solution seemed identical to an equilibrium solution, yet the equilibrium "constant" for the weathering reaction varies with discharge. These equations were solved on a daily time step by using the input concentration of meltwater. For periods of rainfall, the model assumed that the "excess" rainfall, as defined above, reacted with the rock and then mixed with the meltwater, which also has reacted with the rock. The model then re-equilibrated this mixture before routing it into the lake.

Within the lake, no chemical reactions, other than carbonate buffering, were assumed to occur. The volume of the epilimnion is increased by inflow from the terrestrial system, thinning of the ice layer, and deepening of the thermocline. The appropriate mass of solutes are advected with the water, and the system is re-equilibrated assuming that the epilimnion is completely mixed. The time step concludes with water of the same quality as the epilimnion being advected from the lake.

Five parameters need to be calibrated within the chemical model. These parameters are the two regression coefficients for the weathering reaction (eq. 3), the portion of nitrate retained by the biota, the date at which the biota become active, and the partial pressure of carbon dioxide. Necessary hydrologic and chemical inputs for ALF are summarized in table 2.

Table 2.--Hydrologic and chemical inputs to the Alpine Lake Forecaster

| Hydrologic | Chemical |
|---------------------------------------|--|
| Daily discharge from lake | total mass of solutes at maximum snowpack accumulation |
| Rainfall quantity (during snowmelt) | rainwater quality |
| Thermocline depth | initial lake water quality |
| Ice thickness | initial chemical composition of ice on lake |
| Temperature of inflows and epilimnion | |

Although the mass of solutes in the snowpack is input to ALF, the quality of the meltwater must be calculated. The first meltwater from the snowpack typically contains a high concentration of solutes (Johannessen and Henriksen, 1978). This first "pulse" of solutes from acidic snowpacks is thought to be the cause for the sharp pH depressions during the spring snowmelt (Skartveit and Gjessing, 1979) and has been linked to fish kills in Norway (Leivestad and Muniz, 1976). Therefore, the intensity of the acidic pulse is a key factor in determining the effect of acidic contaminants contained within the snowpack on aquatic biota. Previous models have assumed an exponential decline in the release of solutes from the snowpack (Christophersen and others, 1984). Specifically, the concentration factor (the ratio of the concentration of the meltwater to the bulk concentration of the snowpack) is assumed to decline exponentially.

Because knowing the pattern of solute release is critical, particularly when considering different depositional scenarios, the solute release was modeled differently in ALF. An elution rule in the form of x percent of the solutes released in the first y percent of the meltwater (for example, 80/20 rule means 80 percent of the solutes are released in the first 20 percent of the meltwater) and a maximum concentration factor for the first day (the ratio of concentration on that day to the average concentration of the solute in the snowpack) are specified. Two exponential curves, one curve for the period when the first y percent of the water drains from the pack and a second curve for the remainder of the melt period, define the meltwater concentration. These curves meet the specified elution rule and concentration factor together with a continuity condition that the concentration does not change abruptly between the two curves. The results of this approach agreed well with laboratory studies (Hooper, West, and Peters, 1990, p. 15).

Multivariate Soil-Solution Mixing Model

Variations in streamwater chemistry can be considered as stemming from a dynamic mixture of source solutions, such as ground water and precipitation (Johnson and others, 1969); event and pre-event water (Pilgrim and others, 1979; Sklash and Farvolden, 1979); ground water, water in the unsaturated zone, and rainfall directly intercepted by the stream (DeWalle and others, 1988); or soil-water solutions (Neal and Christophersen, 1989; Christophersen and others, 1990; Hooper, Christophersen, and Peters, 1990).

When soil-water and ground-water solutions are used as sources for the mixing model, the controlling soil environments can be used to compartmentalize the watershed. For example, Hooper, Christophersen, and Peters (1990) determined that, at the Panola Mountain Research Watershed in Georgia, soil solutions from the saturated zone in the flood plain of the watershed, from the mineral horizon at the base of the hillslope, and from the soil A-horizon could describe variations in streamwater chemistry for six solutes (or solute combinations): alkalinity, sulfate, sodium, magnesium, calcium, and silica. The mixing model was used in conjunction with a long-term hydrochemical model to identify controlling soil environments, to determine hydrologic routing through the catchment, and to predict streamwater chemistry during future storms (Hooper and Christophersen, 1992).

This approach to compartmentalization is less arbitrary than imposing a "box" model on the watershed, such as the Integrated Lake-Watershed Acidification Study (ILWAS) model (Chen and others, 1983), which has a fixed structure. Furthermore, the approach avoids the difficulty of determining hydrologic routing parameters, which, although chemically important, are difficult to determine from hydrologic data (Hooper and others, 1988).

The mixing model can be posed in either a "forward" or "inverse" mode. In the forward mode, potential source solutions are evaluated as to whether they can be mixed together in some set of proportions to yield the observed streamwater concentration. This has been termed "end-member mixing analysis" (EMMA) by Christophersen and others (1990) because the source solutions have more extreme concentration than the streamwater mixture, and, hence, are "end members." Alternately, the mixture (that is, the streamwater samples) can be analyzed to determine the number and composition of the end members. Traditionally, a standard multivariate statistical technique known as principal components analysis (PCA) has been used for the inverse analysis. However, Christophersen and Hooper (1992) have demonstrated that only the number, and not the composition, of the end members can be determined from PCA.

Geometrically, if a conservative mixture of $n-1$ solutes can be explained by fewer than n end members, the mixture does not fully "fill" $n-1$ dimensions defined by the solutes¹. For example, if two end members are mixed, all mixtures will lie along a line between the two end members regardless of the number of solutes that the end members contain. Thus, the "solute space" may have a high dimensionality (the number of measured solutes), but the mixture may have a lower dimensionality because the solutes do not vary independently; rather, the possible ratio of solutes to one another is determined by their ratios in the end members.

PCA is based on an eigenvalue analysis of the correlation matrix². New variables, which are linear combinations of the solutes, are defined in such a way that the first variable explains the largest variation in the data; the second variable explains the next largest, and so forth. In the analysis of streamwater solution, the first variable typically explains 50 percent or more of the variation, and the first few variables normally explain the vast majority of the variation. For example, at the Panola Mountain Research Watershed in Georgia, the first variable explained 82.4 percent of the variation in a six solute-data set; the second, 11.5 percent; the third, 3.1 percent; and the sixth variable explained only 0.5 percent of the variation in the data. Thus, by retaining only two variables, nearly 94 percent of the variation in the data was captured, even though the data set was defined by six solutes.

¹. More precisely, the mixture does not span the $n-1$ dimensional vector space where each axis is defined by one solute. Throughout this discussion, the n end members are assumed to be linearly independent.

². Any symmetric matrix may be used, but for analyzing streamwater where a large range in variation occurs across solutes, the correlation matrix should be used. For a more complete discussion on the choice of symmetric matrix, see Christophersen and Hooper (1992).

At least $p+1$ end members are required to reproduce the amount of variation in the data captured by p principal components³. For example, three end members can reproduce at most 93.9 percent of the variation in the streamwater data at Panola Mountain.

Once the decision is made as to the number of principal components to retain⁴, these principal components, which are orthogonal to each other, form the basis for a new coordinate system (a Euclidean vector space), which will be called U-space. For a streamwater observation to be explained as a mixture of end members, it is a necessary and sufficient condition that the end members lie in U-space and bound the observations, in the sense that the concentrations are more extreme than the mixture. It is likely that the end members, often defined as the median concentration of soil-water and ground-water solutions, do not lie in U-space. An end-member solution that is within U-space, but that has the smallest change from the original end member, can be calculated⁵.

Christophersen and Hooper (1992) recommend the following five steps to construct a mixing model:

1. construct linear plots of every pairwise combination of solutes (mixing diagrams) containing streamwater observations and potential end members (ground-water and soil-water solutions);
2. perform a PCA on the streamwater data to determine the number of end members;
3. project potential end members into U-space defined by the streamwater PCA;
4. chose the set of end members whose orthogonal projections best bound the streamwater observations and are closest to U-space. Compare the chemistry of the orthogonal projection of the projected end members to the original end members. Differences may indicate spatial variability in the end-member composition or reactions occurring that violate simple mixing-model assumptions;
5. perform EMMA (that is, the forward analysis) using the orthogonal projections of the end members to determine their ability to reproduce streamwater observations. Poor prediction indicates that a mixing model may be inappropriate or that additional characterization of the site may be necessary.

³. The different number arises because the vector of mean concentrations is subtracted from the data in calculating the correlation matrix. If the data are uncentered, then the number of end members and principal components are the same.

⁴. Although objective criteria for this decision have been proposed (for example, Preisendorfer and others, 1981), generally, the number of principal components selected to be retained is based upon the marginal gain in variation explained by retaining an additional principal component relative to the variation already explained. For the analysis described, this decision is not critical. The amount of variation explained by the principal components retained is the upper bound of the variation that can be explained by the mixing model.

⁵. That is, the orthogonal projection of the original end member. Mathematically, this is given by the following expression

$$\mathbf{b}_j^* = \mathbf{b}_j \mathbf{V}^T (\mathbf{V} \mathbf{V}^T)^{-1} \mathbf{V}$$

where \mathbf{b}_j^* is the orthogonal projection of the end member solution vector, \mathbf{b}_j is the original end member, \mathbf{V} is the matrix of eigenvectors, and \mathbf{V}^T is the transpose of \mathbf{V} .

APPLICATION OF THE ALPINE LAKE FORECASTER TO FOUR ALPINE WATERSHEDS

This application of the model was intended to investigate the relevance of the hydrogeochemical formulation in ALF, which was derived from the Emerald Lake data, to the other lake watersheds and to determine if sufficient data exist to apply ALF to these watersheds. Discharge and chemical data used in the application of ALF are from Sickman and Melack (1989).

Approach

The mechanism for generating acid neutralizing capacity (ANC) in ALF is primary mineral weathering that consumes hydrogen ion (H^+) and produces base cations (SBC, which includes Ca^{2+} , Mg^{2+} , Na^+ , and K^+) and dissolved silica (SiO_2) by the stoichiometry of reaction 1. Because weathering is kinetically controlled, the residence time of water in the system is another factor affecting the concentration of solutes in surface water released by this reaction. Therefore, it was necessary to calibrate the weathering ratio, K (eq. 2), using some measure of residence time. The "best" measure of residence time for Emerald Lake was the 10-day average discharge prior to sampling. This measure was determined by comparing regression models relating K to a variety of time averages for the discharge prior to sampling. The "best" of these relations was determined on the basis of variance explained and analysis of residuals.

To test the applicability of ALF to the Pear, Ruby, Topaz, and Crystal Lake watersheds, regression models relating SBC to SiO_2 and ANC were developed for the data available for each lake. All data for a given lake were combined in an initial analysis, and models were developed using data from individual sampling sites within each watershed. These regression models were evaluated with respect to the basic geochemical formulation in ALF.

Geochemical Results

The results for all data for Crystal Lake indicate that, although SBC is highly correlated with ANC, SBC has no apparent relation to SiO_2 (fig. 6). However, three inlets were sampled at Crystal Lake, and, although little data exist for each separately, the analysis of combined data from the three inlets is consistent with the formulation in ALF (fig. 7). This result indicates that in-lake processes, which are not included in ALF, may be differentially removing more SiO_2 than SBC. To examine this hypothesis, SiO_2 and SBC concentrations were plotted for those dates when both inflow and outflow samples were available (fig. 8). Although for some combinations of inflow and outflow samples there is a decrease in SiO_2 concentration and little change in SBC, not all combinations exhibit this pattern.

On three occasions when five inflow samples having low SBC concentrations were collected (May 25, June 4, and June 10, 1988), the outflow samples had a higher SBC concentration and the same or lower SiO_2 concentration than the inflow samples. Temporal differences in the size of the decrease in SiO_2 concentration also occurred; the largest decreases occurred on October 11, 1986, May 25, 1988, and June 4, 1988. On June 10, 1988, SBC concentration increased, and little change occurred in SiO_2 . The chemistry between the inflow and outflow was unchanged on July 9, 1988. These temporal patterns may be related to phytoplankton blooms. In 1988, the ice cover rapidly melted in late May, and was completely gone on June 1; thus, the light levels probably increased in the lake (Sickman and Melack, 1989, p. 80). However, chlorophyll data during this period which would have allowed a more definite conclusion to be made were not collected. Regardless of the precise process, evidence exists that processes occurring within Crystal Lake can substantially change the major ion chemistry of the water, whereas such processes were not evident for Emerald Lake.

The results of the analysis of all data for Ruby Lake are consistent with ALF, but these regressions are controlled mainly by the inclusion of data from the Mono Pass inlet, which correspond to the four high SBC values shown on figure 9. However, the regression results for the 1-m depth sampling location in the lake, the outflow, and the combined inlets produce comparable results, although the ranges in SBC for the lake and outflow are smaller than for the combined inlets (fig. 10).

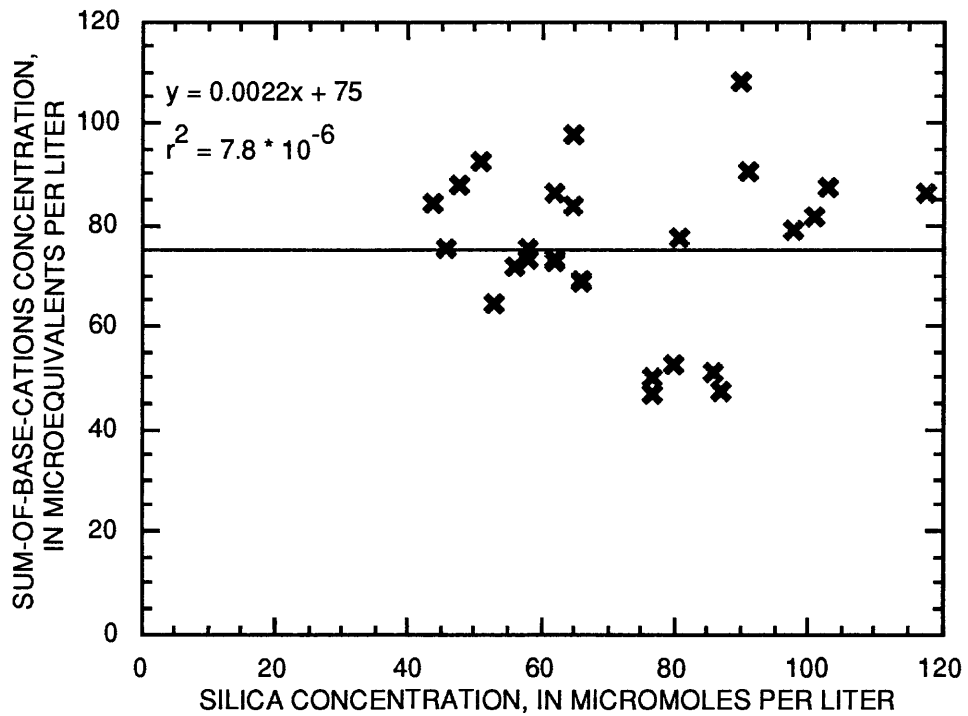
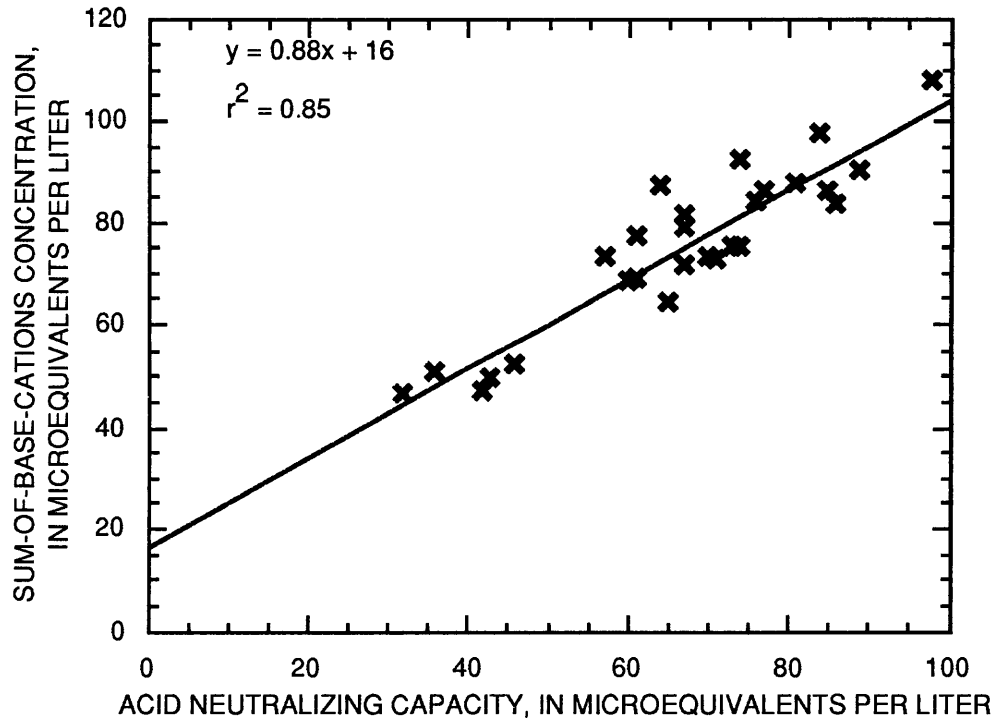


Figure 6.—Relation between sum-of-base-cations concentration and both acid neutralizing capacity and silica concentration for inlet and lake samples at Crystal Lake.

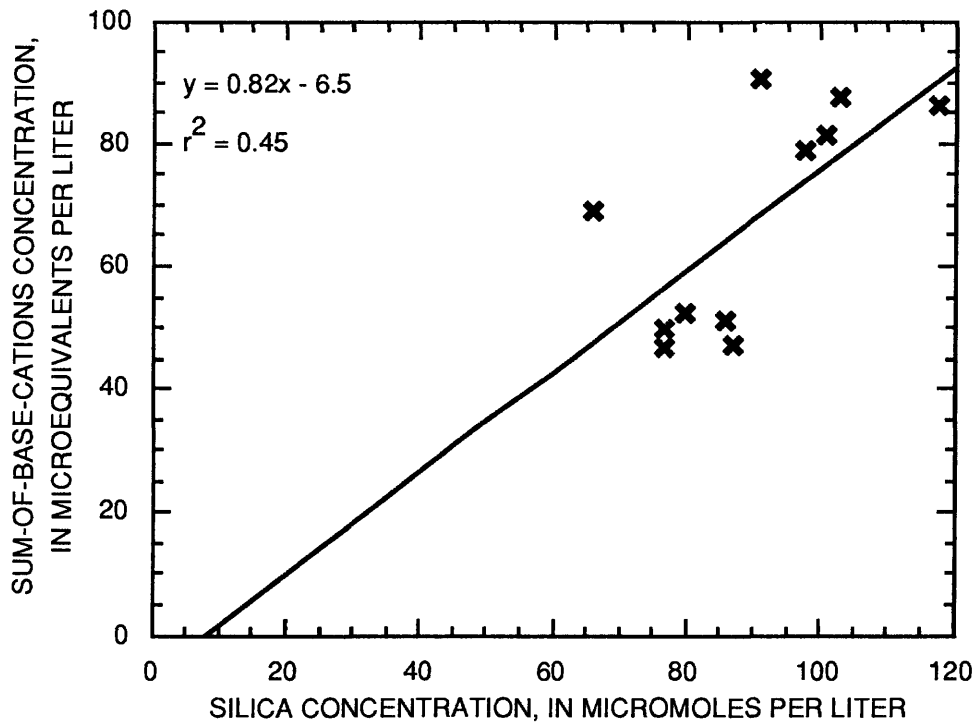
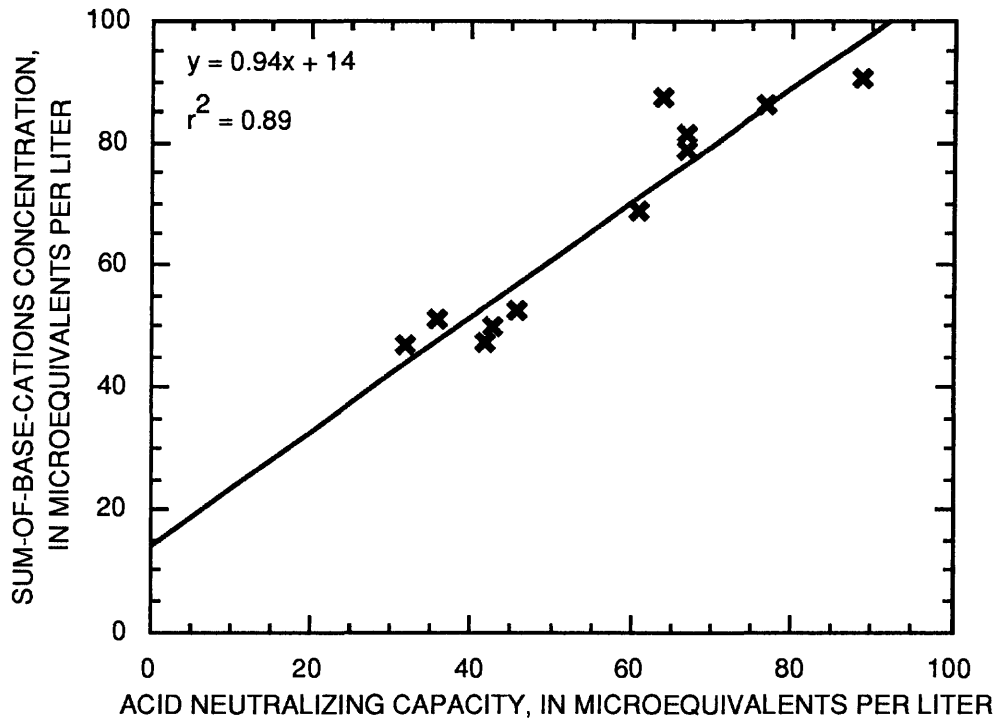


Figure 7.—Relation between sum-of-base-cations concentration and both acid neutralizing capacity and silica concentration for the combined inlets at Crystal Lake.

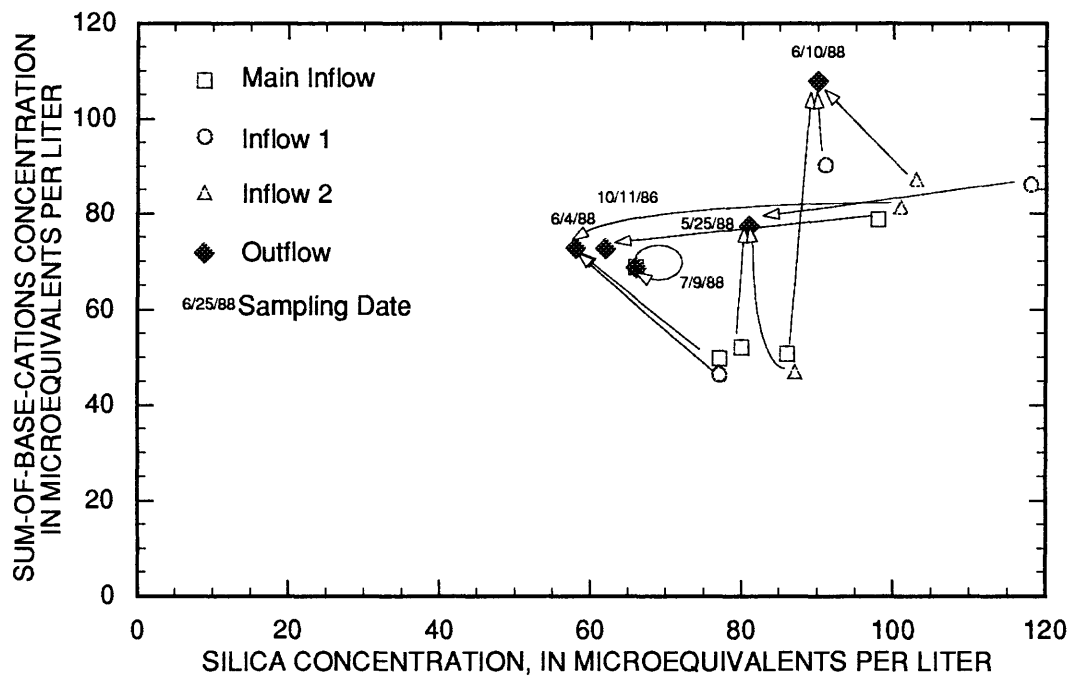


Figure 8.—Relation between silica and sum-of-base-cations concentrations in inflow and outflow samples at Crystal Lake on various sampling dates.

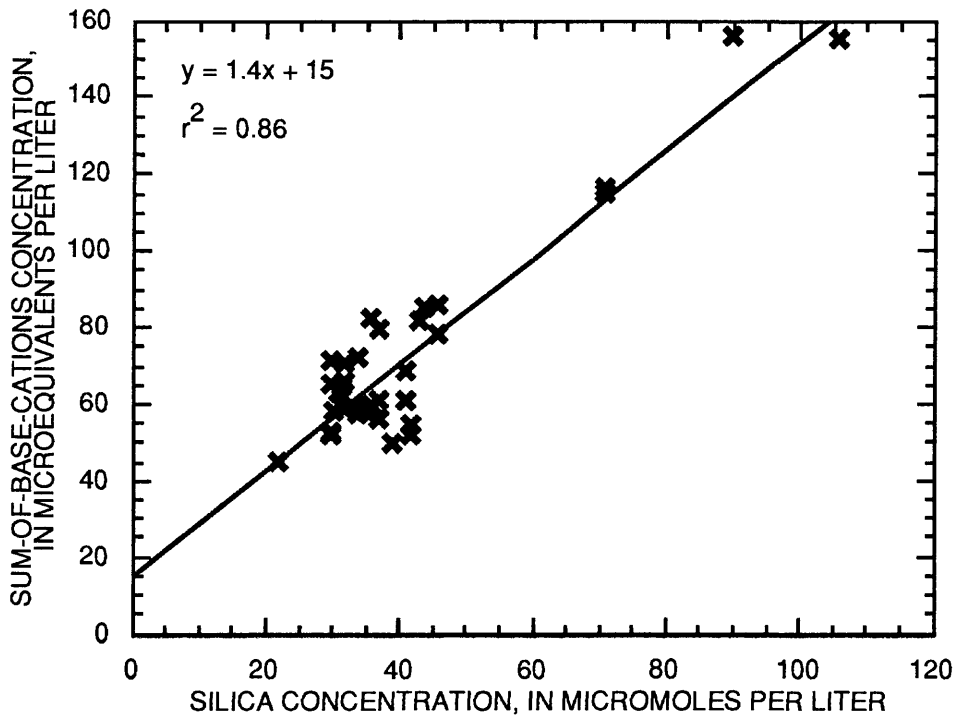
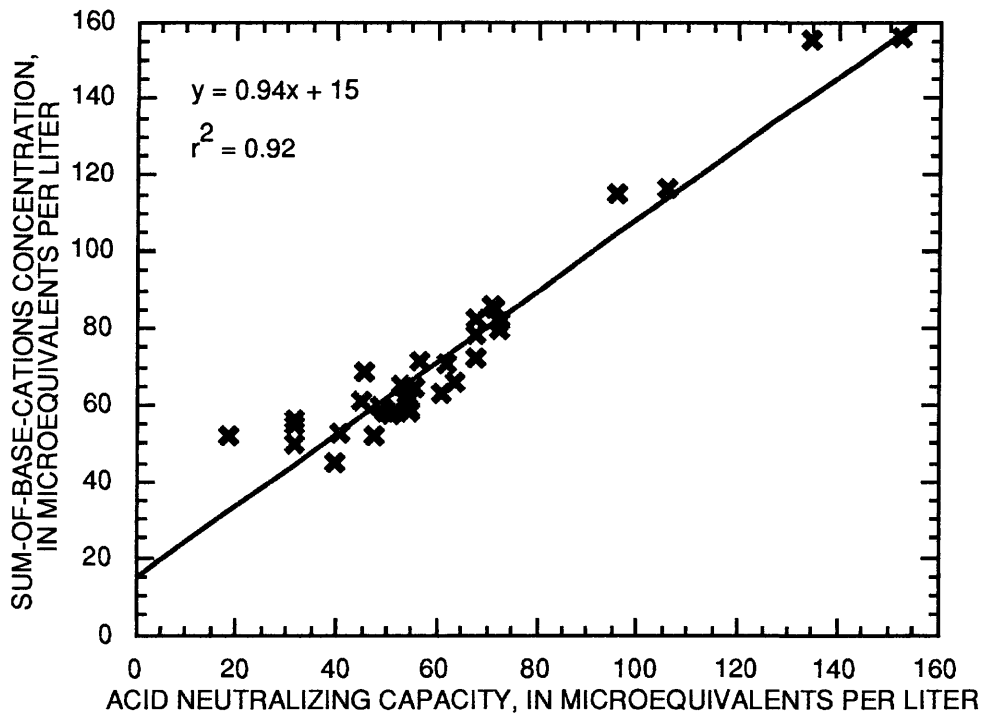


Figure 9.—Relation between sum-of-base-cations concentration and both acid neutralizing capacity and silica concentration for Ruby Lake.

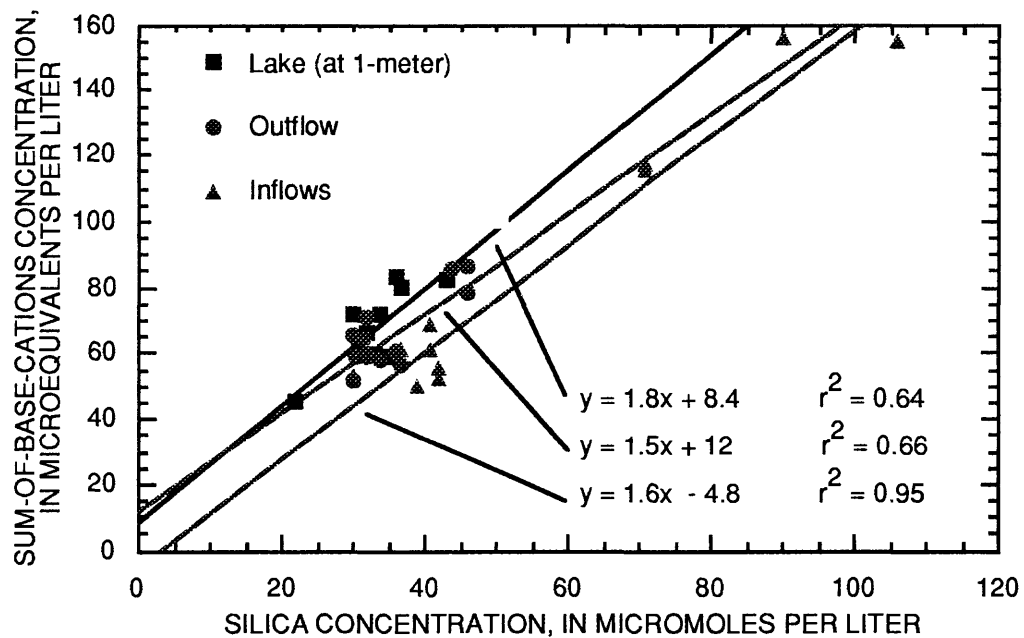
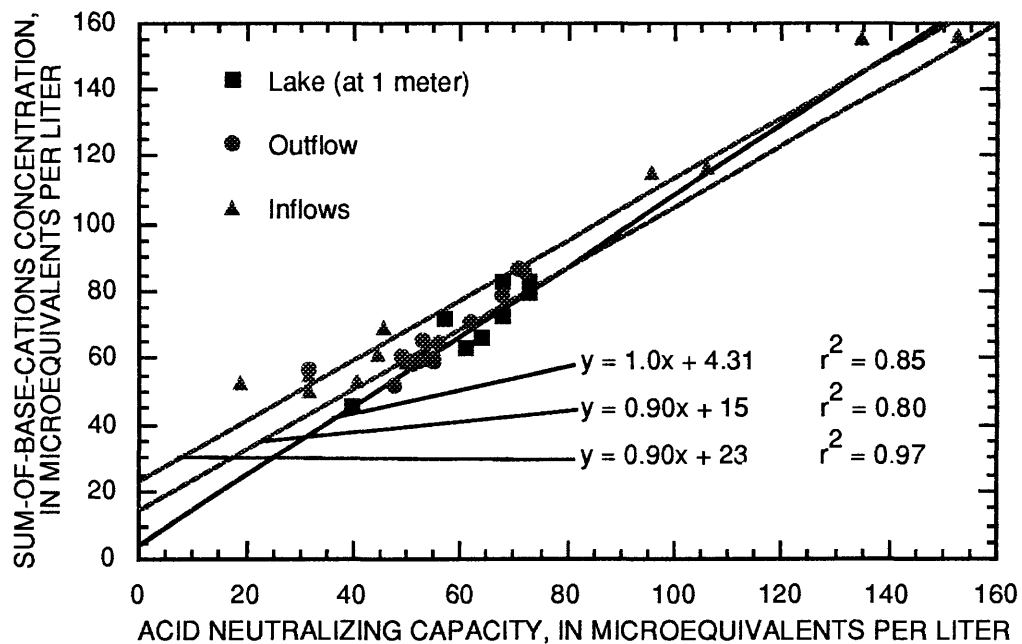


Figure 10.—Relation between sum-of-base-cations concentration and both acid neutralizing capacity and silica concentration for the 1-meter sampling site in the lake, the outflow, and combined inlets, Ruby Lake.

Results of the regression analyses of data from Topaz Lake were consistent with the ALF formulation (fig. 11). The slope of the regression of SBC on SiO_2 for Topaz Lake was similar to that for Emerald Lake, although the intercept was considerably higher. Furthermore, the intercepts of the regression of SBC on SiO_2 for Ruby, Topaz, and Crystal Lakes, in general, were 10 times higher (10-20 $\mu\text{eq/L}$) than that for Emerald Lake ($\sim 2 \mu\text{eq/L}$). The intercept was expected to be comparable to the SBC in precipitation (corrected for evaporation). Because all lakes were expected to receive precipitation of comparable quality, the higher intercepts may allude either to an additional source of base cations, such as cation exchange, or a nonlinear relation between SBC and SiO_2 .

Pear Lake differs from Ruby, Crystal, and Topaz Lakes in that ANC was not controlled by SBC (fig. 12). The range of SBC concentration is much smaller than the range in ANC concentration in Pear Lake. At the other lakes, the concentrations have approximately the same range. The two high ANC values have high particulate carbon concentrations—approximately 200 and 300 $\mu\text{mol/L}$ (Sickman and Melack, 1989, p. 80)—a correlation indicating control of ANC by biological, rather than geochemical processes. Even if these two high ANC values are removed from the analysis, the relation between SBC and ANC remains weak (fig. 13). The slope of the regression line relating the two solutes also is far from 1.0, unlike the regression lines relating SBC and ANC for the other lakes.

The particulate carbon concentration in water from Pear Lake is unusually high for an alpine lake underlain by relatively unreactive bedrock (Wetzel, 1975). These high concentrations have been attributed to infrequent lake turnover because of the depth of the lake relative to the watershed area (J.M. Melack, University of California, Santa Barbara, oral commun., 1991). The relation between ANC and SBC for the inlet is consistent with ALF, but this result is based on only three observations. It may be appropriate to use ALF for the terrestrial part of the watershed, but the model would be unable to predict lakewater chemistry because of the unusual geomorphometry of Pear Lake.

Evaluation of Residence-Time Formulation

The next step in the analysis was an evaluation of the relation between the weathering ratio (K) and daily mean discharge (Q) to determine if K is a function of Q at these sites. The SBC power term in the weathering reaction (eq. 2) was set equal to the slope of linear regression line between the SBC and SiO_2 for each site. For Crystal Lake, the slope was determined from the relation for combined inlet data. For Ruby and Topaz Lakes, the slopes were determined from the relation for all data. Plots and regressions of the log of the weathering ratio on discharge were produced for each site (figs. 14-16).

Few high-flow samples were collected on these lakes, and discharge was not available for some observations. The relations between K and Q generally are poor with the possible exception of the relation for Topaz Lake. The lack of high-flow data to generate this relation precludes the application of ALF to these sites with any degree of confidence. Additional sampling under a broader range of discharges is needed. If the relation between K and Q were to remain weak even with additional high-flow samples, this would indicate that the mineral surfaces in contact with the water are different under high-flow than under low-flow conditions.

Discussion

The generation of alkalinity by rock weathering seems to be applicable to Ruby, Topaz, and Crystal Lakes, but not applicable to Pear Lake. Other processes that affect alkalinity seem to dominate at Pear Lake. For the remaining three lakes, the stoichiometric relations for SBC and SiO_2 , which are needed to calibrate ALF, are not as good as those determined for the Emerald Lake data.

In addition, the calibration of the weathering ratio as a function of discharge is more uncertain for Ruby, Topaz, and Crystal Lakes than for Emerald Lake. In particular, the lack of samples during high flow at Crystal Lake may produce too much uncertainty in the formulation for ALF to be used effectively with these data. However, the analysis indicates that data from Ruby Lake and Topaz Lake are consistent with the ALF formulation and may be the most amenable to its application.

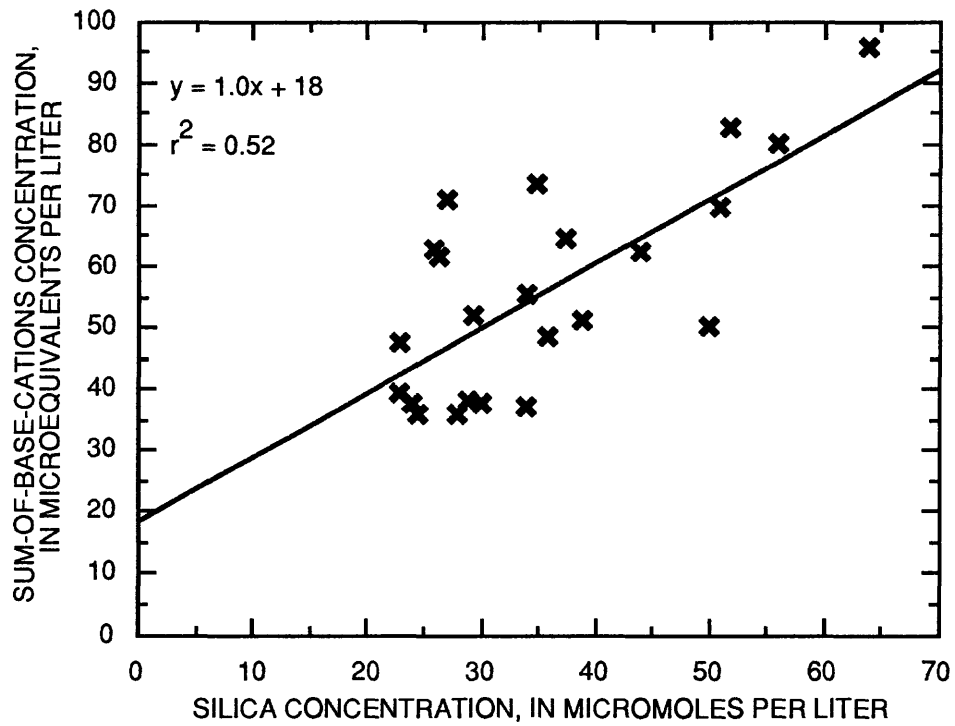
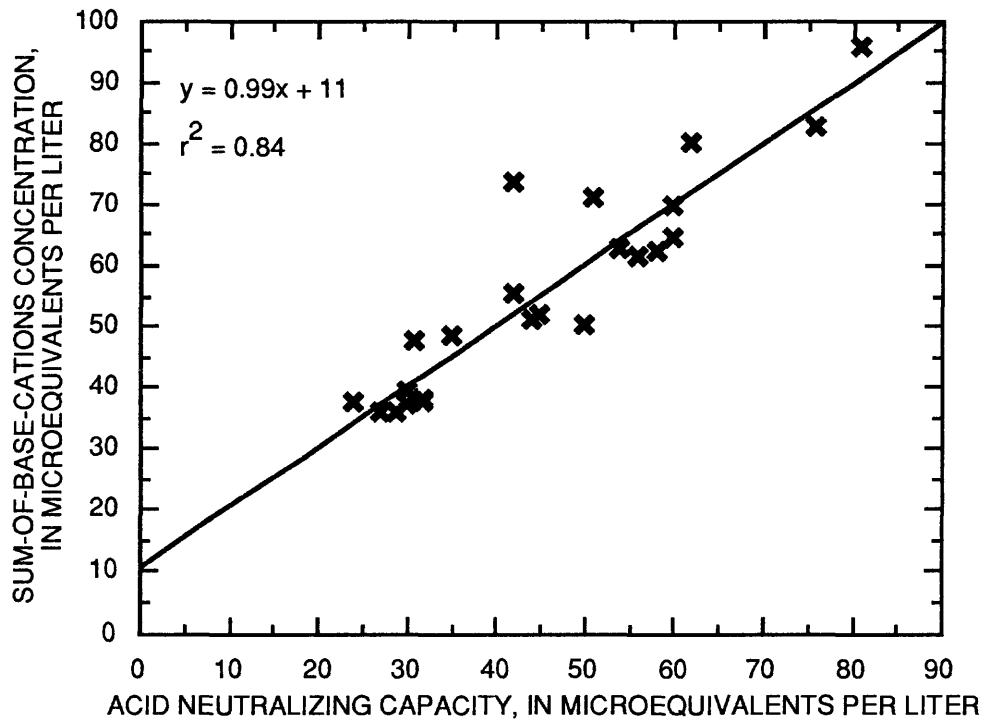


Figure 11. —Relation between sum-of-base-cations concentration and both acid neutralizing capacity and silica concentration for all data at Topaz Lake.

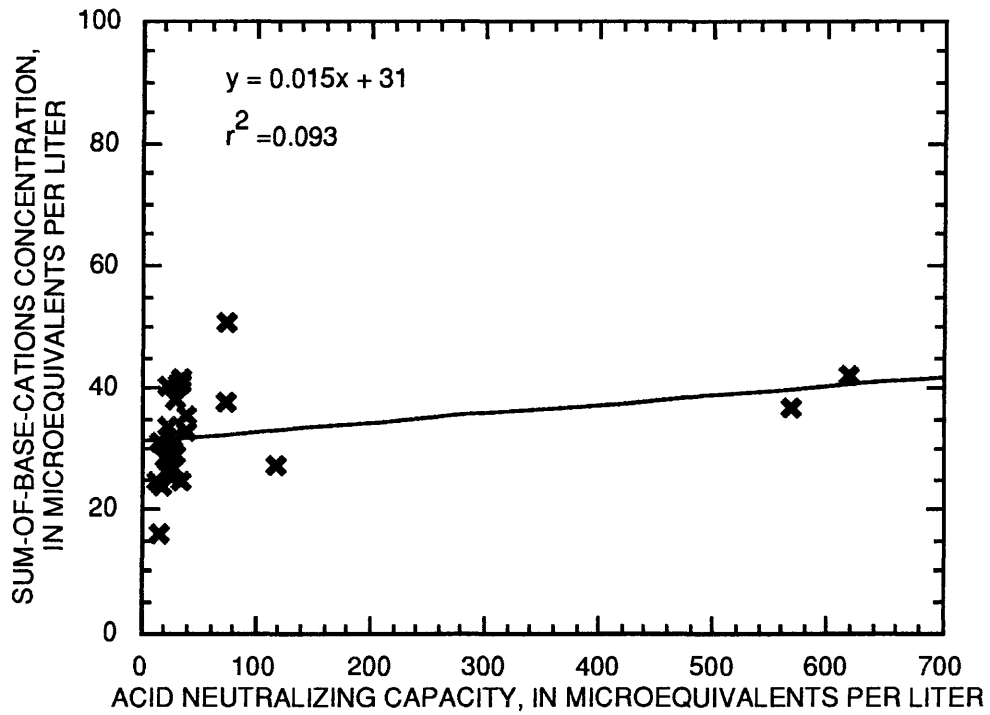


Figure 12.—Relation between sum-of-base-cations concentration and acid neutralizing capacity at Pear Lake.

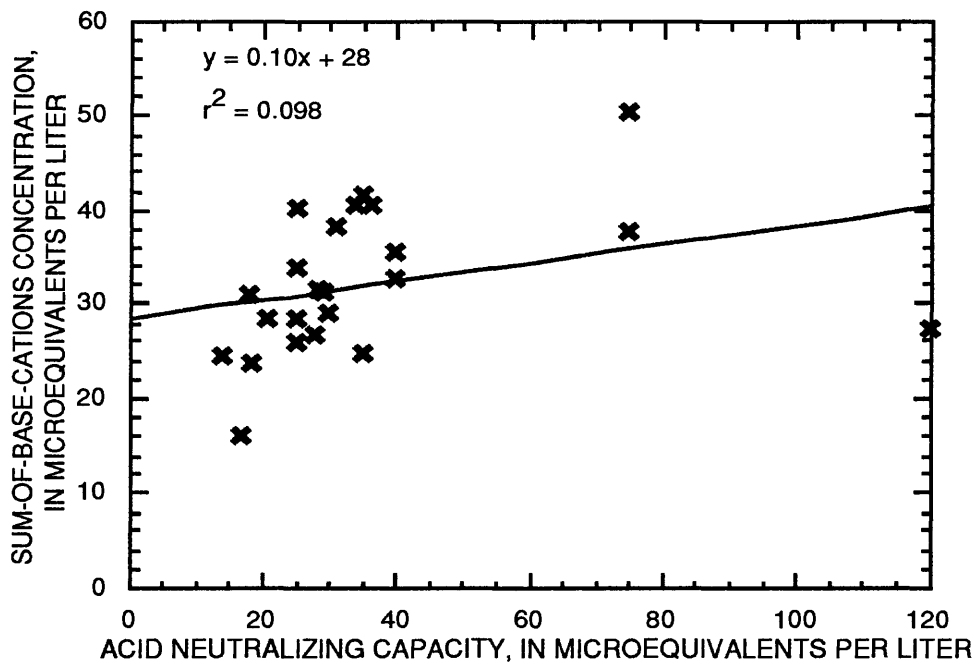


Figure 13.—Relation between sum-of-base-cations concentration and acid neutralizing capacity at Pear Lake, excluding two samples with high acid neutralizing capacity.

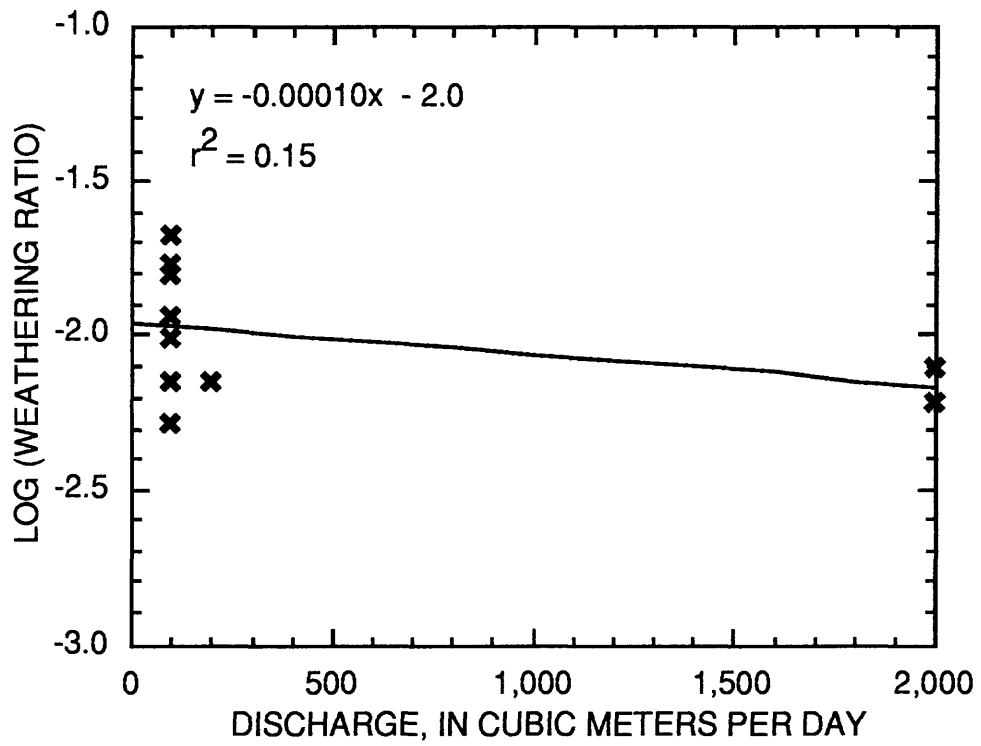
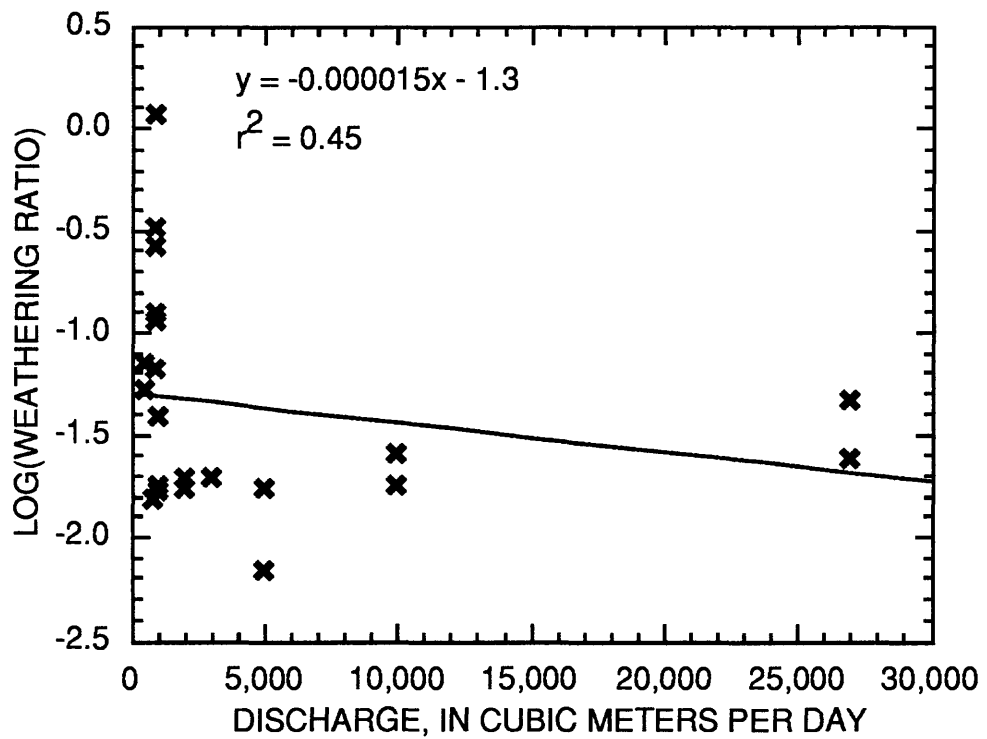


Figure 14.—Relation between the weathering ratio (K) and daily mean discharge for Crystal Lake.



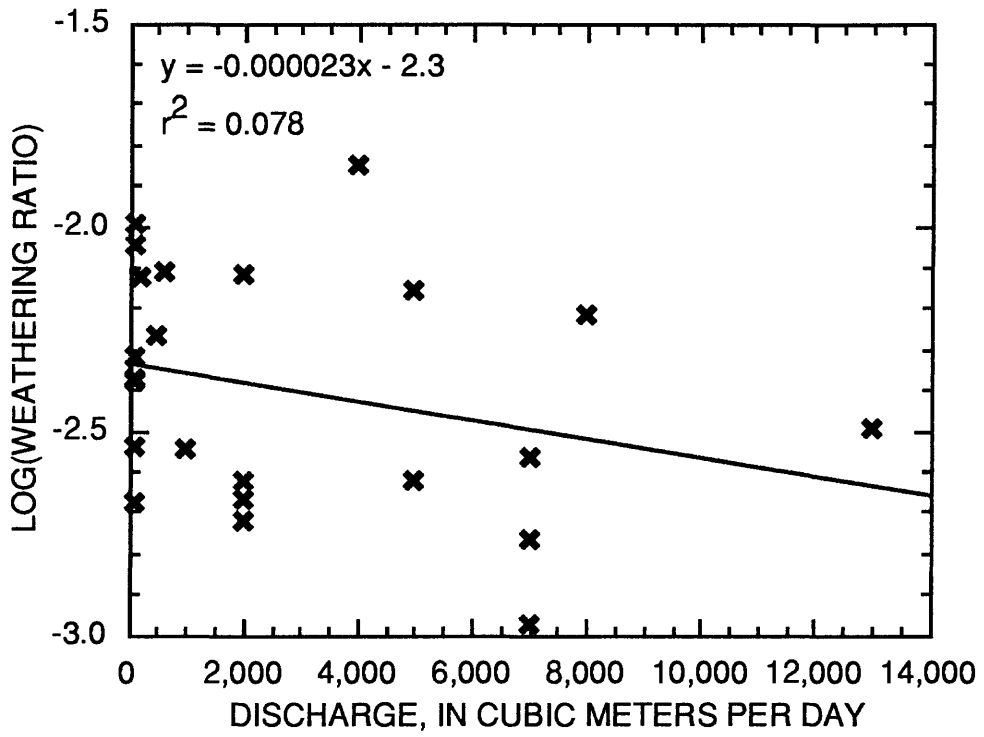
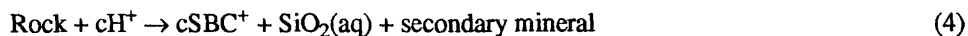


Figure 16.—Relation between the weathering ratio (K) and daily mean discharge for Topaz Lake.

SENSITIVITY ANALYSIS OF THE ALPINE LAKE FORECASTER

As stated in the "Background" section, the hydrologic module of ALF does not contain adjustable parameters, and, therefore, the issue is the accuracy of its formulation, particularly the distributed melt algorithm rather than its sensitivity to parameter values. This verification can best be done by using an energy-based distributed melt model, such as that under development by Dozier (1988); however, that model was not available for comparison. Therefore, the focus of the sensitivity analysis of ALF presented in this section is on the chemical formulations in the model. The data used for the sensitivity analysis is that collected at the Emerald Lake watershed and used in the initial development of ALF.

Reaction 1 was generalized to the form



where the stoichiometric coefficient, c , could be varied. Four additional values for c , 0.0, 0.1, 0.5, and 1.0, were evaluated in addition to the original value of 1.2, which was obtained from the regression model relating SBC and SiO_2 concentration.

The model code was altered to allow the stoichiometric coefficient to vary. This influenced the governing equations and the jacobian matrix necessary for implementation of the modified Newton's method. In addition, new regression models relating the weathering ratio, K (eq. 2), to the 10-day average discharge of the form

$$K = a10^{bQ'} \quad (5)$$

were developed where Q' is the 10-day average discharge. These models and their statistics are presented in table 3; the data and best-fit line for these models are shown in figure 17. Data for these models are the same as those used for the original calibration of ALF, namely samples collected during snowmelt, May through September 1986, from the inlets to Emerald Lake.

Table 3.—*Statistics of regression models relating weathering ratio and 10-day average discharge*

| Stoichiometric coefficient | Intercept | Slope | Variance explained (R^2) |
|----------------------------|----------------------|-----------------------|---------------------------------|
| 1.2 | 8.2×10^{-3} | -4.4×10^{-5} | 0.80 |
| 1.0 | 3.5×10^{-3} | -3.6×10^{-5} | .75 |
| .5 | 3.7×10^{-4} | -2.3×10^{-5} | .74 |
| .1 | 6.1×10^{-5} | -1.3×10^{-5} | .62 |
| .0 | 3.9×10^{-5} | -1.0×10^{-5} | .52 |

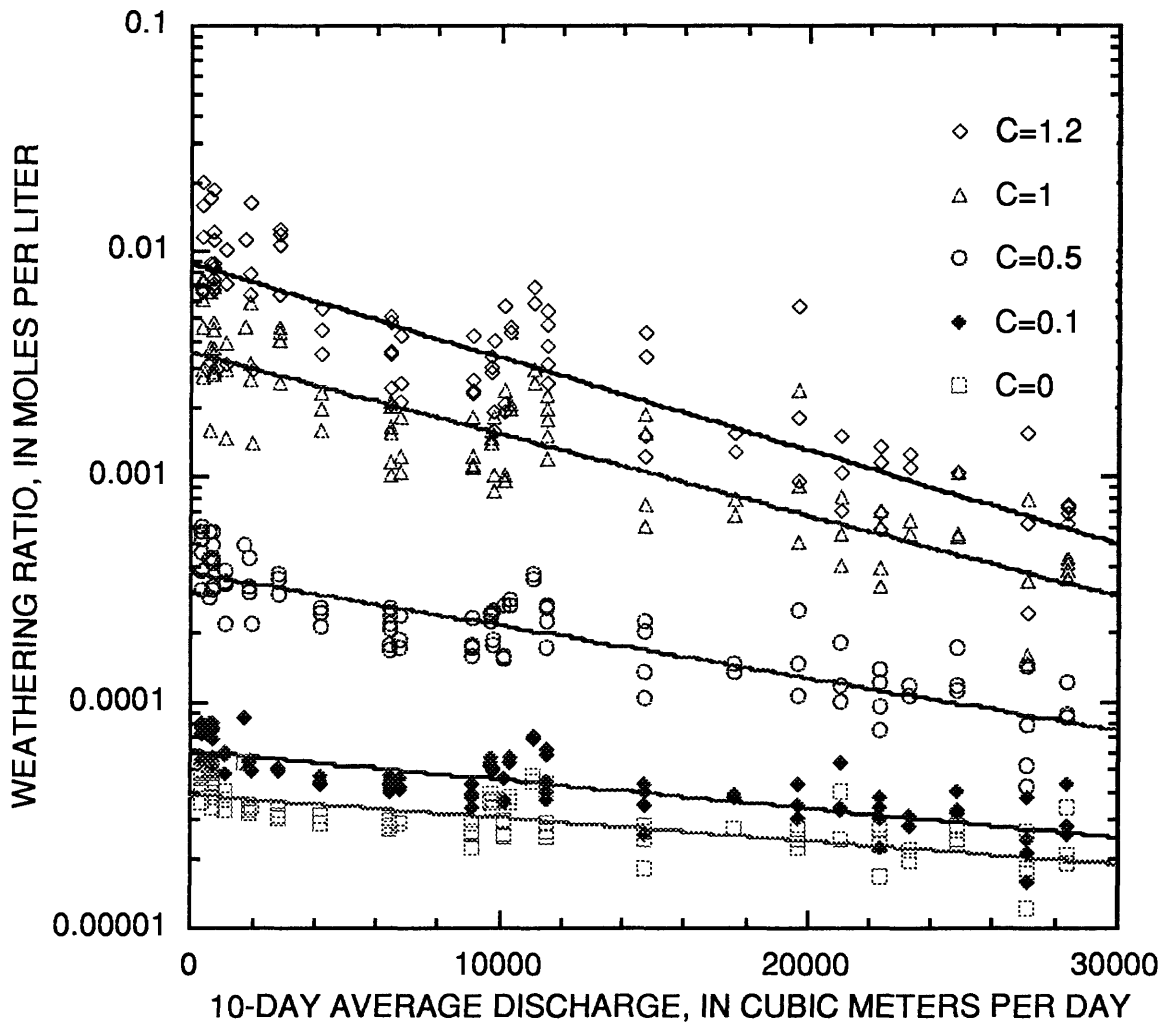


Figure 17.—Relation between weathering ratio and 10-day average discharge for a range of stoichiometric coefficients.

To assess the influence of the stoichiometric coefficient, alkalinity concentrations for the main inlet to Emerald Lake in 1986 were calculated using ALF (fig. 18). These calculations were made using a 40/20 solute release rule with a maximum concentration factor of 3. This release rule provided the best fit for the 1986 data. For coefficients greater than 0.5, the usual pattern of an acidic pulse followed by a dilution pulse was observed. For the two lowest coefficients, the streamwater had negative alkalinity, which slowly increased as the increasingly dilute meltwater drained from the snowpack. The change in calculated alkalinity between coefficients of 1.2 and 1.0 was slight; the model predictions changed substantially only when the coefficient was reduced to 0.5 or less. The three “spikes” in alkalinity seen in figure 18 are associated with rainfall that occurred during the melt period.

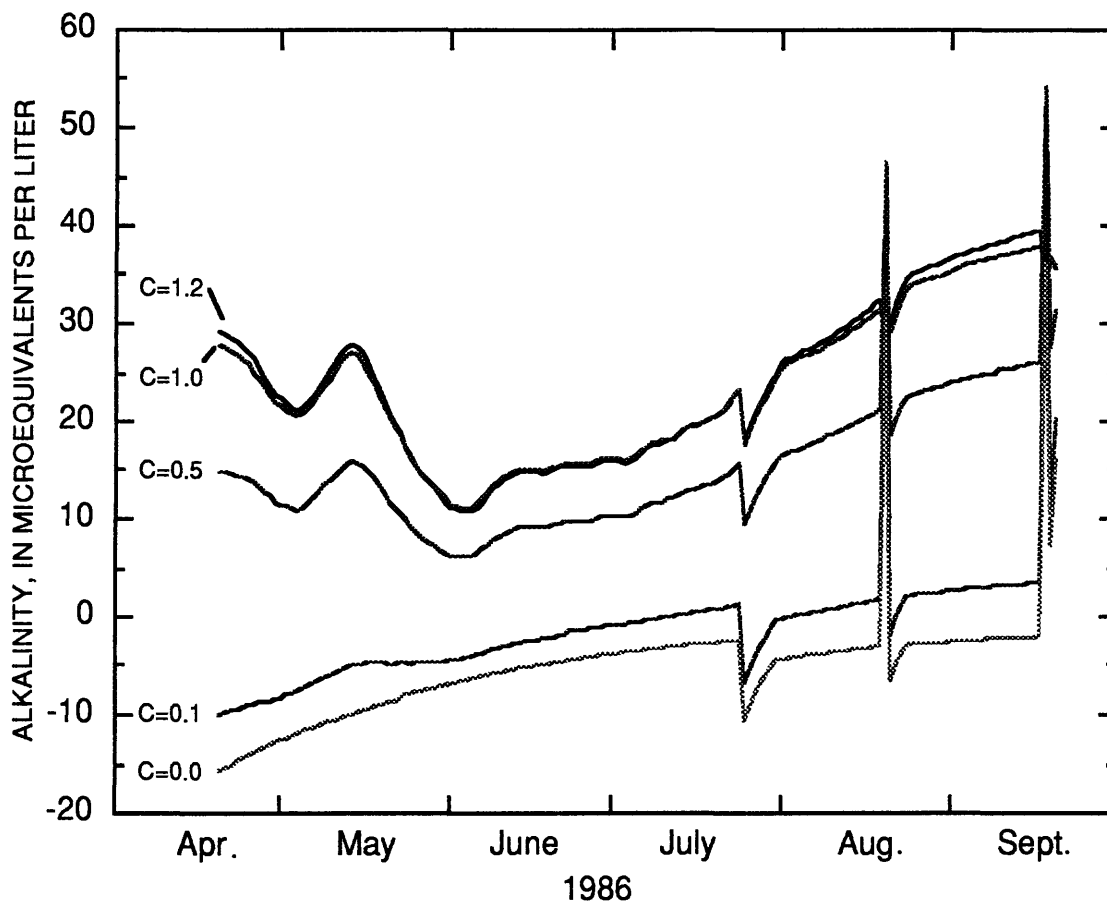


Figure 18.—Calculated alkalinity for an inlet to Emerald Lake during 1986 for a range of stoichiometric coefficients (c).

Physically, the stoichiometric coefficient is related to the mineralogy of the rock. The larger the proportion of readily weatherable minerals (for example, hornblende) contained in the granite, the higher the coefficient will be. Alternately, if the granite is more silicic (containing, for example, a high proportion of quartz) the coefficient becomes lower. Watersheds that have substantially more silicic bedrock than Emerald Lake could be expected to have lower alkalinity streamwaters and to be more sensitive to acidic inputs.

The stoichiometric coefficient may be utilized to predict the sensitivity of other watersheds in the Sierra Nevada that have hydrologic regimes similar to that at Emerald Lake. The relation between silica and SBC can be evaluated under a range of flow conditions for the outlet. If the slope of the regression model is about 1.0, the watershed should have about the same sensitivity as the Emerald Lake watershed. If less than 1.0, it is more sensitive (fig. 18).

The stoichiometric coefficient does not reflect the kinetics of primary weathering nor how the kinetics will be influenced by greater hydrogen ion concentrations. The “equilibrium” formulation of ALF assumes a linear response with increased deposition; the more acid added, the more SBC and alkalinity that must be generated to maintain the weathering ratio. The equilibrium formulation is consistent with laboratory experiments using soils from Emerald Lake, which demonstrated that the “long-term” weathering kinetics (after readily soluble aluminum minerals have been depleted) followed an approximately linear rate law with respect to hydrogen ion (Brown and Lund, 1991). Other studies have demonstrated a sub-linear response with the reaction kinetics related to hydrogen ion only to the 0.8 power (Asolekar and others, 1991). Therefore, when predictions are generated under much higher hydrogen ion loadings, ALF may overstate SBC and SiO_2 production and understate the loss of alkalinity. It must be emphasized that the stoichiometric coefficient is not related to the dependence of the weathering kinetics on hydrogen ion concentration, but is related only to the mineralogy of the rock.

ANALYSIS OF STREAM TRANSECT DATA

ALF can be used to identify and quantify important chemical reactions affecting meltwater and precipitation. Although a possible set of reactions have been identified that are consistent with the watershed inputs and outputs, a more precise identification can be made by analyzing streamwater and soil solutions from the catchment. Synoptic surveys of streamwater chemistry at eight sites along the major inflow to Emerald Lake (referred to as the transect data set) were conducted as part of the Integrated Watershed Study (fig. 19). Details of sampling procedures, chemical analysis techniques, and quality assurance protocols are contained in reports by Lund and others (1987) and Brown and others (1990).

Generally, the concentration of weathering products (for example, dissolved silica and base cations) would be expected to increase as the contact time of water and rock increases. In watersheds, that expectation translates into higher concentrations of weathering products in streamwater low in the watershed, where the water has, on average, a longer residence time than it does in more elevated areas of the watershed. At Emerald Lake, however, this pattern is not evident as neither SBC (fig. 20) nor silica (fig. 21) exhibit a tendency toward higher concentrations downstream, either on average or on individual sampling dates. The only pattern that emerges is one of greater or lesser variability at the various sampling locations.

Possible explanations for the lack of a systematic increase in concentration for weathering products include the following:

- Streamwater is being diluted continually by water having a shorter residence time as it flows toward the lake;
- Streamwater does not exhibit hydrologic continuity over its entire length. Rather, over the series of soil benches the stream crosses, it is alternately gaining water from local soils (having shorter residence time, and then losing water to soils or bedrock fractures; and
- Biogeochemical processes occur that utilize the weathering products. For example, diatoms can utilize silica, and the base cations can be utilized by phytoplankton and zooplankton.

Determining the processes at work in the Emerald Lake watershed is difficult using the available data. If discharge had been measured along the entire course of the stream from the headwaters to the lake, however, it might have been possible to calculate mass fluxes to determine if solute mass were actually lost. Also, greater hydrogeological characterization could identify gaining or losing reaches of the stream.

Despite the limitations of the data, the transect data indicate that modeling the watershed as a simple series of connecting landscapes, one feeding into the next, connected by a stream where chemical reactions do not take place, is not applicable. A reliable deterministic representation of hydrologic flowpaths through the catchment, as contained in the ILWAS model (Chen and others, 1983), requires better hydrologic characterization of Emerald Lake than is currently available. An alternate approach to determine flowpaths is considered in the following section.

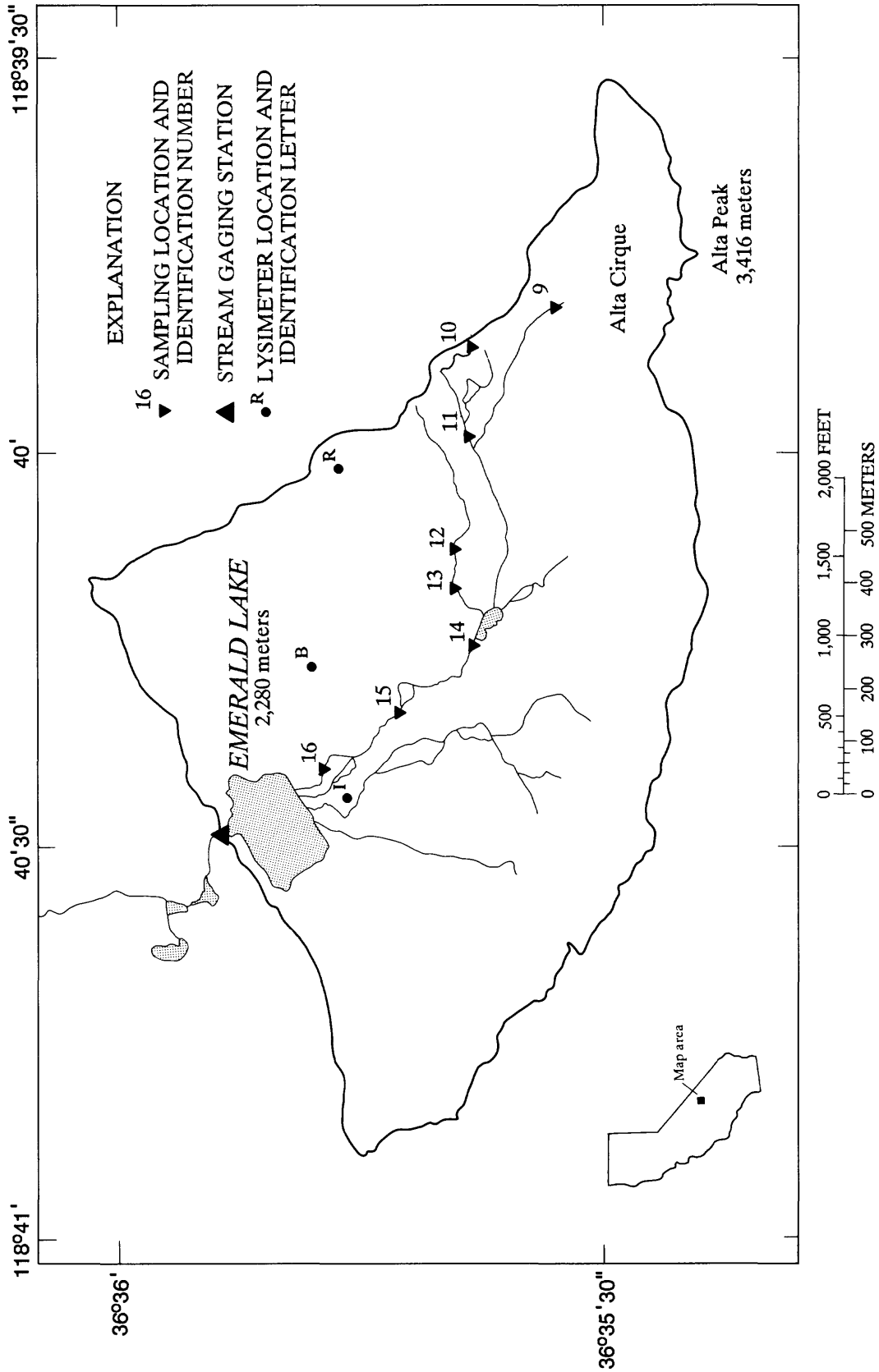


Figure 19.—Location of stream and lysimeter sites sampled along a major inlet to Emerald Lake.

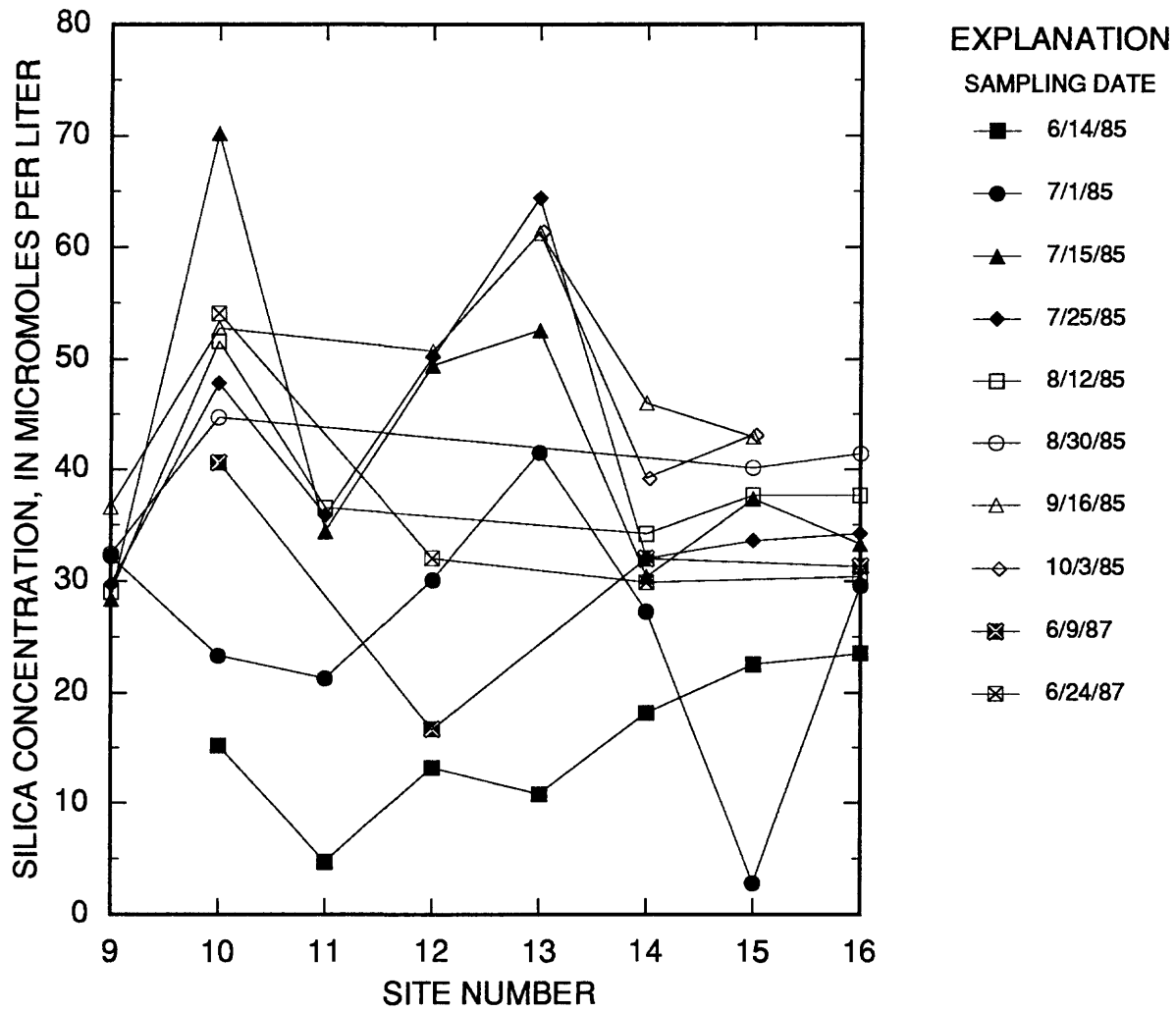


Figure 20.—Silica concentration along the major inflow to Emerald Lake on various sampling dates.

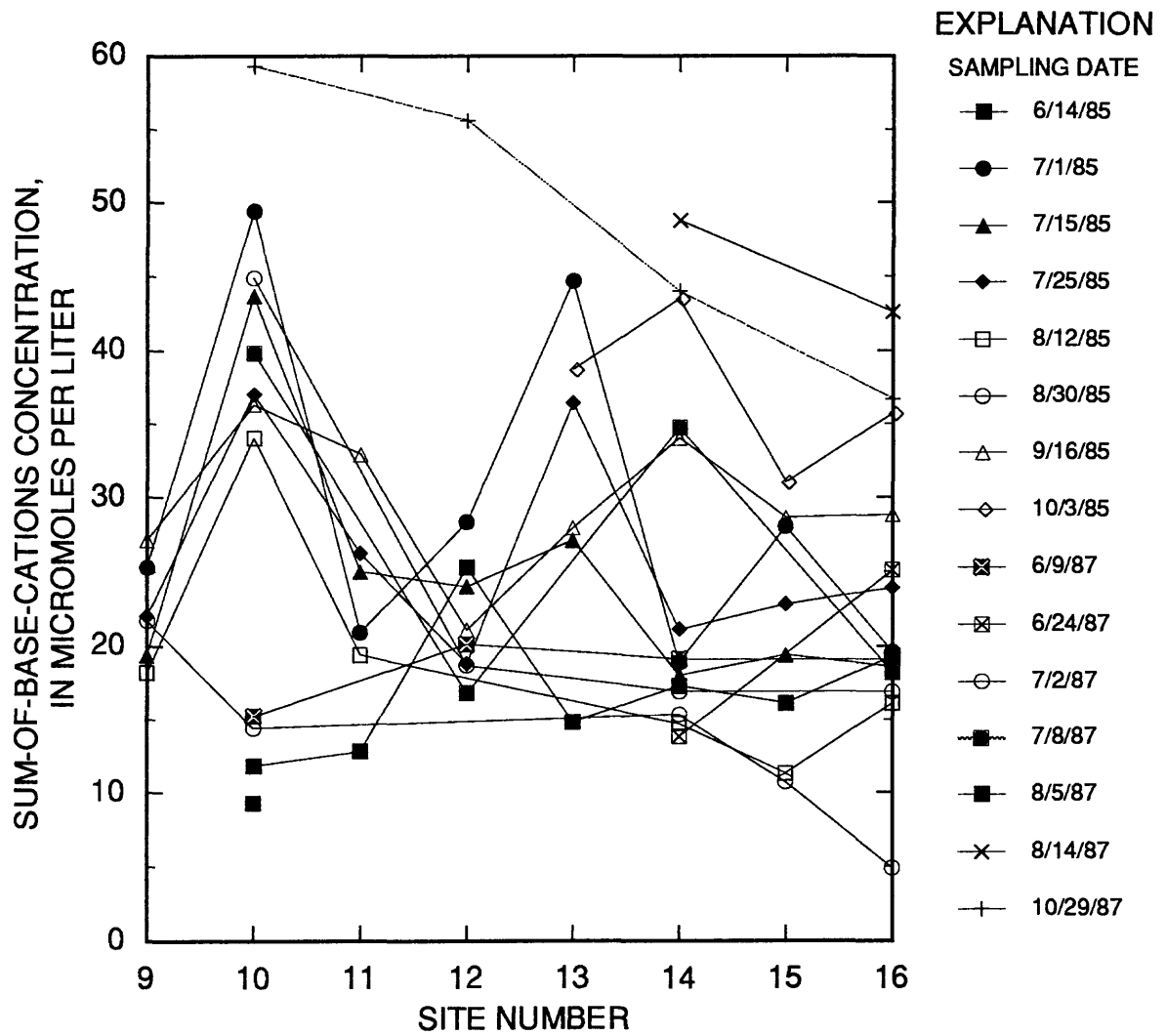


Figure 21.—Sum of base cations concentration along the major inflow to Emerald Lake on various sampling dates.

MULTIVARIATE SOIL-SOLUTION MIXING MODEL

Soil-solution data collected at two depths at three locations in the Emerald Lake watershed: the inlet meadow, the bench meadow, and the ridge site (fig. 19). Soil solutions collected during 1985 were excluded from this analysis because of soil disturbance caused by the lysimeter installation that year. Details of sampling procedures, chemical analysis techniques, and quality assurance protocols are contained in reports by Lund and others (1987) and Brown and others (1990).

Mixing diagrams were constructed for every pairwise combination of nine solutes—alkalinity, chloride, nitrate, sulfate, calcium, magnesium, sodium, potassium, and silica (figs. 22-57 in the appendix). The streamwater data values were determined from analyses of samples collected from all inlets to Emerald Lake between 1985 and 1988. Soil solutions are represented by the median value of the samples collected during 1986 through 1988 at three sites (designated R for the ridge site, I for the inlet meadow, and B for the bench meadow) at two depths (designated S for shallow and D for deep). Replicate samples at each of these six locations were combined for purposes of calculating the median and the two quartiles (the 25th and 75th percentiles). The quartiles are represented on the mixing diagrams as error bars.

The purpose of the mixing diagrams is to determine whether the soil solutions can be end members for a mixing model. That is, can the medians be connected to enclose the streamwater observations? Connecting three soil-solution medians yields a triangle--four medians, a quadrilateral, and so forth. The values that lie inside the triangle (or quadrilateral) can be explained as a mixture of the end members for those solutes. Mathematically, they are said to lie in the convex set defined by the end members. When more than two solutes are being considered simultaneously, it is a necessary, but not sufficient, condition that the streamwater sample lie in the convex set for each pair of solutes considered (that is, inside the convex set as it appears in the mixing diagrams)⁶. If the streamwater sample is outside the convex set for any pair of solutes, then it cannot be described exactly as a mixture of the solutes.

In analyzing real data, the situation is not so straightforward. Commonly, end members that enclose most of the data for streamwater samples may adequately describe the data, particularly if the values outside the convex set are not too far outside. Furthermore, both spatial and temporal variability exist in the soil solution that is being used as the end member. If that variability is small relative to the variability of the mixture, the use of the soil-solution median as an end member can be justified. Similarly, assessing how different the orthogonal projections of the soil solutions are from the original solutions should be considered relative to the variability of the soil solutions. For example, if the orthogonal projection lies within the quartiles of the soil solution, the orthogonal projection may be comparable to the original.

In evaluating the mixing diagrams (figs. 22 - 57, in the appendix at the back of this report), the most notable feature is the large variability in the soil solution relative to the streamwater. Although the medians for many of the solutes are not significantly different from one another, the median values from the bench meadow, ridge, and inlet meadow sites usually are more different from each other than are the median values from the two different depths. This variability may be the result of the large volume of water flowing through the soil during snowmelt that overwhelms the ability of the soil to regulate the solution concentration. However, not only are the soil solutions quite variable, the median concentration of the soil solutions generally do not enclose the concentration observed in the streams.

Another important feature of these plots is that the calcium concentration in the soil solutions is too low to explain calcium concentrations in many of the streamwater samples. Identifying the source of the calcium in the streamwater is important geochemically and, possibly, hydrologically. It is possible that the calcium comes from ground-water sources which are difficult to sample, such as deep fractures in the bedrock. Alternately, there may be a mineralogic explanation. In Loch Vale, an alpine watershed in the Rocky Mountains, finely disseminated calcite was an important contributor to calcium in the streamwater despite being a minor mineral in granitic bedrock (Mast and others, 1990).

⁶. The sufficient condition is that it lies within the convex set in n dimensions, where n is the number of solutes. The mixing diagrams are two-dimensional projections of the n -dimensional convex set.

A PCA of the correlation matrix for the same nine solutes shown in the mixing diagrams indicates that the first two principal components (PC) could explain 73 percent of the variation of the data (table 4). Therefore, a mixing model having as few as three end members could also explain this same percentage of the variation. By restricting the analysis to the first two PC's, one mixing diagram captures the entire problem rather than the 36 plots that were necessary for nine solutes (fig. 58). The streamwater concentrations lie between concentrations in samples from the bench meadow lysimeters on the upper part of the plot and from the inlet meadow and ridge lysimeters on the lower part of the plot. Deep and shallow lysimeters exhibit little difference within a plot or between the inlet and ridge sites

Table 4.—*Variance explained by principal components*

| Principal component rank | Variance explained (in percent) | Cumulative variance explained (in percent) |
|--------------------------|---------------------------------|--|
| First | 54 | 54 |
| Second | 19 | 73 |
| Third | 8.0 | 81 |
| Fourth | 5.8 | 87 |
| Fifth | 4.9 | 92 |
| Sixth | 3.6 | 95 |
| Seventh | 2.4 | 98 |
| Eighth | 1.3 | 99 |
| Ninth | .8 | 100 |

To be able to explain the streamwater as a mixture of water from these sources, however, the soil solutions must lie in the same subspace as the streamwater (U-space). The orthogonal projections for the medians of the six soil solutions are presented in tables 5 through 10. The median concentration of samples from the bench meadow lysimeters have the most solutes lying outside the quartiles (calcium, silica, and potassium for both depths and nitrate for the deep lysimeter and sulfate for the shallow lysimeter). The orthogonal projection of the median concentrations from the ridge site has a high calcium and alkalinity concentration. The projection of median concentrations from the inlet meadow site has the fewest solutes outside the quartiles; only the potassium concentration is outside the quartiles at both depths. As could be anticipated from the mixing diagrams in the appendix, calcium is the solute that generally must have a higher concentration for end members in a mixing model than the sampled soil solutions.

The major variation in streamwater chemistry may be explained as mixing between soil solutions from the bench meadow and from the ridge or inlet meadow sites. These two locations would be the areas of the watershed on which to focus process-level research, because, if the soil solutions from these areas change in response to changes in acid deposition, the stream chemistry also would be expected to change. In any distributed hydrologic model for Emerald Lake, it is critical to determine the discharge from these sites.

The similarity between the inlet meadow and the ridge site soil solutions in U-space was unexpected. The soil solutions from the inlet and bench meadows were expected to be more similar than those from the inlet and ridge sites as both have deeper soil deposits than does the ridge site. Perhaps the salient difference is the residence time of the water, which must be longer at the bench site to achieve the observed higher ionic strengths. Determining the reasons for the similarity indicated by the PCA could be the subject for additional field investigations.

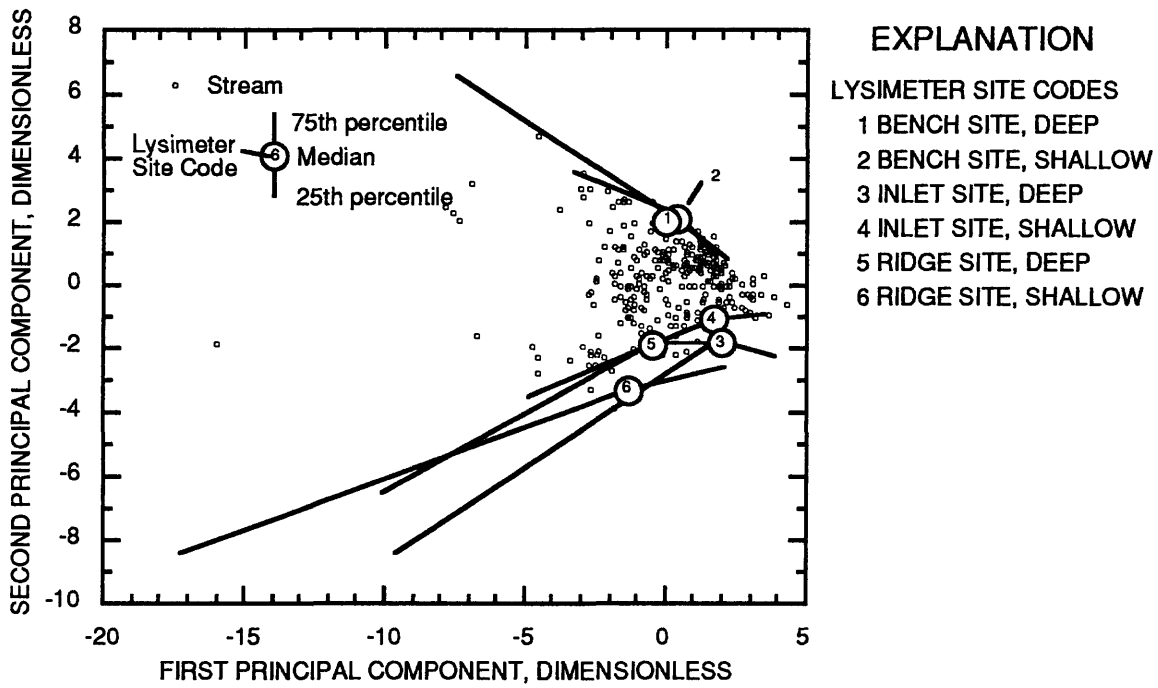


Figure 58.—Relation between first and second principal components for streamwater and soil solutions.

Table 5.—*Soil-solution statistics for shallow lysimeter at bench meadow site*
 [Underlined numbers indicate that the orthogonal projection lies outside the two quartiles;
 silica values are in micromoles per liter]

| Solute | Median concentration (microequivalents per liter) | Concentrations for indicated quartiles (microequivalents per liter) | | Orthogonal projection (microequivalents per liter) |
|------------|--|--|------|---|
| | | 25th | 75th | |
| Alkalinity | 42 | 21 | 68 | 43 |
| Calcium | 15 | 9.4 | 21 | <u>33</u> |
| Magnesium | 4.4 | 2.8 | 6.4 | 4.6 |
| Sodium | 23 | 14 | 28 | 15 |
| Potassium | 3.4 | 2.1 | 4.6 | <u>1.4</u> |
| Silica | 50 | 48 | 61 | <u>47</u> |
| Chloride | 2.4 | 1.8 | 4.4 | 4.3 |
| Nitrate | .7 | 0 | 1.7 | 1.6 |
| Sulfate | 4.2 | 3.4 | 5.0 | <u>6.2</u> |

Table 6.—*Soil-solution statistics for deep lysimeter at bench meadow site*
 [Underlined numbers indicate that the orthogonal projection lies outside the two quartiles;
 silica values are in micromoles per liter]

| Solute | Median concentration (microequivalents per liter) | Concentrations for indicated quartiles (microequivalents per liter) | | Orthogonal projection (microequivalents per liter) |
|------------|--|--|------|---|
| | | 25th | 75th | |
| Alkalinity | 30 | 16 | 82 | 42 |
| Calcium | 10 | 4.4 | 18 | <u>32</u> |
| Magnesium | 4.2 | 2.4 | 6.4 | 4.6 |
| Sodium | 22 | 15 | 33 | <u>14</u> |
| Potassium | 4.2 | 1.8 | 6.8 | <u>1.7</u> |
| Silica | 64 | 59 | 140 | <u>45</u> |
| Chloride | 2.9 | 1.8 | 10 | 4.3 |
| Nitrate | .1 | 0 | 1.7 | <u>2.3</u> |
| Sulfate | 4.4 | 2.4 | 9.4 | 6.3 |

Table 7.—*Soil-solution statistics for shallow lysimeter at ridge site*
 [Underlined numbers indicate that the orthogonal projection lies outside the two quartiles;
 silica values are in micromoles per liter]

| Solute | Median concentration (microequivalents per liter) | Concentrations for indicated quartiles (microequivalents per liter) | | Orthogonal projection (microequivalents per liter) |
|------------|--|--|------|---|
| | | 25th | 75th | |
| Alkalinity | -3.5 | -7.5 | 5.5 | <u>14</u> |
| Calcium | 13 | 7.8 | 17 | <u>31</u> |
| Magnesium | 7.2 | 4.8 | 11 | 8.6 |
| Sodium | 28 | 12 | 66 | 15 |
| Potassium | 6.5 | 3.4 | 14 | 11 |
| Silica | 36 | 23 | 67 | 30 |
| Chloride | 6.2 | 3.3 | 49 | 9.3 |
| Nitrate | 28 | 7.0 | 100 | 18 |
| Sulfate | 15 | 11 | 24 | 11 |

Table 8.—*Soil-solution statistics for deep lysimeter at ridge site*
 [Underlined numbers indicate that the orthogonal projection lies outside the two quartiles;
 silica values are in micromoles per liter]

| Solute | Median concentration (microequivalents per liter) | Concentrations for indicated quartiles (microequivalents per liter) | | Orthogonal projection (microequivalents per liter) |
|------------|--|--|------|---|
| | | 25th | 75th | |
| Alkalinity | 8.5 | 0 | 19 | <u>20</u> |
| Calcium | 10 | 6.2 | 17 | <u>29</u> |
| Magnesium | 6.8 | 4.2 | 10 | 7.0 |
| Sodium | 23 | 12 | 32 | 14 |
| Potassium | 9.4 | 4.3 | 15 | 7.7 |
| Silica | 41 | 33 | 44 | <u>32</u> |
| Chloride | 5.6 | 4.5 | 34 | 7.1 |
| Nitrate | 10 | 5.0 | 53 | 18 |
| Sulfate | 10 | 5.8 | 15 | 9.3 |

Table 9.—*Soil-solution statistics for shallow lysimeter at inlet meadow site*
 [Underlined numbers indicate that the orthogonal projection lies outside the two quartiles;
 silica values are in micromoles per liter]

| Solute | Median concentration (microequivalents per liter) | Concentrations for indicated quartiles (microequivalents per liter) | | Orthogonal projection (microequivalents per liter) |
|------------|--|--|------|---|
| | | 25th | 75th | |
| Alkalinity | 25 | 3.2 | 42 | 19 |
| Calcium | 17 | 11 | 30 | 20 |
| Magnesium | 2.7 | 2.0 | 5.7 | 4.6 |
| Sodium | 8.7 | 5.6 | 16 | 11 |
| Potassium | 1.1 | 0.40 | 1.7 | <u>4.2</u> |
| Silica | 38 | 32 | 47 | <u>29</u> |
| Chloride | 4.7 | 1.9 | 12 | 3.6 |
| Nitrate | 26 | 5.5 | 71 | 9.1 |
| Sulfate | 6.0 | 3.8 | 8.8 | 6.4 |

Table 10.—*Soil-solution statistics for deep lysimeter at inlet meadow site*
 [Underlined numbers indicate that the orthogonal projection lies outside the two quartiles;
 silica values are in micromoles per liter]

| Solute | Median concentration (microequivalents per liter) | Concentrations for indicated quartiles (microequivalents per liter) | | Orthogonal projection (microequivalents per liter) |
|------------|--|--|------|---|
| | | 25th | 75th | |
| Alkalinity | 18 | 3.5 | 28 | 16 |
| Calcium | 22 | 12 | 39 | 20 |
| Magnesium | 5.6 | 3.6 | 16 | 5.1 |
| Sodium | 8.8 | 4.6 | 14 | 11 |
| Potassium | 3.1 | 1.4 | 4.4 | <u>5.4</u> |
| Silica | 30 | 7.3 | 59 | 27 |
| Chloride | 3.6 | 1.8 | 12 | 4.3 |
| Nitrate | 20 | 6.2 | 120 | 12 |
| Sulfate | 6.2 | 3.1 | 8.9 | 7.0 |

SUMMARY

The Alpine Lake Forecaster, a computer model that simulates the chemical effects of acidic deposition on streamwater and lakes in alpine catchments, was applied to four alpine catchments in the Sierra Nevada, California, that were studied between 1986 and 1988. The geochemical processes contained within the model seem to be applicable to three of the four lakes. At one lake, which turns over infrequently because of its geomorphology, alkalinity seems to be controlled by biological, rather than geochemical processes, thereby rendering ALF unsuitable. Even where applicable, however, parameter estimation for ALF requires that calibration data be collected over a large range of discharge. Therefore, it is critical that peak discharge during snowmelt be sampled.

Qualitatively, the smaller the amount of more readily weatherable minerals, such as hornblende, that are contained in the granitic bedrock, the more sensitive the watershed is to acidic pulses. A sensitivity analysis of ALF has quantified this relation using data for Emerald Lake, another watershed in the Sierra Nevada of California, for which the model was originally developed. The more extensive data set at Emerald Lake was required for this analysis. Changing the stoichiometric coefficient from 1.2 to 1.0 has little effect on the chemistry of the streamwater, but a stoichiometric coefficient of 0.5 or less substantially lowers the alkalinity of the streamwater. This coefficient may be used as an index value to compare other watersheds to Emerald Lake.

Additional insights into the geochemical and hydrologic processes operating in the catchment can be gained by comparing the chemistry of soil-water solutions to the chemistry of streamwater. A multivariate mixing model that relates these solutions was developed using data from Emerald Lake, the only site for which soil solution data were available. This analysis indicates that streamwater may be considered a mixture of soil solutions from the bench meadow and the ridge or inlet meadow site. The similarity between the ridge and inlet meadow soil solutions was unexpected. The higher solute concentrations at the bench site indicate that the residence time of the soil solution may be longer at this site than at the other two sites. This mixing model presents a method for the determination of hydrologic flowpaths that can affect streamwater quality, and may serve as a means of parameterizing compartmentalized hydrochemical models.

TOPICS FOR ADDITIONAL STUDY

Applicability of stoichiometric coefficient as an index. This analysis indicated that the stoichiometric coefficient, that is, the slope of the regression model relating sum of base cation (SBC) concentration to silica concentration, may be a useful indicator of the sensitivity of a watershed to acidification. To test the use of this coefficient, the lake inlets at Emerald Lake and at additional sites could be monitored during snow melt for major ion chemistry. The hypothesis is that the ANC of the inlets with a coefficient value similar to that of Emerald Lake would decline during snowmelt much like the ANC of Emerald Lake and that watersheds with smaller coefficients would experience greater ANC depressions.

Soil process studies. The bench meadow and inlet meadow or ridge sites seem to be important in the control of surface-water chemistry at Emerald Lake. *In situ* acidification studies could help to determine processes that control the response of these soil solutions to changes in atmospheric deposition or to changes in the relative amounts of nitrate and sulfate. Further hydrologic and chemical characterization of these soil environments also may indicate why soil solutions at the inlet and ridge sites seem to have a similar composition.

Source of "missing" calcium. Soil solutions measured to date (1992) do not have a sufficiently high calcium concentration to explain the streamwater chemistry of Emerald Lake. Additional field research is needed to determine if the discrepancy can be explained hydrologically (for example, a deep ground-water source that is rich in calcium), or mineralogically (for example, a small quantity of a readily weatherable mineral, such as calcite).

Distributed hydrochemical model development. The multivariate soil-solution mixing model indicates that the bench meadow and inlet meadow or ridge site soil environments should be included in a distributed model of Emerald Lake. The development of a distributed hydrologic model would require a representation of the physical processes linking snowmelt or rainfall inputs with discharge from these soil environments.

REFERENCES CITED

- Asolekar, S.R., Valentine, R.L., and Schnoor, J.L., 1991, Kinetics of chemical weathering in B horizon spodosol fraction: *Water Resources Research*, v. 27, p. 527-532.
- Brown, A.D., Lund, L.J., and Lueking, M.A., 1990, Integrated soil processes studies at Emerald Lake watershed: Sacramento, Calif., California Air Resources Board, Final Report, Contract A5-204-32, 173 p.
- Brown, A.D., and Lund, L.J., 1991, Kinetics of weathering in soils from a subalpine watershed: *Soil Science Society of America Journal*, v. 55, p. 1767-1773.
- Chen, C.W., Gherini, S.A., Hudson, R.J.M., and Dean, J.D., 1983, The integrated lake-watershed acidification study: Model principles and application procedures: Lafayette, Ca., Tetra Tech, Inc., EPRI Report EA-3221, v. 1, RP 1109-5, 188 p.
- Christophersen, Nils, Dymbe, L.H., Johannessen, Merete, and Seip, H.M., 1984, A model for sulphate in streamwater at Storgama, southern Norway: *Ecological Modelling*, v. 21, p. 35-61.
- Christophersen, Nils, Neal, Colin, and Hooper, R.P., 1990, Modeling streamwater chemistry as a mixture of soil-water end members—a step towards second generation acidification models: *Journal of Hydrology*, v. 116, p. 307-320.
- Christophersen, Nils, and Hooper, R.P., 1992, Multivariate analysis of streamwater quality: The use of principal components for the end-member mixing problem: *Water Resources Research*, v. 28, p. 99-107.
- DeWalle, D.R., Swistock, B.R., and Sharp, W.E., 1988, Three-component tracer model for storm flow on a small Appalachian forested catchment: *Journal of Hydrology*, v. 104, p. 301-210.
- Dozier, Jeff, 1988, Topographic distribution of solar radiation over an alpine, snow-covered drainage basin [*abs*]: *Eos Transactions of American Geophysical Union*, v. 69, p. 1198.
- Dozier, Jeff, Melack, J.M., Marks, Daniel, Elder, Kelly, Kattelman, Richard, and Williams, Mark, 1989, Snow deposition, melt, runoff, and chemistry in a Sierra Nevada watershed: Sacramento, Calif., California Air Resources Board, Final Report, Contract A6-147-32, 268 p.
- Hooper, R.P., and Christophersen, Nils, 1992, Predicting episodic stream acidification in the southeastern United States: Combining a long-term acidification model and the end-member mixing concept: *Water Resources Research*, v. 28, p. 1983-1990.
- Hooper, R.P., Christophersen, Nils, and Peters, N.E., 1990, Modeling streamwater chemistry as a mixture of soil-water end members—an application to the Panola Mountain watershed, Georgia, USA: *Journal of Hydrology*, v. 116, p. 321-343.
- Hooper, R.P., Stone, Alexander, Christophersen, Nils, de Grosbois, Edward, and Seip, H. M., 1988, Assessing the Birkenes model of stream acidification using a multi-signal calibration methodology: *Water Resources Research*, v. 24, p. 1308-1316.
- Hooper, R. P., West, C.T., and Peters, N.E., 1990, Assessing the response of Emerald Lake, an alpine watershed in Sequoia National Park, California, to acidification during snowmelt by using a simple hydrochemical model: U.S. Geological Survey Water-Resources Investigations Report 90-4000, 68 p.
- Johannessen, Merete, and Henriksen, Arne, 1978, Chemistry of snow meltwater—changes in concentration during melting: *Water Resources Research*, v. 14, p. 615-619.
- Johnson, N.M., Likens, G.E., Bormann, F.H., Fisher, D.W., and Pierce, R.S., 1969, A working model for the variation in streamwater chemistry at Hubbard Brook Experimental Forest, New Hampshire: *Water Resources Research*, v. 5, p. 1353-1363.
- Leivestved, H., and Muniz, I.P., 1976, Fish kill at low pH in a Norwegian river: *Nature*, v. 259, p. 391-392.
- Lund, L.J., Brown, A.D., Lueking, M.A., Nodvin, S.C., Page, A.L., and Sposito, Garrison, 1987, Soil processes at Emerald Lake Watershed: Sacramento, Calif., California Air Resources Board, Final Report, Contract A3-105-32, 114 p.
- Marks, Daniel, 1988, Climate, energy exchange, and snowmelt in Emerald Lake watershed, Sierra Nevada: Santa Barbara, Calif., University of California, unpublished Ph.D. thesis, 158 p.

REFERENCES CITED--Continued

- Mast, M.A., Drever, J.I., and Baron, J., 1990, Chemical weathering in the Loch Vale watershed, Rocky Mountain National Park, Colorado: *Water Resources Research*, v. 26, p. 2971-2978.
- Melack, J.M., Cooper, S.D., Jenkins, T.M., Jr., Barmuta, Leon, Hamilton, Scott, Kratz, Kimberly, Sickman, James, and Soiseth, Chadwick, 1989, Chemical and biological characteristics of Emerald Lake and the streams in its watershed, and the responses of the lakes and streams to acidic deposition: Sacramento, Calif., California Air Resources Board, Final Report, Contract A6-184-32, 377 p.
- Morel, François, and Morgan, J.J., 1972, A numerical method for computing equilibria in aqueous chemical systems: *Environmental Science and Technology*, v. 6, p. 58-66.
- Neal, Colin, and Christophersen, Nils, 1989, Inorganic aluminum-hydrogen ion relationship for acidified streams: the role of water mixing processes: *Science of the Total Environment*, v. 80, p. 195-203.
- Pilgrim, D.H., Huff, D.D., and Steele, T.D., 1979, Use of specific conductance and contact time relations for separating flow components in storm runoff: *Water Resources Research*, v. 15, p. 329-339.
- Preisendorfer, R.W., Zweirs, F.W., and Barnett, T.P., 1981, Principal component selection rules: La Jolla, Calif., Scripps Institute of Oceanography, SIO Reference Series 81-4, 200 p.
- Sickman, J.O., and Melack J.M., 1989, Characterization of year-round sensitivity of California's montane lakes to acidic deposition: Sacramento, Calif., California Air Resources Board, Final Report, Contract A5-203-32, 104 p.
- Skartveit, A., and Gjessing, K.T., 1979, Chemical budgets and chemical quality of snow and runoff during spring snowmelt: *Nordic Hydrology*, v. 10, p. 141-154.
- Sklash, M.G., and Farvolden, R.N., 1979, The role of ground water in storm runoff: *Journal of Hydrology*, v. 43, p. 45-65.
- Swift, L.W., 1976, Algorithm for solar radiation on mountain slopes: *Water Resources Research*, v. 12, p. 108-112.
- Tonnessen, K.A., 1991, The Emerald Lake watershed study: Introduction and site description: *Water Resources Research*, v. 27, p. 1537-1539.
- Weintraub, Jill, 1986, An assessment of the susceptibility of two alpine watersheds to surface water acidification—Sierra Nevada, California: Bloomington, Ind., Indiana University, unpublished masters thesis, 186 p.
- Wetzel, R.G., 1975, *Limnology*: Philadelphia, Pa., W.B. Saunders Co., 743 p.

APPENDIX—MIXING DIAGRAMS

In the figures in this appendix, the following codes are used to identify the lysimeter locations:

| | |
|-----------|---|
| BD | Bench site, deep lysimeter |
| BS | Bench site, shallow lysimeter |
| ID | Inlet meadow site, deep lysimeter |
| IS | Inlet meadow site, shallow lysimeter |
| RD | Ridge site, deep lysimeter |
| RS | Ridge site, shallow lysimeter |

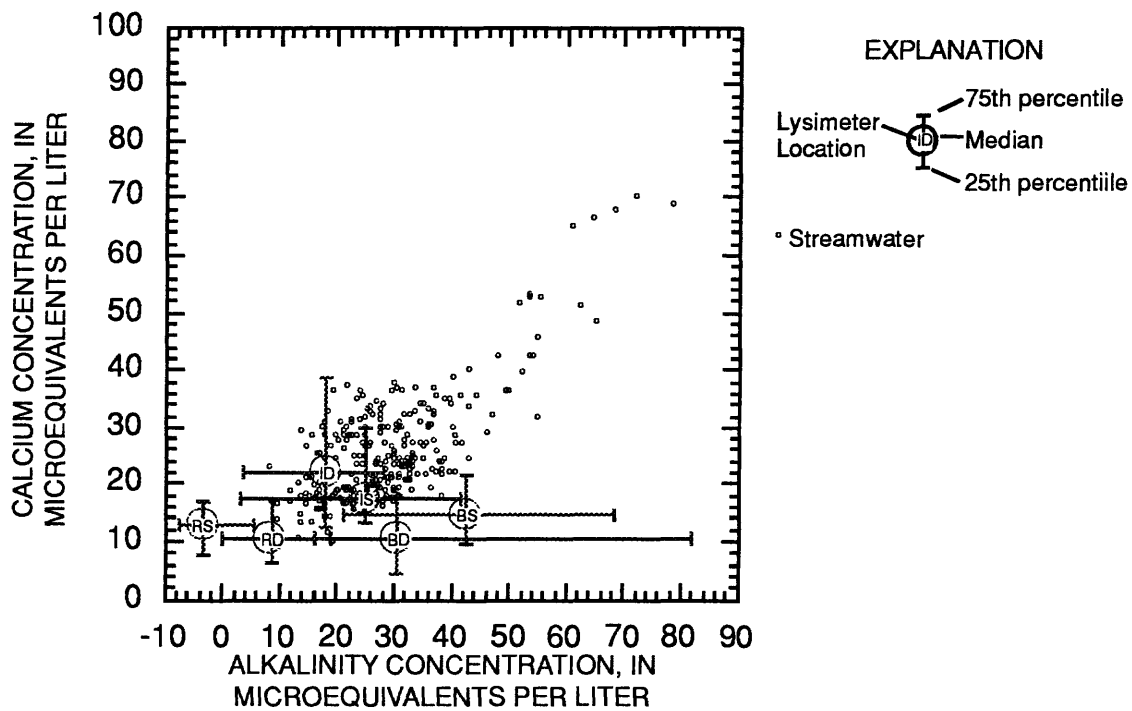


Figure 22.— Mixing diagram relating calcium and alkalinity.

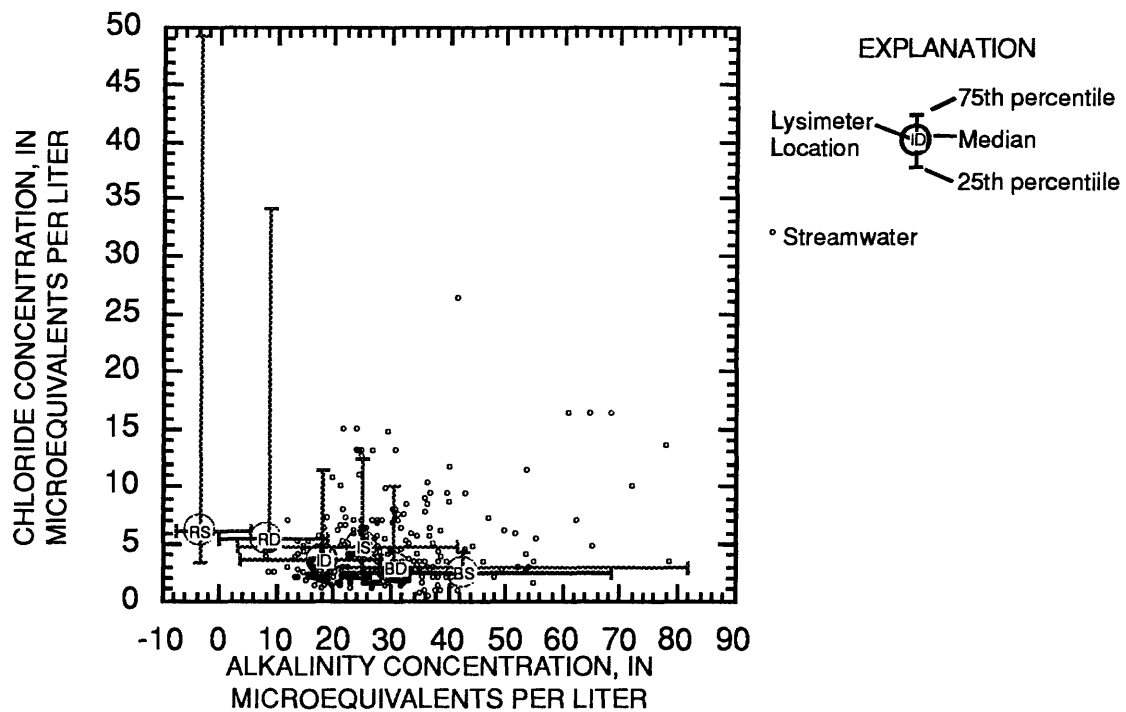


Figure 23.— Mixing diagram relating chloride and alkalinity.

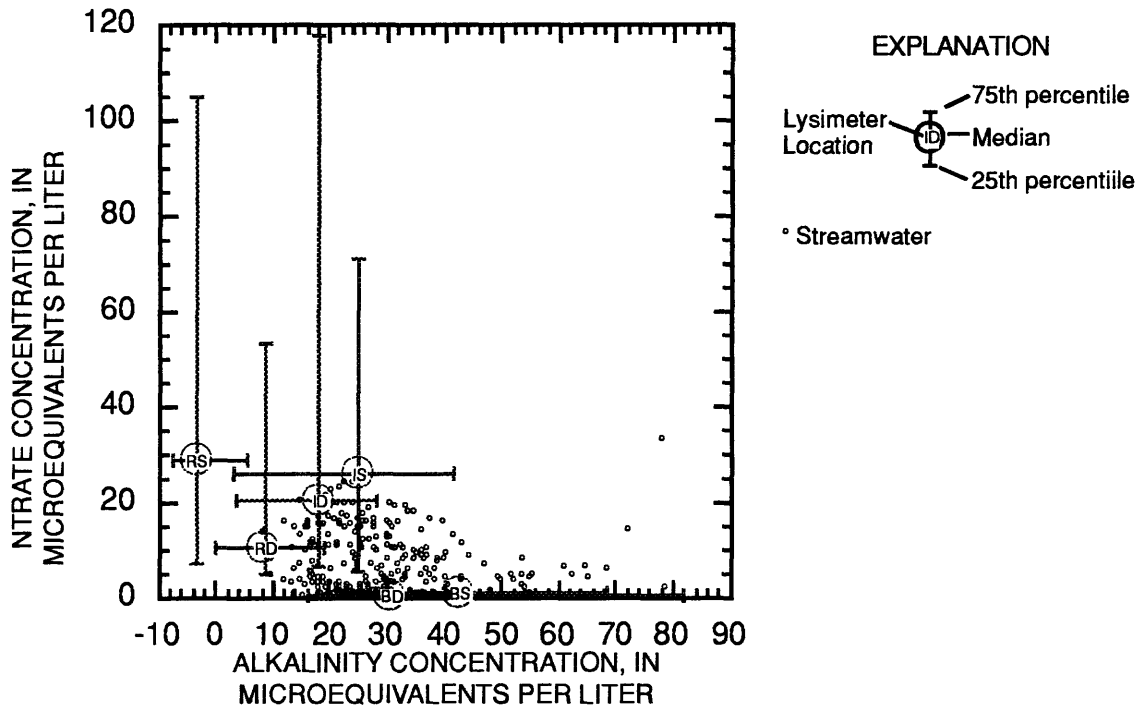


Figure 24.— Mixing diagram relating nitrate and alkalinity.

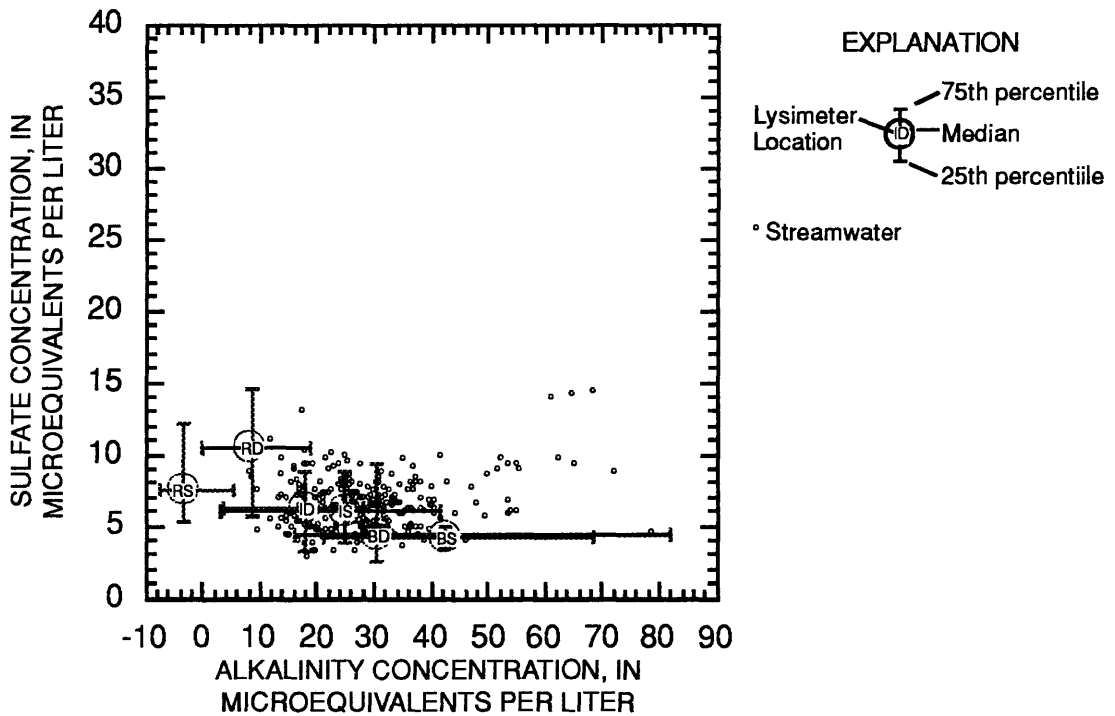


Figure 25.— Mixing diagram relating sulfate and alkalinity.

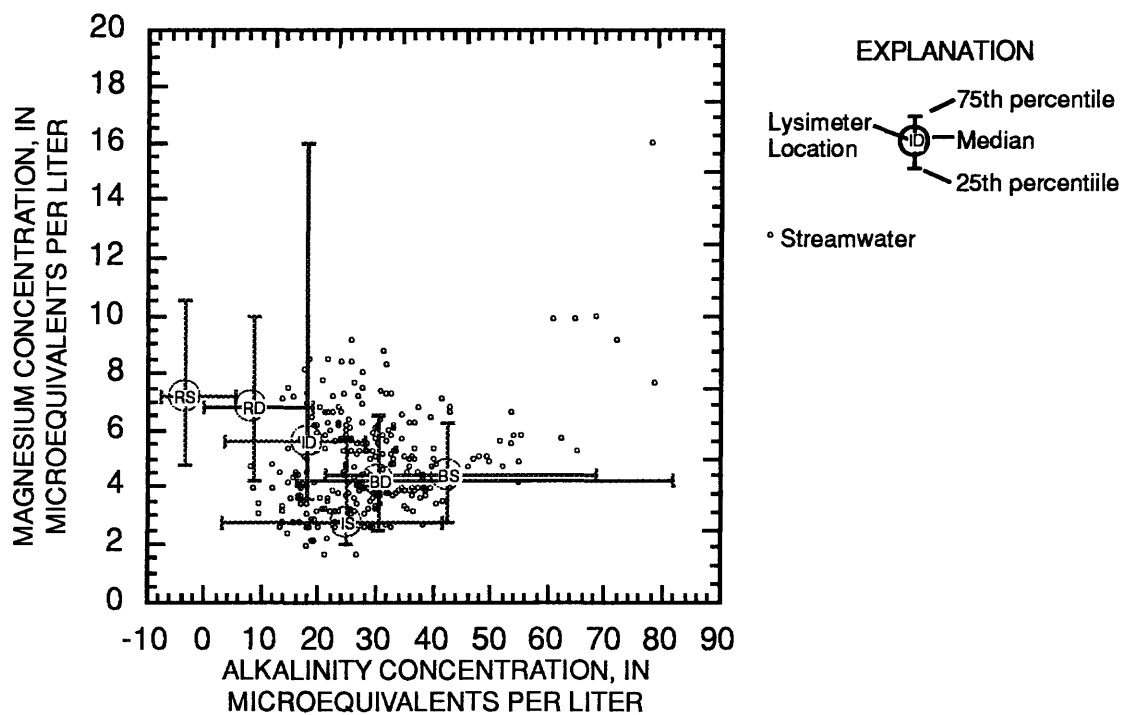


Figure 26.—Mixing diagram relating magnesium and alkalinity.

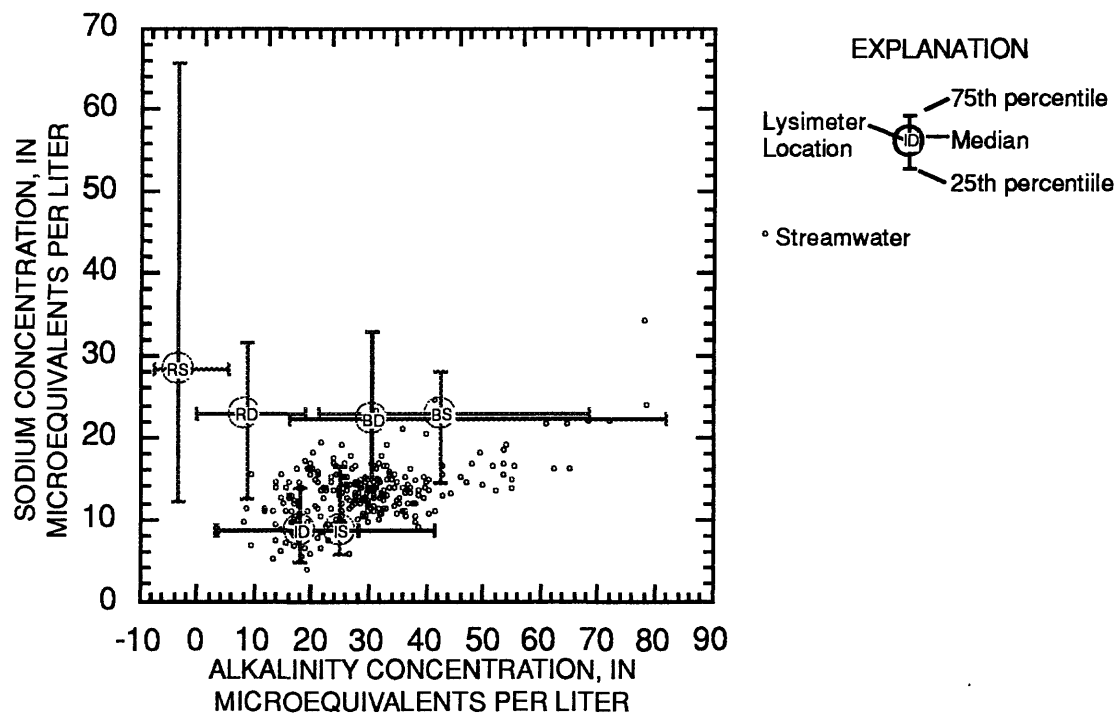


Figure 27.—Mixing diagram relating sodium and alkalinity.

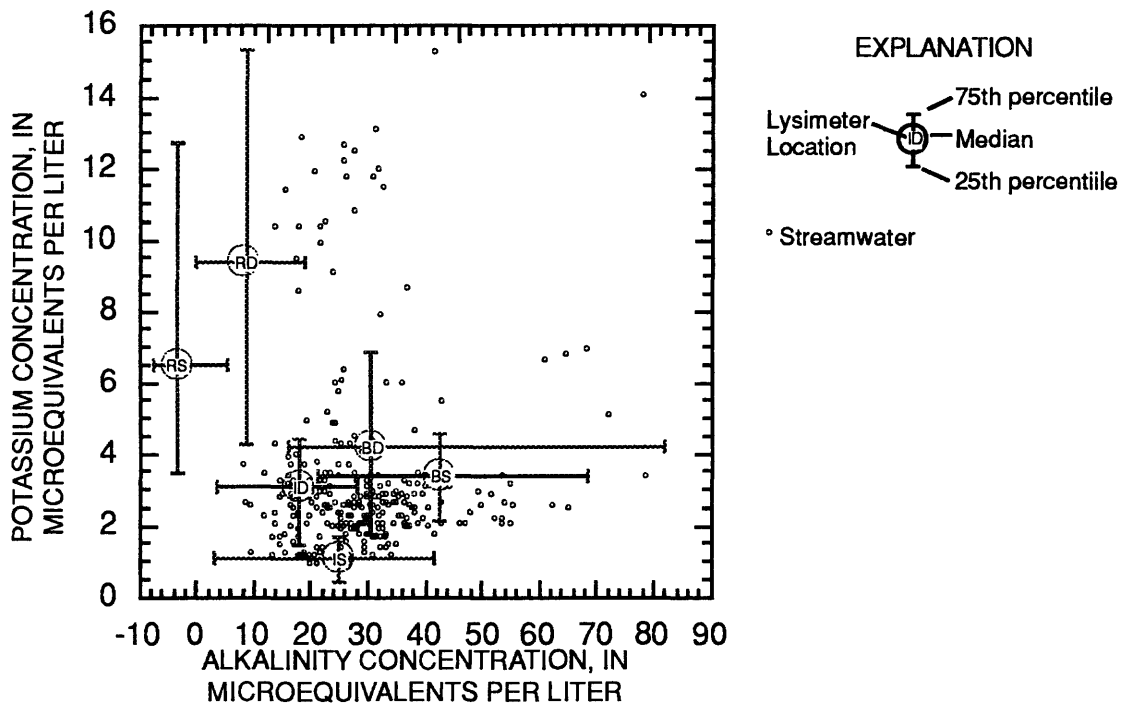


Figure 28.—Mixing diagram relating potassium and alkalinity.

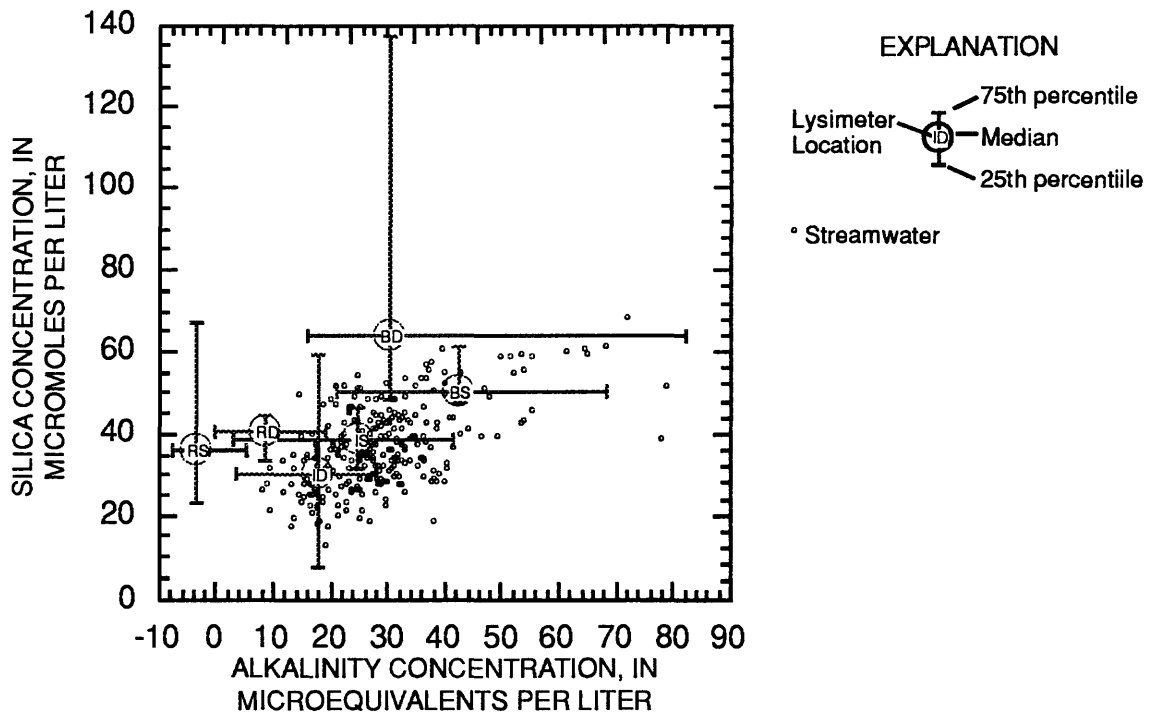


Figure 29.—Mixing diagram relating silica and alkalinity.

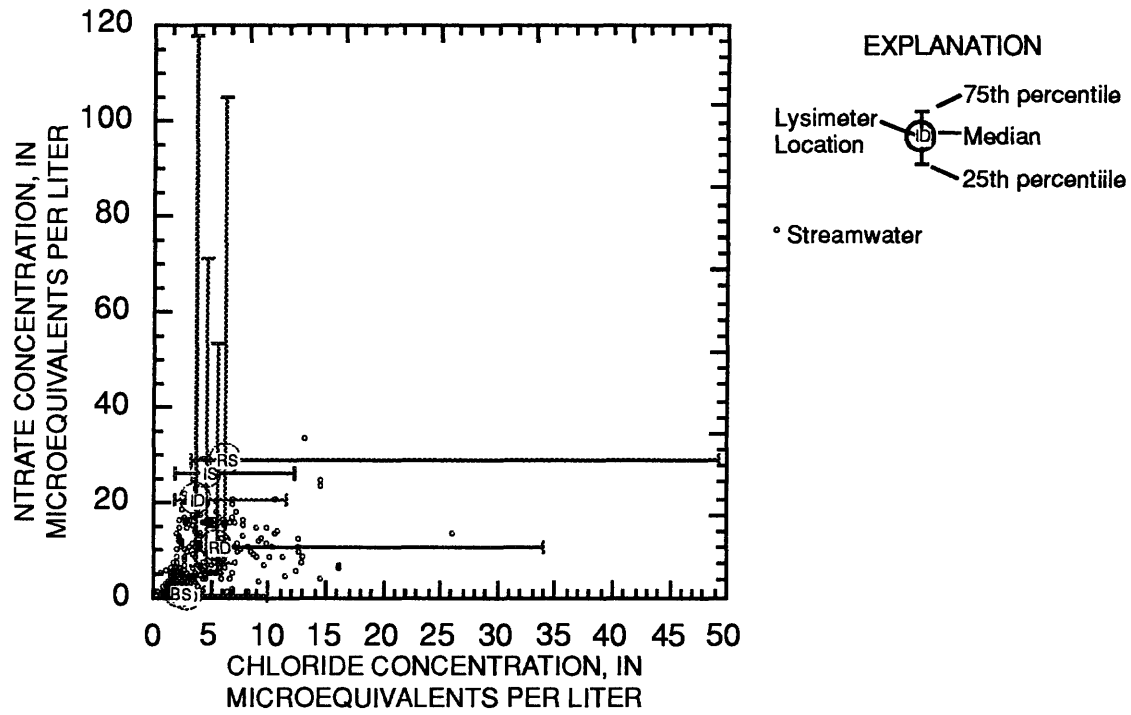


Figure 30.—Mixing diagram relating nitrate and chloride.

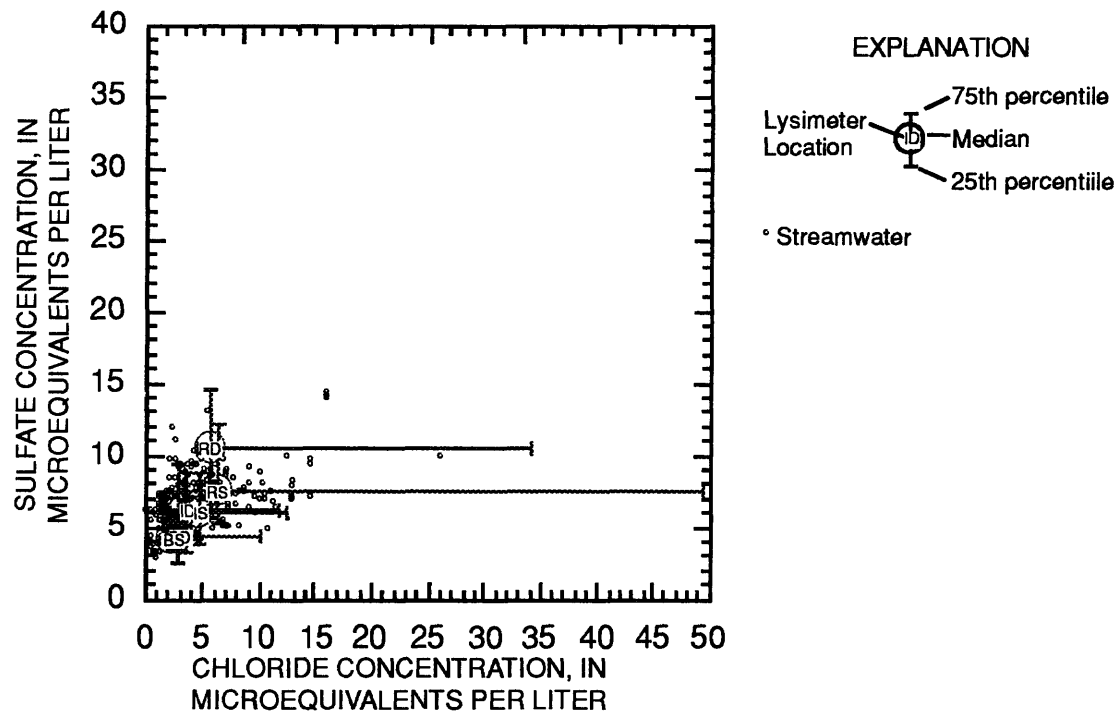


Figure 31.—Mixing diagram relating sulfate and chloride.

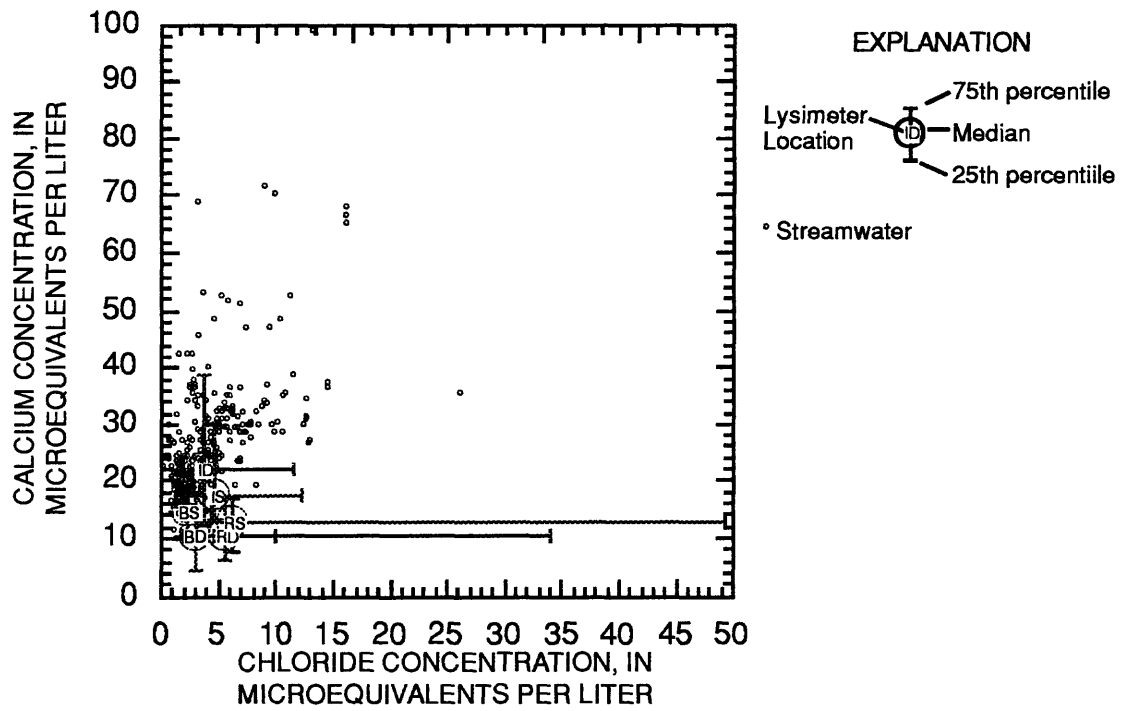


Figure 32.—Mixing diagram relating calcium and chloride.

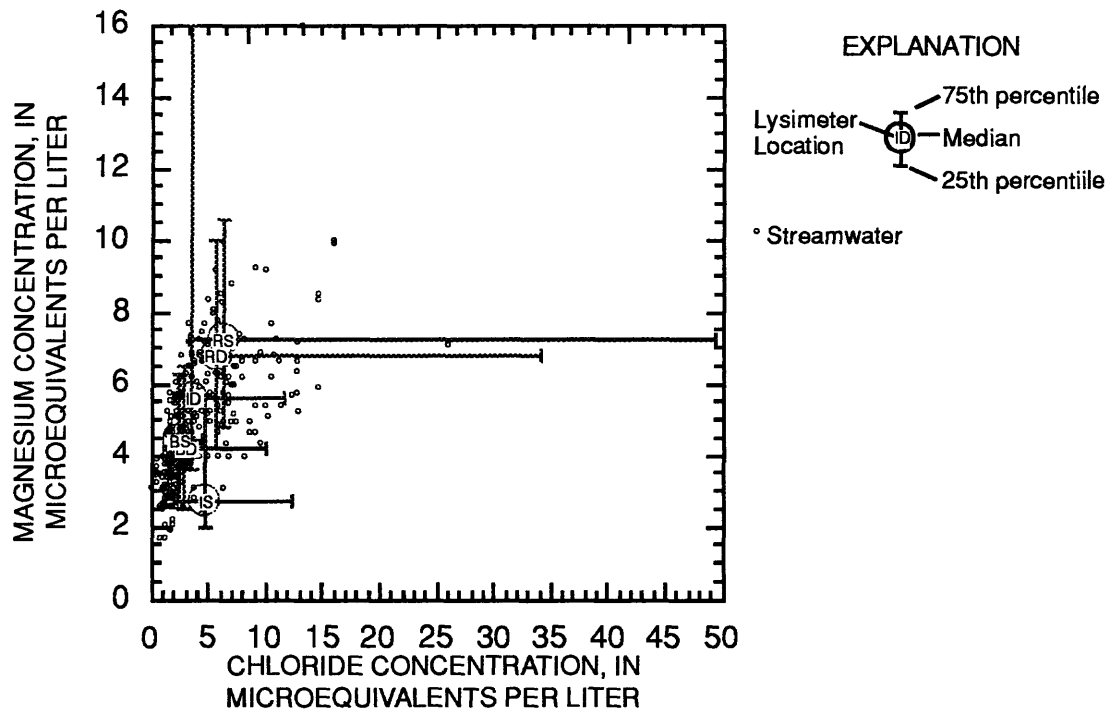


Figure 33.—Mixing diagram relating magnesium and chloride.

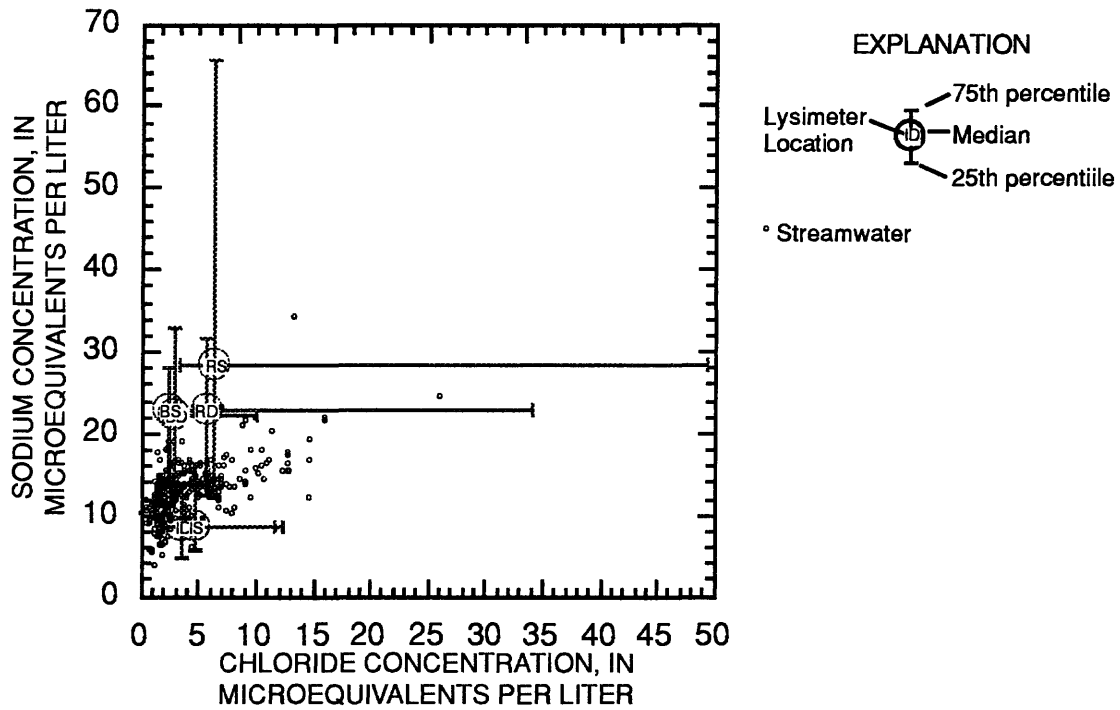


Figure 34.—Mixing diagram relating sodium and chloride.

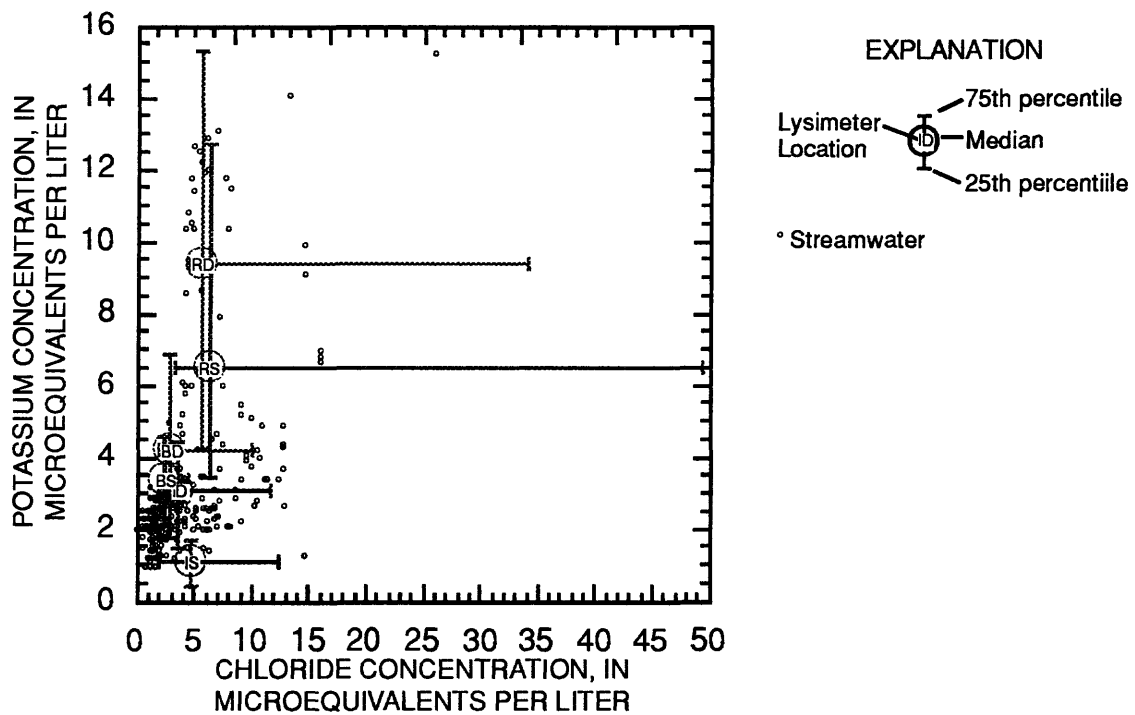


Figure 35.—Mixing diagram relating potassium and chloride.

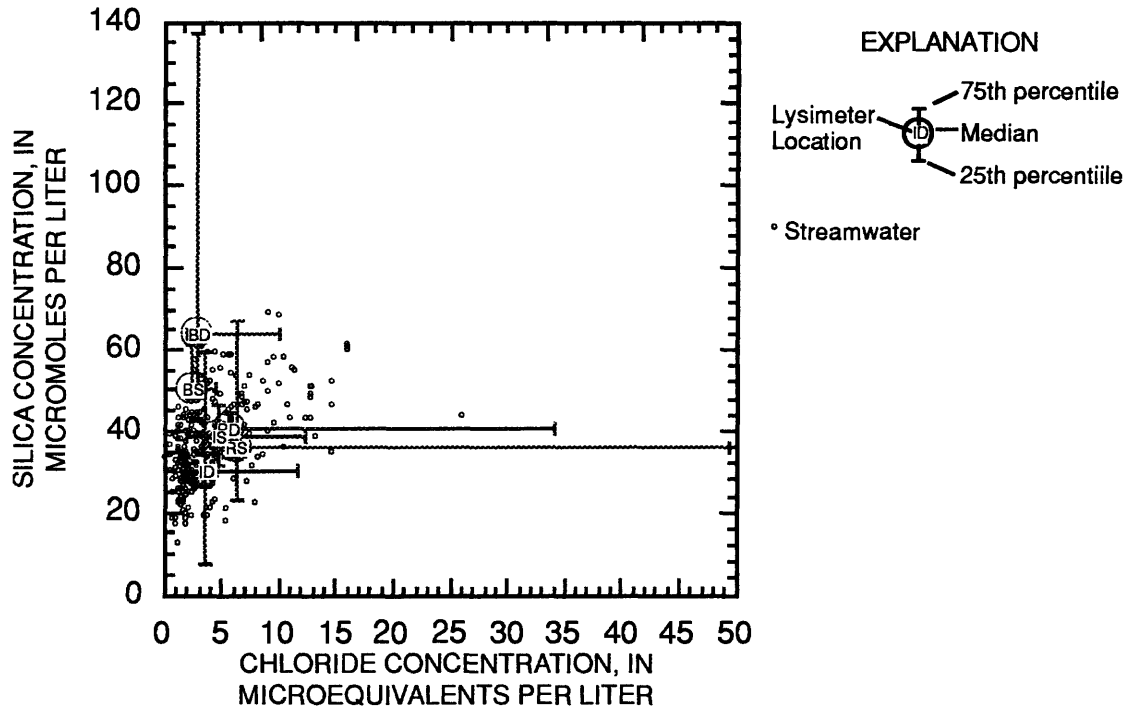


Figure 36.—Mixing diagram relating silica and chloride.

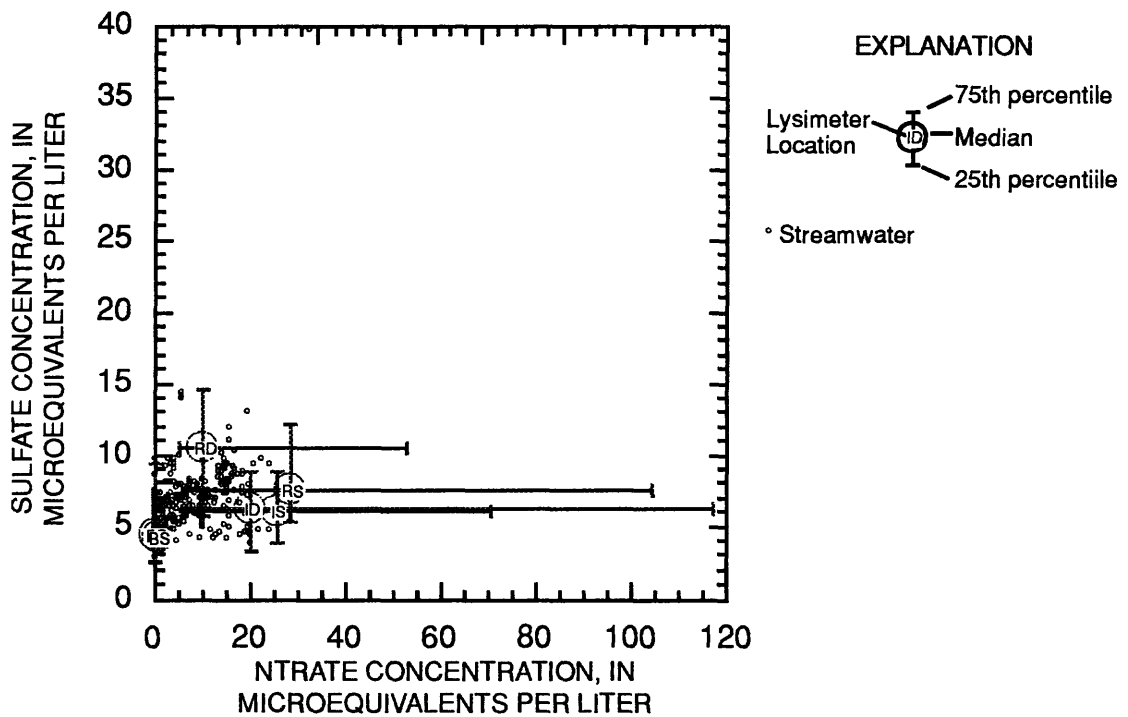


Figure 37.—Mixing diagram relating sulfate and nitrate.

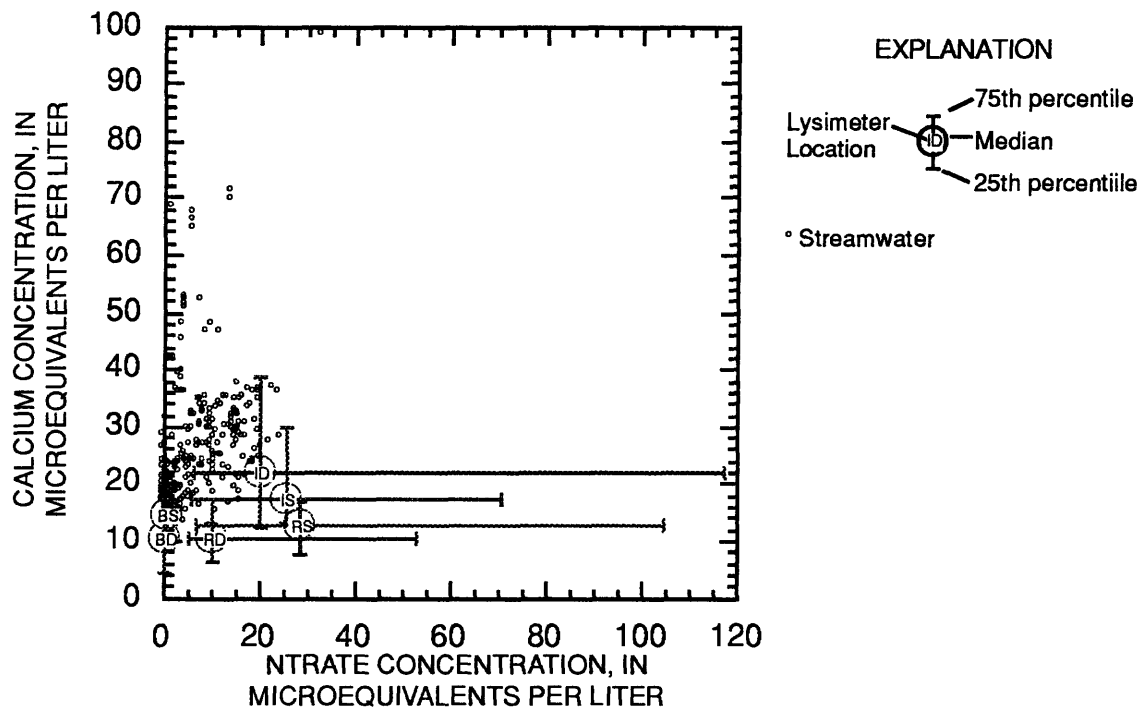


Figure 38.—Mixing diagram relating calcium and nitrate.

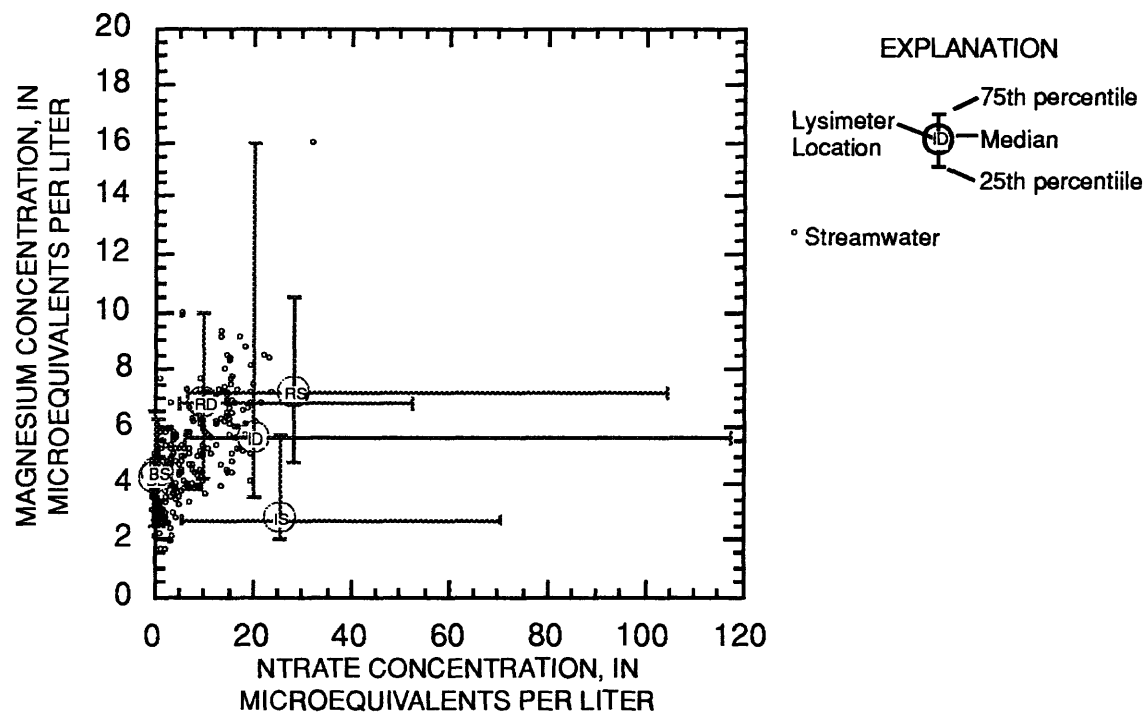


Figure 39.—Mixing diagram relating magnesium and nitrate.

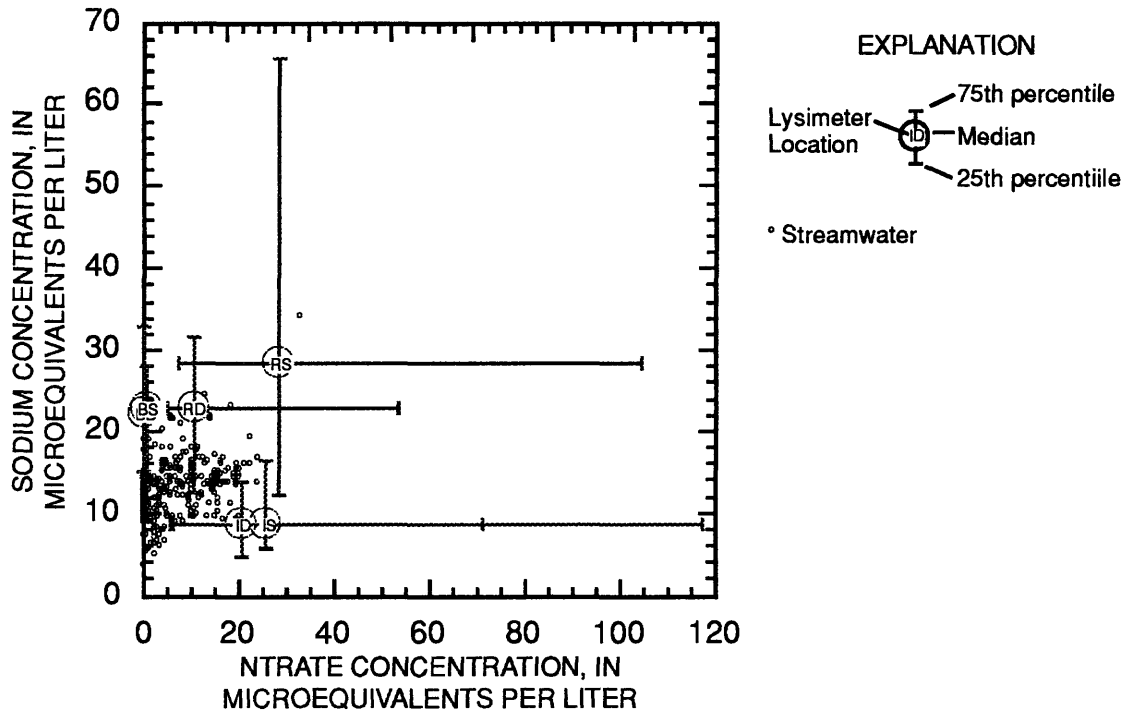


Figure 40.—Mixing diagram relating sodium and nitrate.

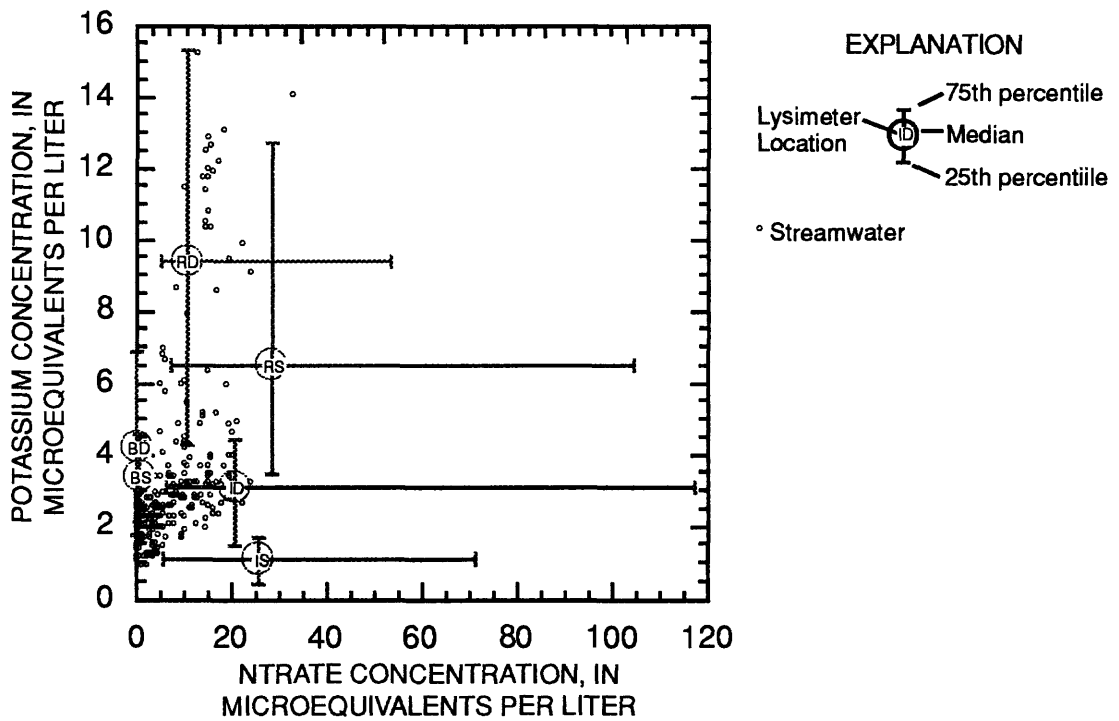


Figure 41.—Mixing diagram relating potassium and nitrate.

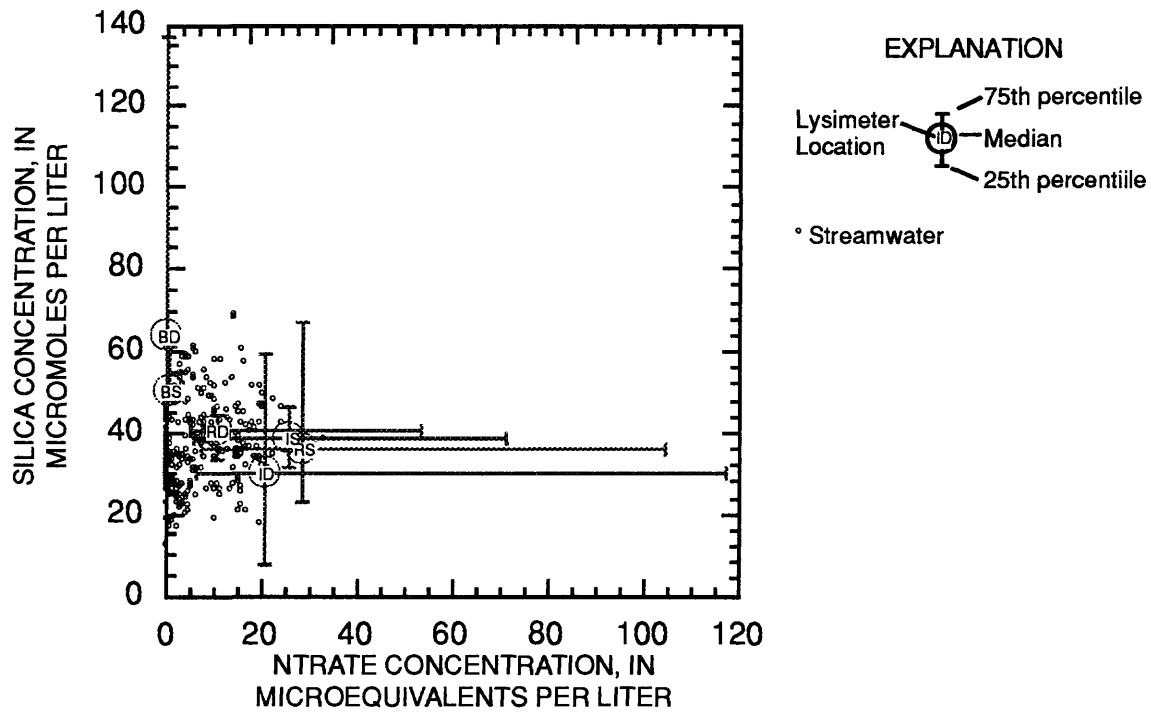


Figure 42.—Mixing diagram relating silica and nitrate.

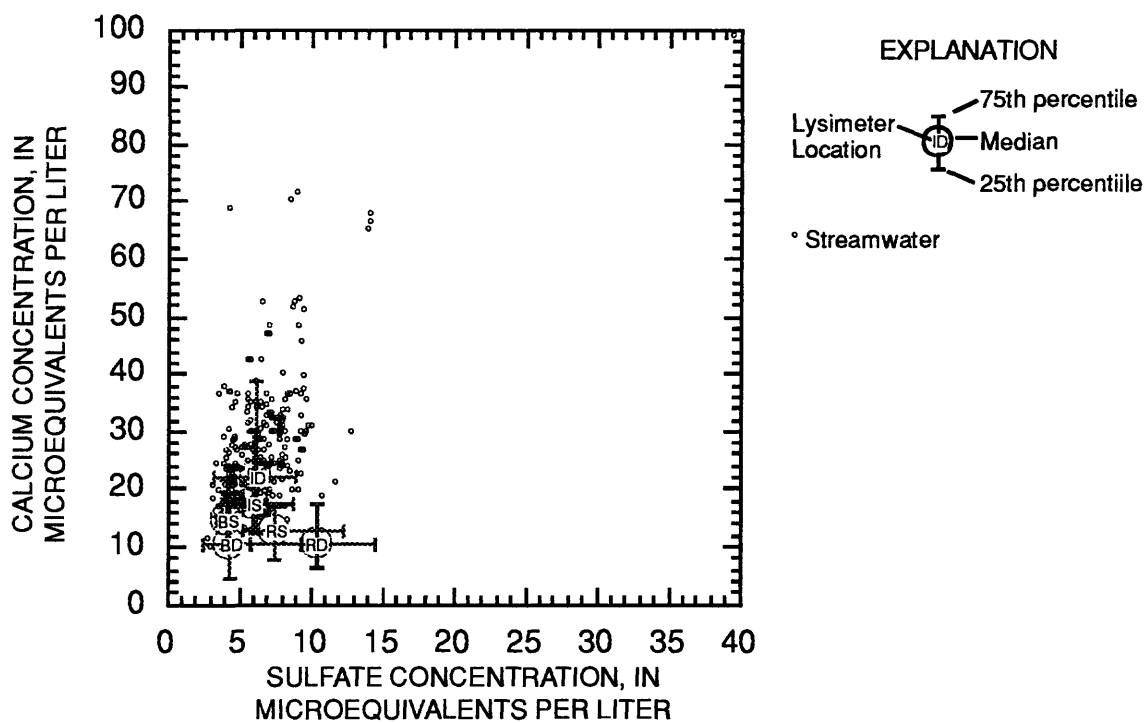


Figure 43.—Mixing diagram relating calcium and sulfate.

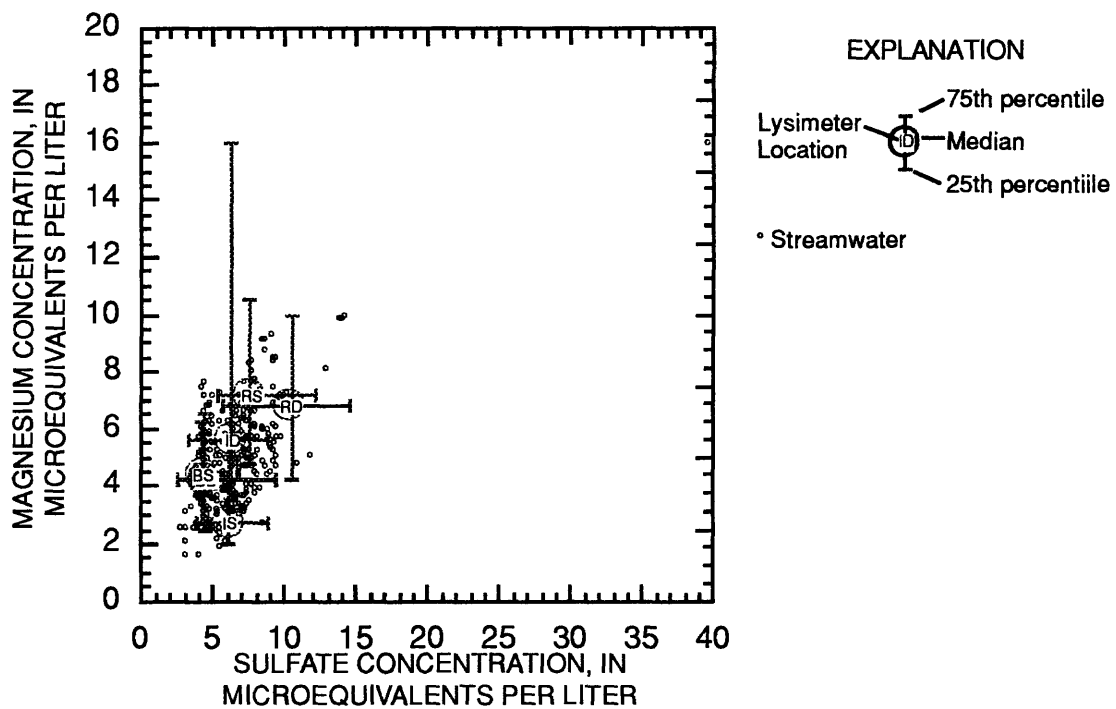


Figure 44.—Mixing diagram relating magnesium and sulfate.

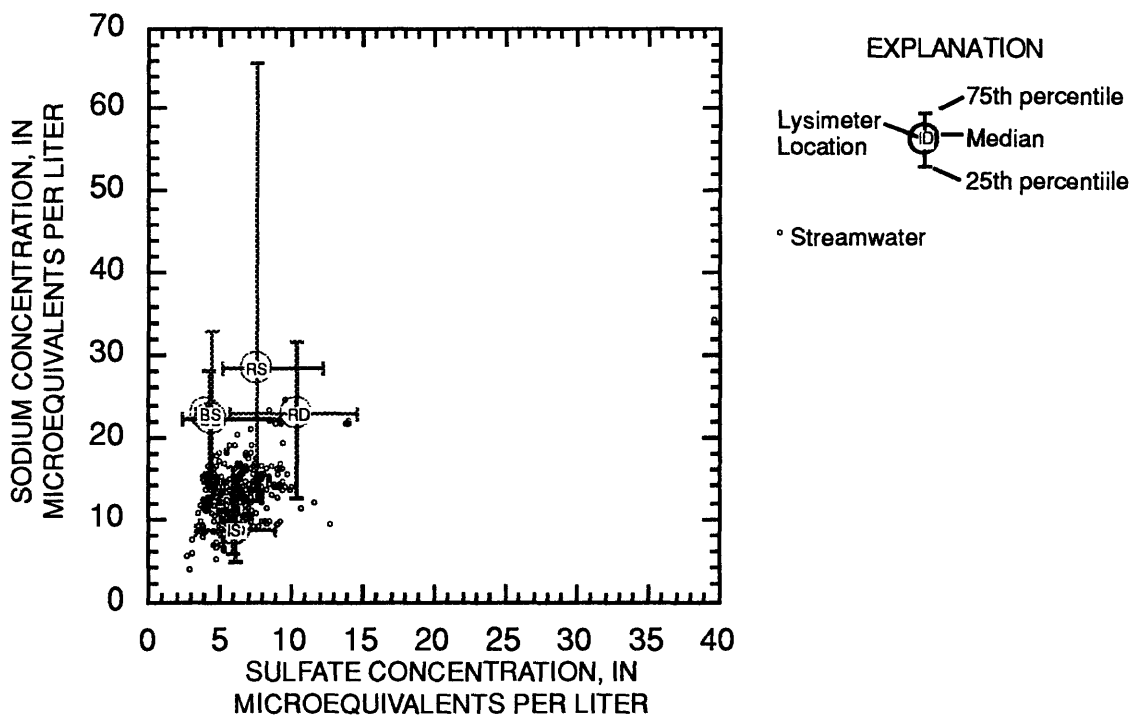


Figure 45.—Mixing diagram relating sodium and sulfate.

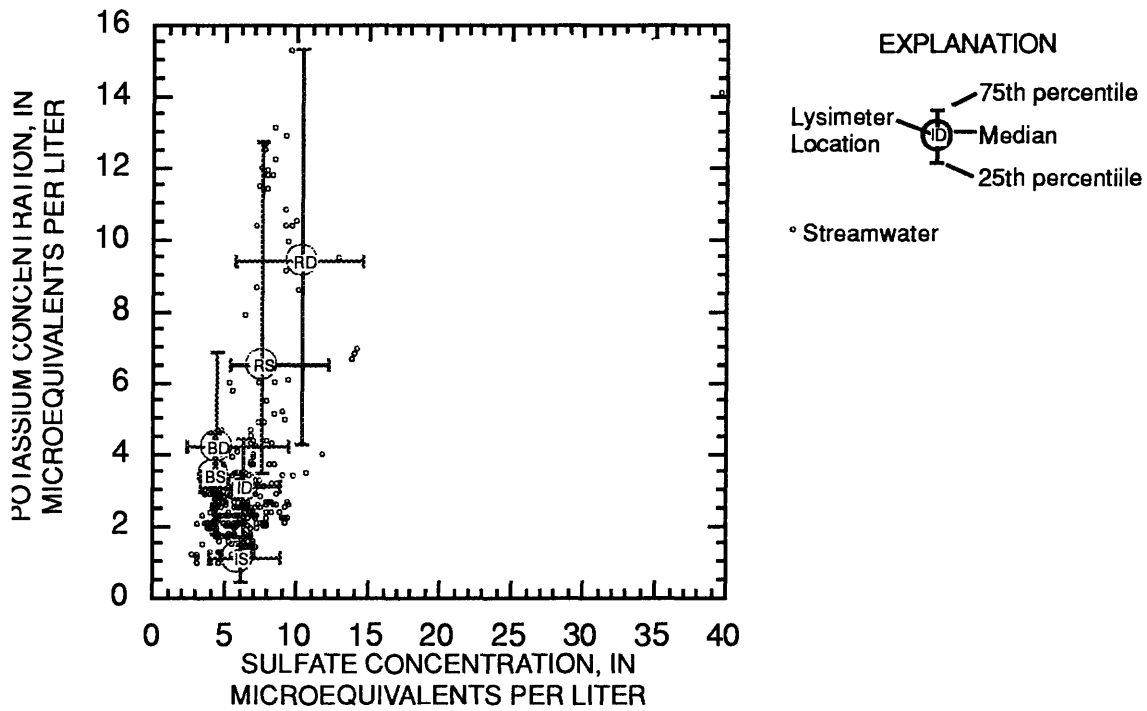


Figure 46.—Mixing diagram relating potassium and sulfate.

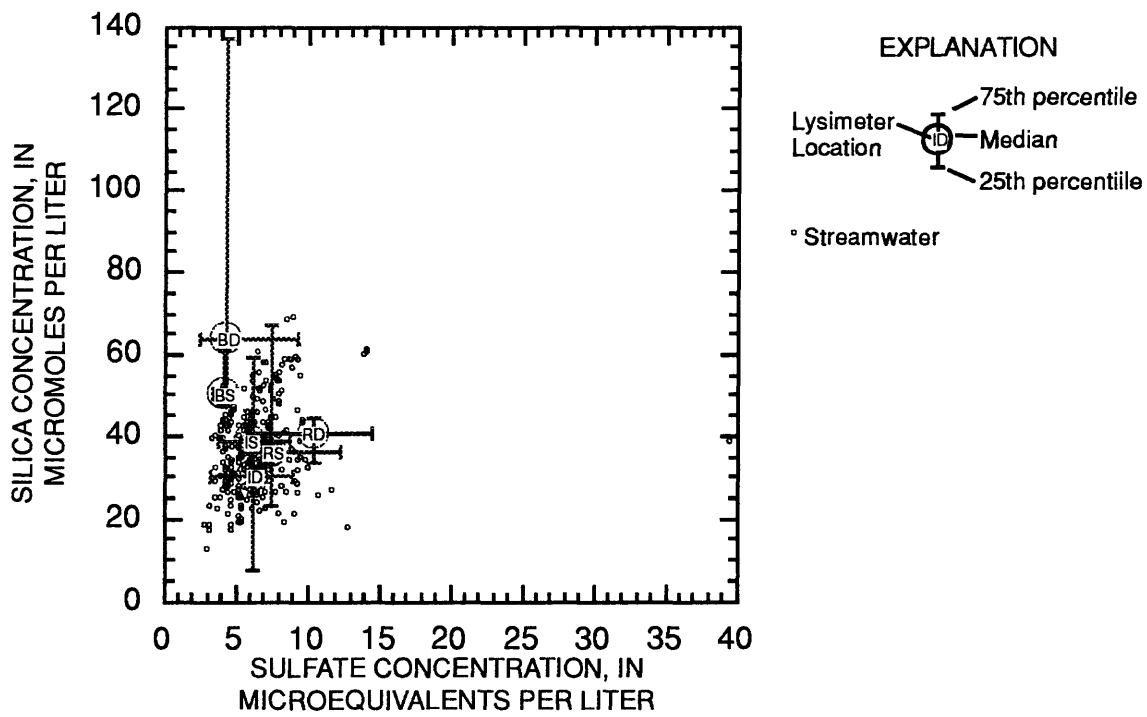


Figure 47.—Mixing diagram relating silica and sulfate.

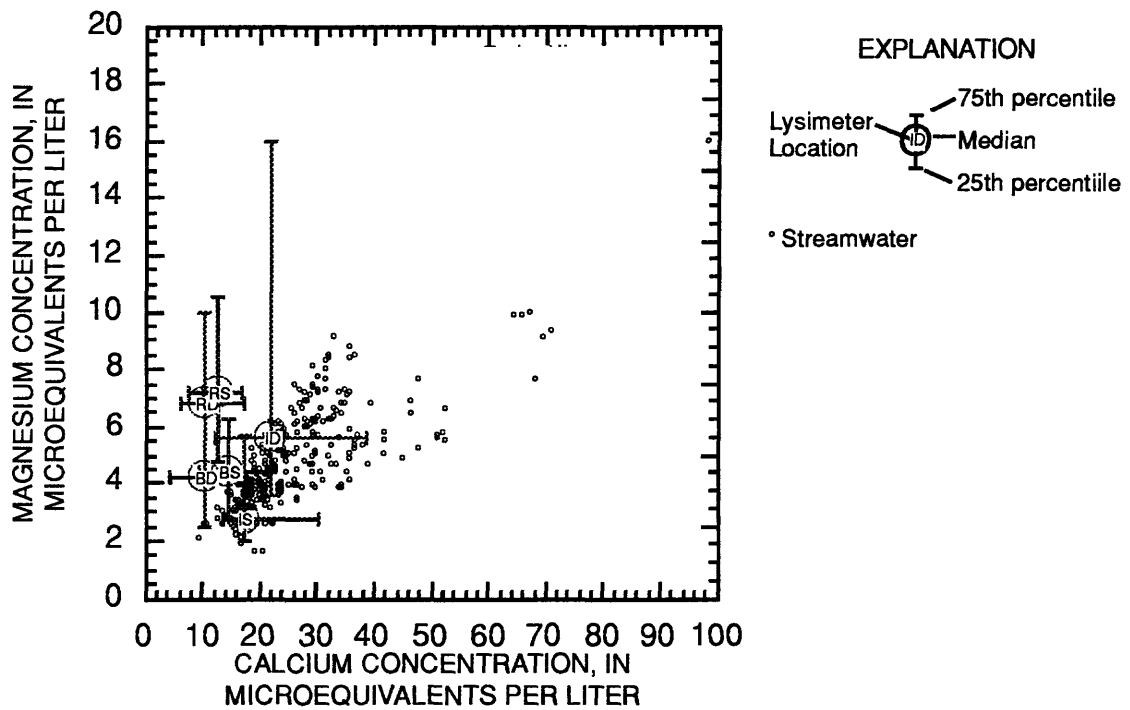


Figure 48.—Mixing diagram relating magnesium and calcium.

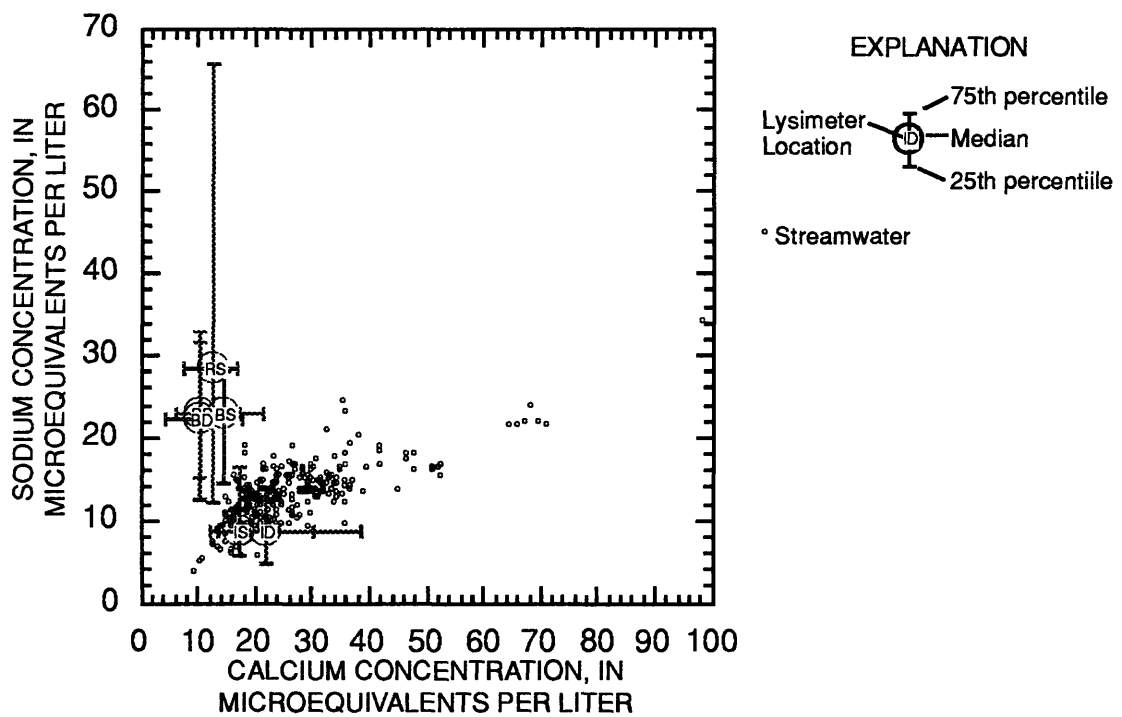


Figure 49.—Mixing diagram relating sodium and calcium.

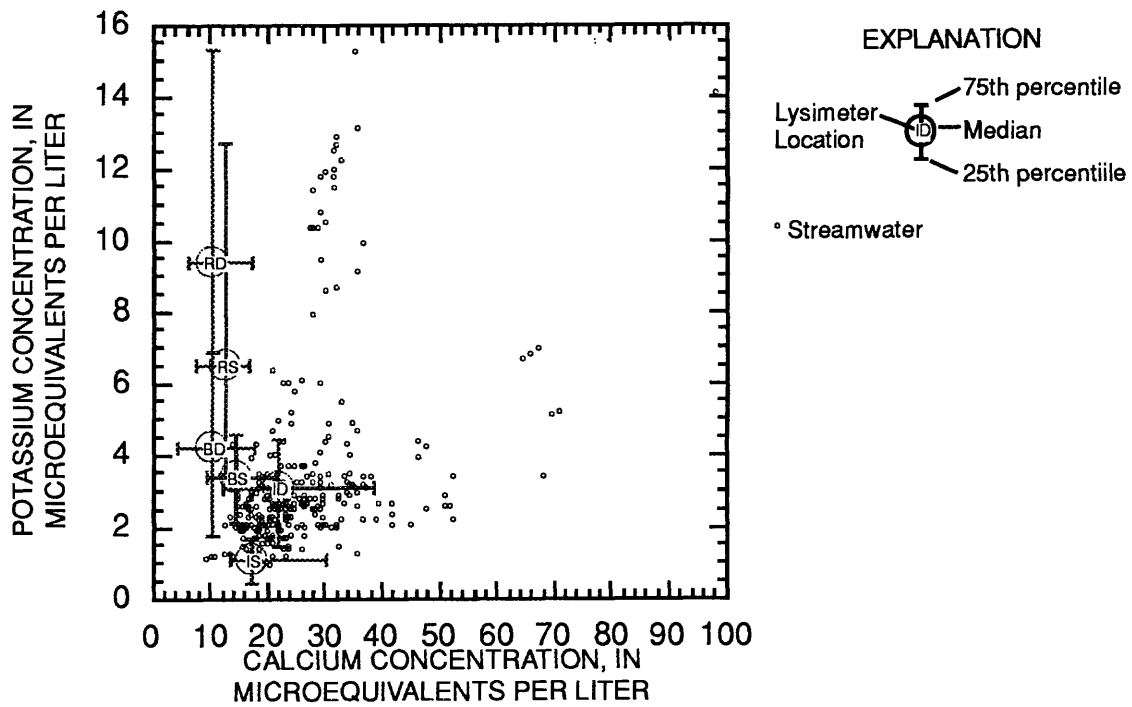


Figure 50.—Mixing diagram relating potassium and calcium.

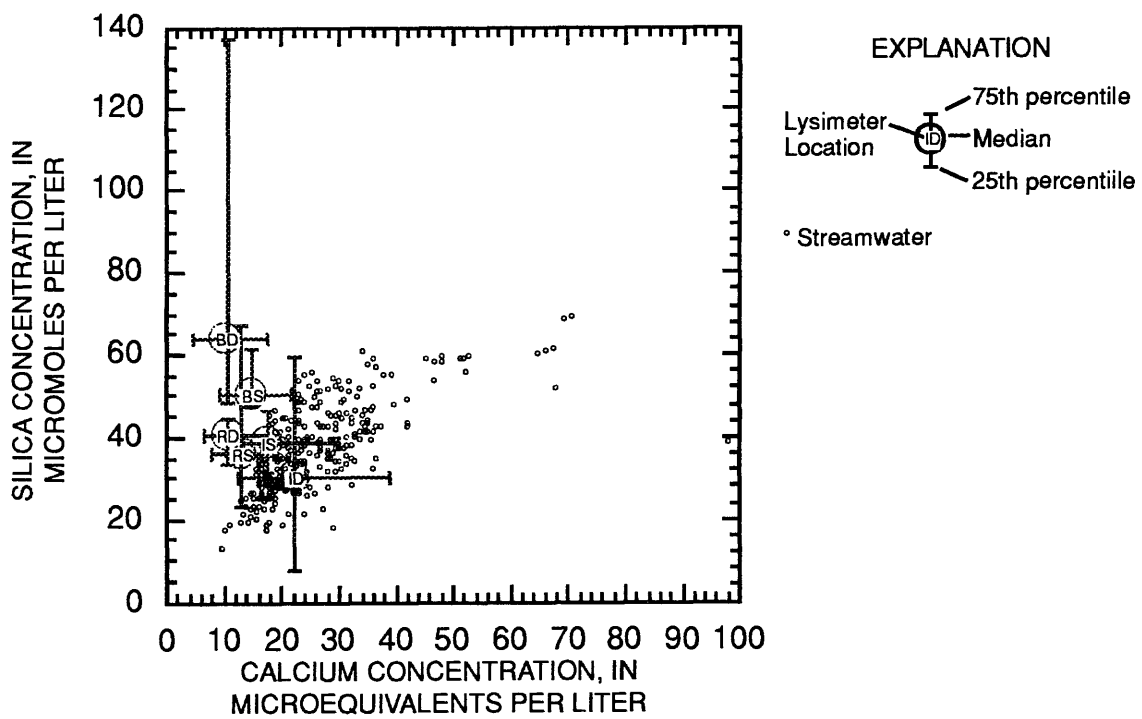


Figure 51.—Mixing diagram relating silica and calcium.

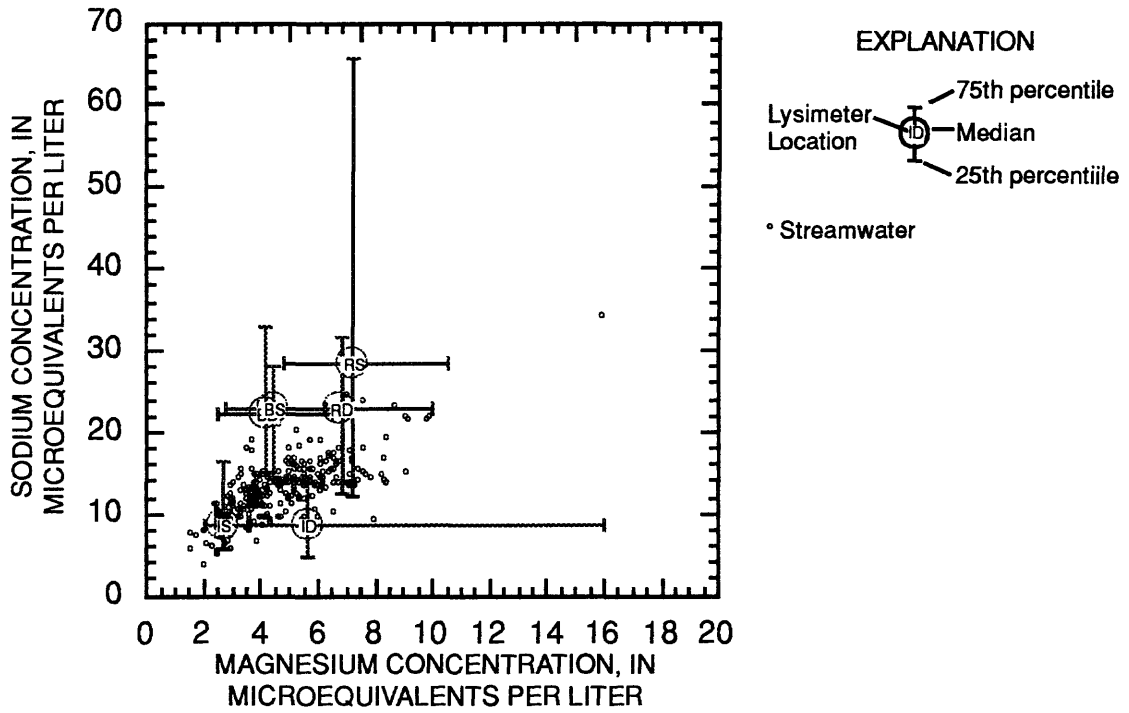


Figure 52.—Mixing diagram relating sodium and magnesium.

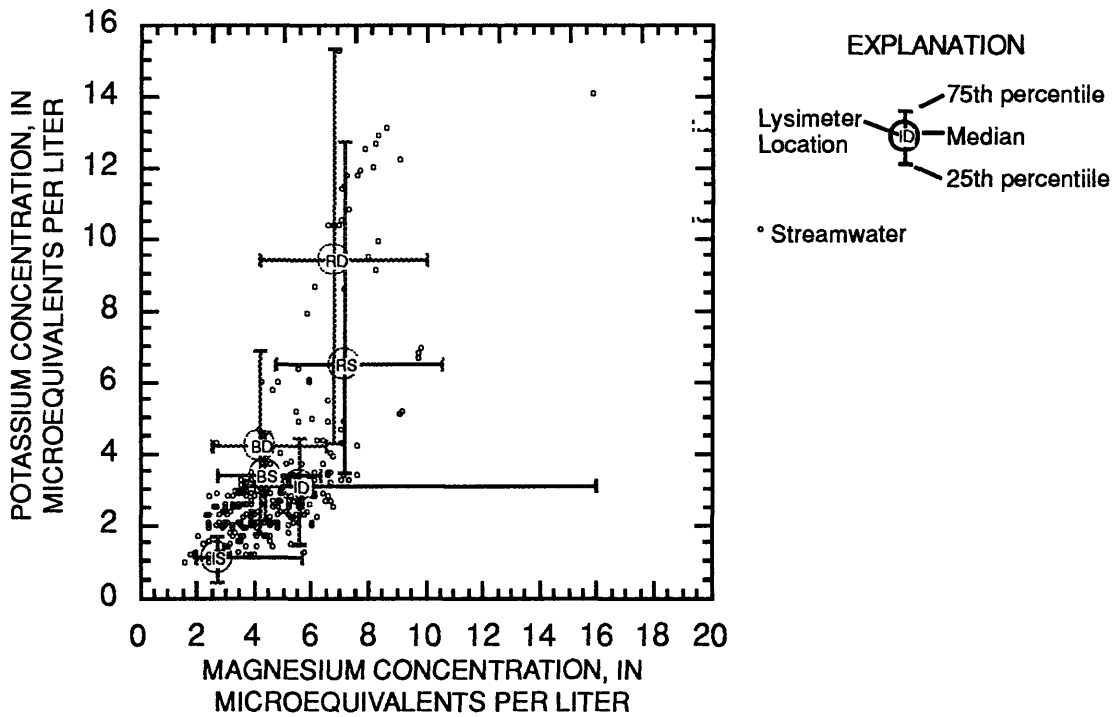


Figure 53.—Mixing diagram relating potassium and magnesium.

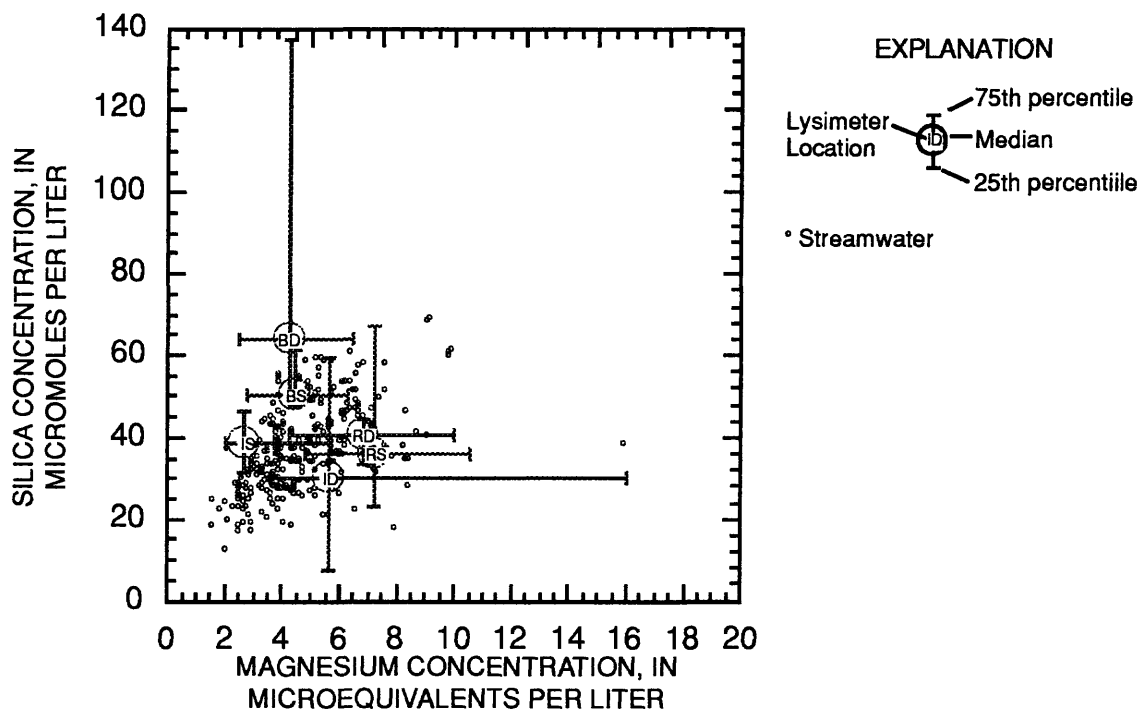


Figure 54.—Mixing diagram relating silica and magnesium.

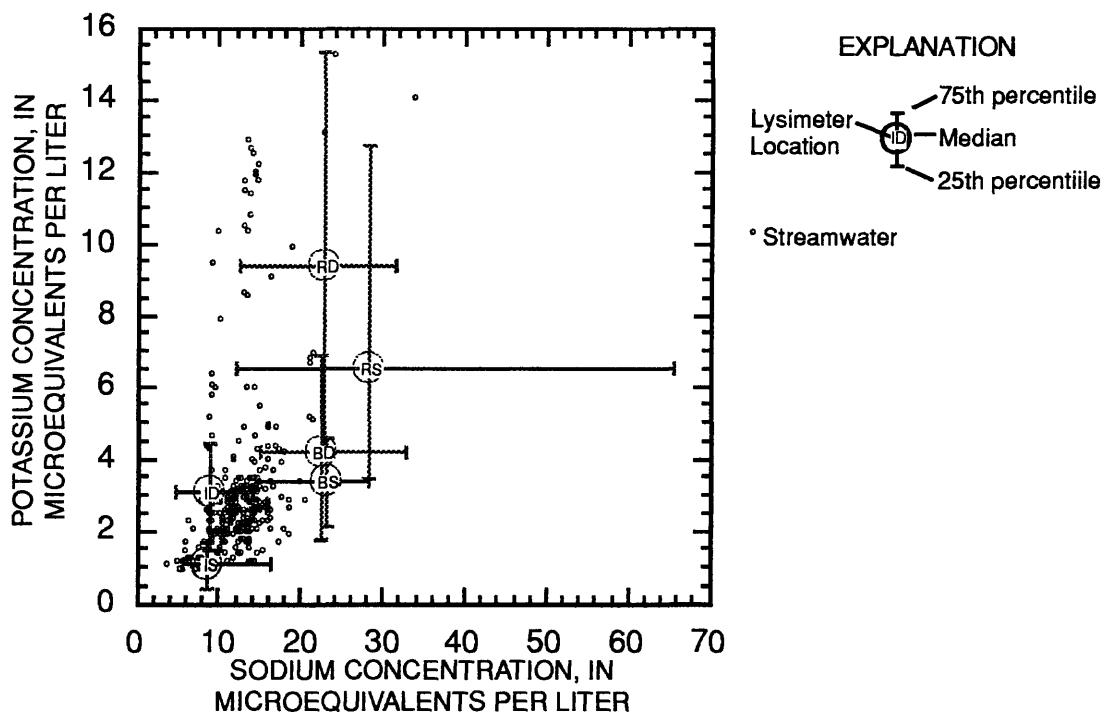


Figure 55.—Mixing diagram relating potassium and sodium.

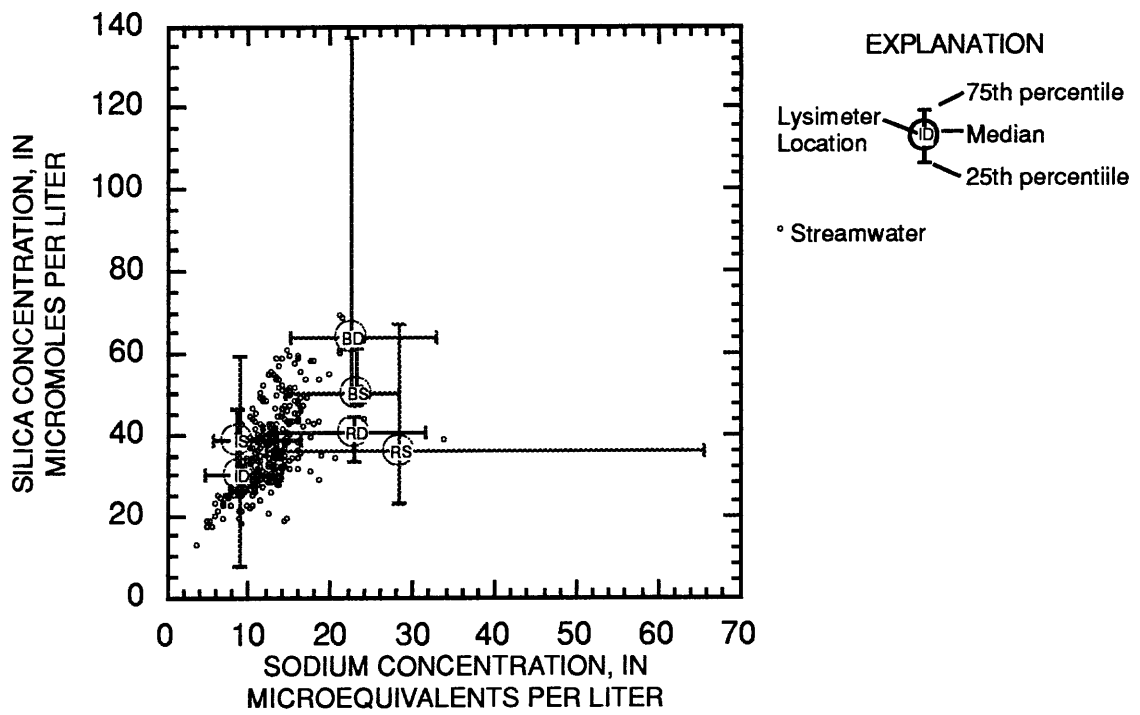


Figure 56.—Mixing diagram relating silica and sodium.

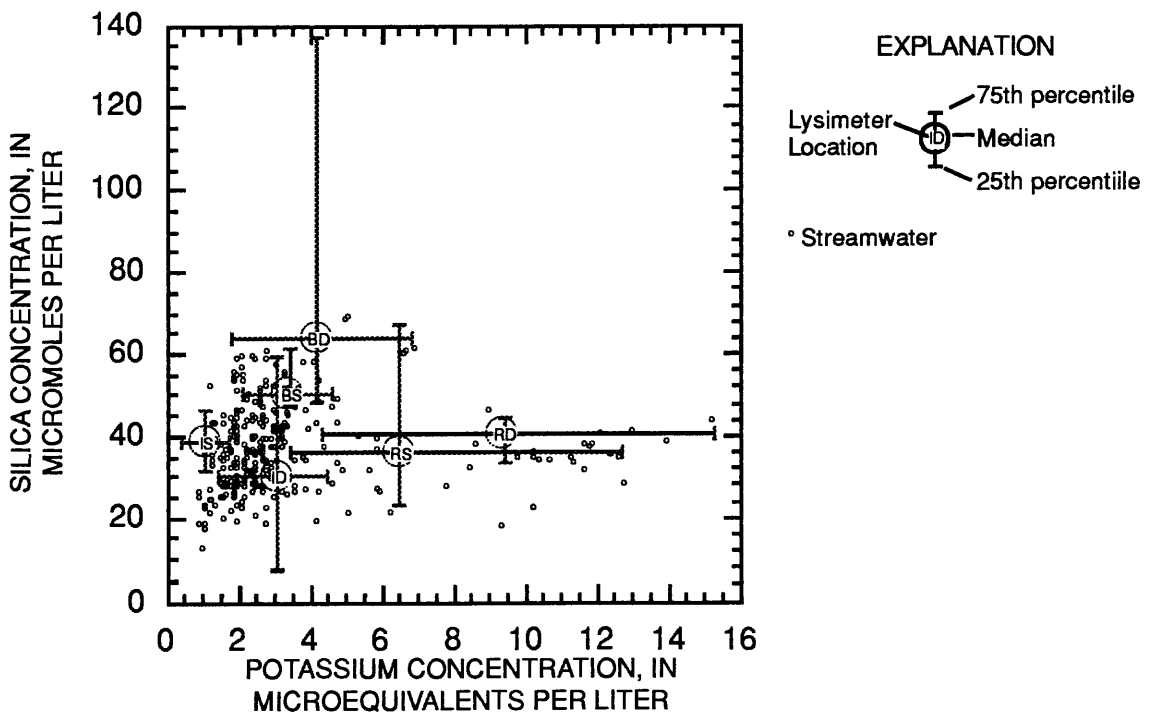


Figure 57.—Mixing diagram relating silica and potassium.